NATIONAL RENEWABLE ENERGY LABORATORY

ACCREDITED
Certificate No. 1239-01

BLADE STATIC TEST REPORT
Test Identifier: SNL_2017

LABORATORY WIND TURBINE BLADE STATIC TESTING OF THE SANDIA NATIONAL ROTOR TESTBED 13-METER WIND TURBINE BLADE

Maximum Flapwise Proof Loading
Minimum Flapwise Proof Loading
Maximum Edgewise Proof Loading
Minimum Edgewise Proof Loading
Flapwise Fatigue Loading
Ultimate Positive Flapwise Static Load

Conducted by:
National Renewable Energy Laboratory
National Wind Technology Center
15013 Denver West Parkway
Golden, CO 80401

Conducted for:
Sandia National Laboratories
P.O. Box 5800
Albuquerque, NM 87185

22 AUGUST 2018

APPROVAL BY Bill Gage — 23 AUG 2018
Bill Gage
Test Technician
Date

APPROVAL BY Ryan Beach — 23 AUG 2018
Ryan Beach
Test Engineer
Date

APPROVAL BY Scott Hughes — 23 AUG 2018
Scott Hughes
Test Manager
Date

TABLE OF CONTENTS

ACROYNMS and INITIALISMS

Phrase	Abb.	Phrase	Abb.
National Wind Technology Center	NWTC	Department of Energy	DOE
National Renewable Energy Laboratory	NREL	National Rotor Testbed	NRT
Sandia National Laboratories	SNL	Scaled Wind Farm Technology	SWiFT
Ethercat Data Acquisition System	EDAS	Lightning Protection System	LPS
National Instruments	NI	Center of Gravity	CG
Damage Equivalent Load	DEL	Leading Edge	LE
Trailing Edge	TE	High Pressure side	HP
Low Pressure side	LP		

1-DISCLAIMER

This report was prepared by the National Renewable Energy Laboratory (NREL), operated for the United States Department of Energy (DOE) by the Alliance for Sustainable Energy, LLC (Alliance), as an account of work sponsored by the United States government. The test results documented in this report define the characteristics of the test article as configured and under the conditions tested.

This report is provided “as is” and neither the government, the Alliance, NREL, nor any of their employees, makes any warranty, express or implied, including the warranties of merchantability and fitness for a particular purpose, or assumes any legal liability or responsibility for the accuracy, completeness, or usefulness of any such information disclosed in the report, or of any apparatus, product, or process disclosed or represents that its use would not infringe privately owned rights.

Neither Alliance nor the U. S. Government shall be liable for special, consequential or incidental damages. Reference herein to any specific commercial product, process, or service by trade name, trademark, manufacturer, or otherwise does not necessarily constitute or imply its endorsement, recommendation, or favoring by the United States government or any agency thereof. The views and opinions of the authors expressed herein do not necessarily state or reflect those of the United States government or any agency thereof or Alliance.

NREL is a DOE Laboratory, and as an adjunct of the United States government, cannot certify wind turbines. The information in this report is limited to NREL’s knowledge and understanding as of this date.

NREL is accredited by the American Association for Laboratory Accreditation (A2LA) and the results shown in this test report have been determined in accordance with the NREL’s terms of accreditation unless stated otherwise in the report.

This report shall not be reproduced, except in full, without the written approval of Alliance or successor operator of NREL.

Results presented in this report are for the NRT Blade 0 tested at NREL. Data used to calculate the applied test moment is based on model information provided by Sandia.

2-EXECUTIVE SUMMARY

The Sandia National Laboratories (SNL or Sandia) National Rotor Testbed (NRT) blade is a new design for experimental research and development at the Sandia Scaled Wind Farm Technology (SWiFT) facility, located at Texas Tech University's National Wind Institute Research Center in Lubbock, TX. Four NRT blades were manufactured, with three blades for operation at the SWiFT facility, and one blade intended for structural validation. A series of structural validation tests including property testing, static strength testing, and fatigue testing were performed at the National Renewable Energy Laboratory (NREL). This report documents the static and fatigue load cases applied to the NRT blade.

Figure 2.1 – Minimum Edgewise Static Test Setup

Figure 2.2. Fatigue Test Setup

3-SCOPE

This test report provides information on the test setup, instrumentation, and load matrix used for laboratory testing of the NRT blade. This report covers the following load cases:

- Maximum Flapwise Proof Load
- Minimum Flapwise Proof Load
- Maximum Edgewise Proof Load
- Minimum Edgewise Proof Load
- Flapwise Fatigue Load
- Ultimate Positive Flapwise Static Load

4-BACKGROUND

Static and fatigue laboratory test loading was performed on the Sandia NRT blade. Prior to static testing, property testing including airfoil profiling and a modal survey was performed. Following the static proof loading described in this report a flapwise fatigue test was performed then followed by an ultimate static test to failure. Table 4.1 provides information and references on each of the experiments and tests performed on the blade.

Table 4.1. Sequence of Property and Structural Testing of the Sandia NRT Blade at NREL

Test	Test Periods	Reference
Blade Delivery	January 2017	n/a
Airfoil profiling	May and June 2017	[1]
Modal Survey	April, May, June 2017	[2]
Static Proof Load Testing	July 2017 – September 2017	This report
Flapwise Fatigue Testing	December 2017 – January 2018	This report
Ultimate Static Test	January 2018	This report
Blade sectioning	May 2018	[3]
Blade removed from NWTC	June 2018	n/a

Work was performed through an inter-agency agreement between Sandia and NREL [4]. DOE program funds were used for the edgewise static load cases as part of the wake dynamics project. NREL subtask WUJJ1000 was used for the inter-agency agreement, and NREL subtask WE163D01 was used for program support.

Testing was performed according to NREL's Quality Assurance Program. NREL is accredited by A2LA for blade testing in accordance with the IEC 61400-23 standard [5], A2LA Certificate Number 1239-01 [6]. Testing operations complied with the NWTC Structural Testing Safe Operating Procedure and were conducted within the scope of the Job Walk [7]. Structural validation testing was performed according to the test plans for static and fatigue testing [8, 9, 10, 11].

5-TEST OBJECTIVE

The objectives of the static proof loading of the blade were to:

1. Validate the blade can sustain the factored extreme negative flapwise bending and static edgewise bending moments.
2. Measure deflections and strains resulting from the applied test loads.

The objectives of the flapwise fatigue were to:

1. Apply a cyclic fatigue load to the blade to an equivalent 20-year damage equivalent load
2. Measure strains and accelerations during fatigue loading

The objectives of the ultimate static test were to:

1. Apply a static load to the blade up to a root moment of 380 kN m (test rig constraint).
2. Measure deflections and strains resulting from the applied test loads. Displacement sensors were removed prior to loading to failure.

6-TEST ARTICLE

The Sandia NRT blade was 13 m in length, with construction materials that include fiberglass, balsa wood, and epoxy. The blade root bolt pattern is (30) M20 bolts on a 508-mm bolt pattern. The nominal maximum chord is 1.473 m. The blade includes pre-bend in the flapwise, upwind direction. The blade was not identified with a unique marking but was identified by Sandia as NRT Blade 0.

The blade was fabricated by TPI Composites from an additive manufactured mold designed by Oak Ridge National Laboratory.

The trailing edge was modified at the 9.46 m and 9.71 m stations. Small (4 mm) triangular sections were cut from the blade for material testing because of visible abnormalities noted upon delivery to NREL (caused by the force exerted by tie-down straps during shipping to NREL).

7-TEST SETUP

7.1-Test Location

Testing was performed inside of the highbay of the Structural Testing Laboratory (STL) at NREL's National Wind Technology Center (NWTC).

7.2-Facility Configuration

The blade was cantilevered to the 5.4 MN m test stand in the STL highbay. The 5.4 MN m test stand was secured to t-slot base plates on the west end of the highbay.

The test stand was tilted back at several angles between load cases to allow adequate clearance for test equipment while keeping the blade relatively close to the laboratory floor. Test stand inclination angles are provided in the test plan.

A T-slot base plate blade was mounted to the highbay floor to react the external load applied by the crane or electric winch for both static load cases and calibration pulls during the fatigue test.

7.3- Blade to Test Stand Connection

The blade was mounted to the test stand through an adapter plate. The adapter plate is a 3" (~75-mm) thick, A-36 steel plate. Bolt torque and mounting configurations are provided in the test plans.

7.4-Blade Pre-twist Orientation

For all static load cases the test loads were applied vertically with respect to the laboratory. For each load case the blade and attached adapter plate was removed from the test stand, keeping the blade mounted to the adapter plate. The blade was rotated and remounted to the test stand for each load case.

Figure 7.1 provides the inclination of the 12.96 m airfoil as mounted to the test stand for each static load case.

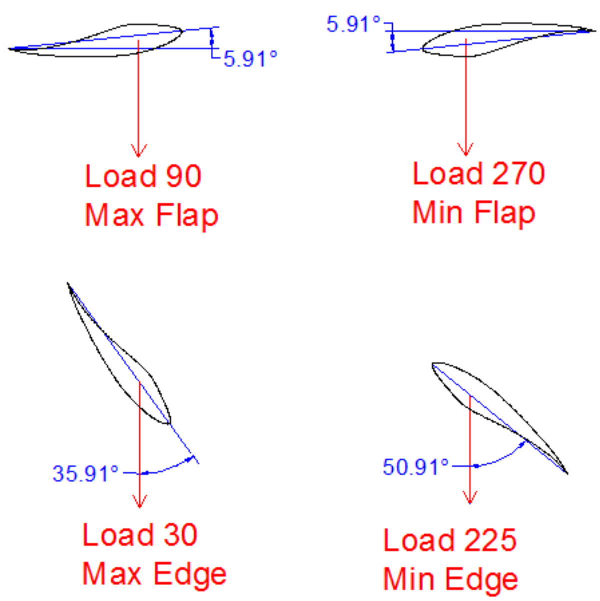

Figure 7.1. Blade Mounting Orientation (view is from root to tip)

The mounting orientation for the flapwise fatigue test and the ultimate positive flapwise (Load 90) was the same as the maximum flapwise proof load, with the inclination of the 12.96 m airfoil at 5.91 degrees.

7.5-Load Introduction Method and Hardware

7.5.1 – Static Proof Load Cases

The applied test bending moment includes blade self-weight, tare load from the weight of the load saddles, and the external loads applied via the overhead crane and ballast weights.

Three load introduction stations at 4.6 m, 7.55 m and 10.85 m were used to apply external loads. A ballast weight was suspended from the blade at the 4.6 m station. External test loads were applied at the the 7.55 m and 10.85 m stations by a test operator controlling the STL's 35 ton overhead bridge crane. A spreader bar was positioned between the 7.55 m and 10.85 m load introduction stations to carry the load applied by the crane to the saddles. Turning blocks mounted to the t-slot base plates reacted and redirected the force from the overhead bridge crane to a force applied to the spreader bar pulling downwards towards the laboratory floor. A 5/8-in Dyneema synthetic rope was used to connect to the spreader bar and run through turning blocks to the overhead crane.

Load saddles were used to apply the external loads to the blade. Load saddles are comprised of wood forms which are shaped to match the airfoil profile; steel frames are built around the wood forms to transfer the test load from the winches to the wood forms. The wood forms are constructed from microlams beams that are cut to the station airfoil profile and fitted to the blade surface with rubber and structural putty, this ensures good surface contact that distributes to point load from the winch across the station chord. The load saddle wood forms were 5.25 in (133.4 mm) thick in the spanwise direction, centered at the nominal blade station. The steel frames are fabricated around the wood forms and secure the load saddle to the blade using four ½-13 grade B7 threaded rods that were torqued to 20 ft-lbf. The torque applied to the threaded rods created a preload of approximately 10.7 kN on the blade. Saddles were designed to apply loads to the blade at the center of a line between the centers of the high-pressure and low-pressure spar caps.

For edge load static cases, chain bridles were attached to the saddles. Unequal length bridles provided the ability to adjust the external load to center through the center of the spar. For all load cases the geometry of the saddle was designed for load to pass through the center of the spar.

7.5.2 – Fatigue Testing

For initial fatigue testing, two UREX exciters were mounted to the 4.6 m saddle. Additional ballast mass was attached to the 4.6 m and 7.55 m saddles, while the metal frame of the 10.85 m station saddle was removed. Saddles were ballasted according to the test plan to provide the appropriate mean load and fatigue load amplitude. The amplitude of the applied moment was controlled by adjusting the displacement amplitude of the UREX actuator(s).

Early in the fatigue test it was noted that the amplitude ranges of accelerometers and strain gages were not steadily tracking the UREX actuator amplitude. It is thought that the first flap frequency at which the test was operating at was near a subharmonic frequency of the second flap mode, and potentially near a subharmonic of a torsional mode. The north UREX was removed from the blade near cycle 109,400, while additional oscillating mass was added to the UREX. The 10.85 m saddle weight was reduced by 14-kg to 21-kg. The test was noted to run steadily following these modifications. Table 7.2 provides the 4.6m saddle mass and total oscillating mass as originally configured and for the modified configuration. Note that these weights are approximate as the saddle was not removed and weighed during this modification.

Table 7.2. Fatigue Test 4.6 m saddle and UREX Weights

Property	Initial configuration	After removal of North UREX at cycle 109,400
Total Saddle Mass [kg]	1352	1197
Total Oscillating mass [kg]	225	170
Test Operating Frequency [Hz]	1.5	1.57

The Lightning Protection System (LPS) was observed (heard) to be contacting the inside blade surface during loading near the tip of the blade. A hole was drilled into the high-pressure blade surface at the 12 m station and then expanding urethane foam was injected to secure the LPS. The amount of foam injected was unmeasured however the weight listed by the foam manufacturer was 0.45 kg.

7.5.3 – Ultimate Positive Flapwise Static Loading

The 4.6 m and 7.55 m saddles were ballasted for the ultimate flapwise loading. An electric winch applied loads to the 10.85 m saddle. The winch line ran through a block and tackle system that created a two-part line connecting to the load saddle. This arrangement is shown in Figure 7.2 during the 75% (of anticipated ultimate) loading, as the load cell is positioned between the saddle and pulley.

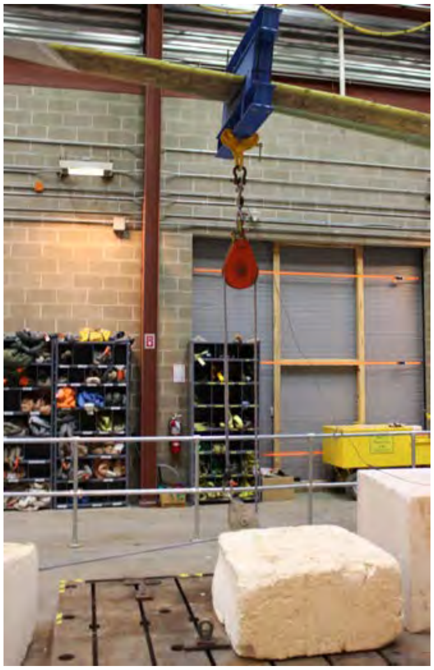

Figure 7.2. Two-part rigging line attached to the 10.85 m station saddle

8-INSTRUMENTATION

The channel map for the sensors used during the test is provided in the test plans [8, 9, 10, 11]. Instrumentation records and calibration certificates are available upon request.

8.1-Load

8.1.1 – Static Proof Load

Two load cells were used to measure the applied test loads during static proof load testing. One load cell was positioned at the 4.6 m station and the second load cell was positioned under the spreader beam connecting to the 7.55 m and 10.85 m station saddles. Table 8.1 provides the specifications for the load cells. Load cells were zeroed without rigging attached beneath the load cell.

Table 8.1. Static Proof Load Cell Specifications

Type	Manufacturer	Model	Serial
Load Cell 1	MTS	661.20E-03	04859C
Load Cell 2	Transducer Techniques	SW-10K	4718C

8.1.2 – Fatigue

A load cell was used for calibration pulls to enable correlation of moment to strain. Table 8.2 provides specifications for the load cell used for moment calibration during fatigue testing.

Table 8.2. Fatigue Calibration Pull Load cell

Type	Manufacturer	Model	Serial
Load Cell	Transducer Techniques	SW-10K	4718C

8.1.3 – Ultimate Static Load

A single load cell was connected to the 10.85 m saddle during ultimate static load testing. During the 75% (of estimated failure load) load ramp the load cell was connected directly underneath the saddle. For the load ramp to failure, the load cell was moved and positioned ahead of the two-part rigging line connected to the saddle. Since the load cell was measuring the load in the winch line before reeving through the turning blocks to the saddle, creating a two-part line, the applied load at the saddle during the failure pull will be approximately twice the reading of the load cell. However, friction in the turning block bearings will decrease the load applied to the blade compared to load cell readings. Table 8.3 provides information on the load cell used during the ultimate static load test.

Table 8.3. Ultimate Static Test Load Cell Specification

Type	Manufacturer	Model	Serial
Load Cell	Transducer Techniques	SW-10K	4718C

8.2-Displacement

8.2.1 – Static Proof Loading

Three string potentiometers were used to measure blade displacements at the 4 m, 7 m, and 11.25 m stations for static testing. String potentiometers were attached between the blade and the ground along the center of the spar cap. A laser distance transducer was positioned to measure blade displacements near the trailing edge of the 7 m station. The laser distance transducer was not used for the edgewise static load cases. String pot and laser distance transducer specifications are provided in Table 8.4.

Table 8.4. String Potentiometer and Laser Distance Transducer Specifications

Type	Manufacturer	Model	Serial
String Pot	Unimeasure	HX-PA-30	32060220
String Pot	Unimeasure	HX-PA-30	32060221
String Pot	Unimeasure	HX-PA-50	32060222
String Pot	Unimeasure	HX-PA-80	31030644
String Pot	Unimeasure	HX-PA-150	32060224
String Pot	Unimeasure	HX-PA-250	32060226
LDT	Balluff	DOD 63M-LA04-S115	1333DE

8.2.2 – Fatigue Loading

For fatigue testing the LDT was positioned at the 1 m station, facing the low-pressure side of the blade. This was the only displacement transducer used during fatigue cycling. For calibration pulls, the Unimeasure string potentiometer was used (s/n 32060222).

8.2.3 – Ultimate Positive Flapwise Loading

Displacement transducers were removed prior to the load ramp to blade failure during ultimate static loading.

8.3-Strain

Resistance strain gages were installed on the blade for strain measurement. The single-axis strain gages are Measurements Group WK-06-250BG-350 and the rosettes are Measurements Group WK-06-250RA-350. All the strain gages have a nominal 350 Ohm resistance and were connected in a three-wire configuration. Single-axis strain gages were orientated at 0 degree (parallel with the spanwise axis and perpendicular to the chordwise axis). Rosettes were oriented such that one gage is 0 degrees, one gage is 45 degrees, and one gage is 90 degrees (parallel with the chordwise axis and perpendicular to the spanwise axis). Table 8.5 provides the location of the strain gages.

Table 8.5. Strain Gage Locations

Strain Gage Name	Span	Surface	Chord Position	Type
SG01-200-LP0	0.2	LP	0°	Uni
SG02-200-LP45	0.2	LP	45°	Uni
SG03-200-LP90	0.2	LP	90°	Uni
SG04-200-LP135	0.2	LP	135°	Uni
SG05-200-HP180	0.2	HP	180°	Uni
SG06-200-HP225	0.2	HP	225°	Uni

Strain Gage Name	Span	Surface	Chord Position	Type
SG07-200-HP270	0.2	HP	270°	Uni
SG08-200-HP315	0.2	HP	315°	Uni
SG09-1900-HP-AP-0	1.9	HP	Aft Panel at Spar Interface	Rosette
SG10-1900-HP-AP-45	1.9	HP	Aft Panel at Spar Interface	Rosette
SG11-1900-HP-AP-90	1.9	HP	Aft Panel at Spar Interface	Rosette
SG12-2500-HP-AP-0	2.5	HP	Aft Panel at Spar Interface	Rosette
SG13-2500-HP-AP-45	2.5	HP	Aft Panel at Spar Interface	Rosette
SG14-2500-HP-AP-90	2.5	HP	Aft Panel at Spar Interface	Rosette
SG15-2750-HP-TE	2.75	HP	TE	Uni
SG16-2750-LP-TE	2.75	LP	TE	Uni
SG17-2900-LP-SC-0	2.9	LP	Center of Sparcap	Rosette
SG18-2900-LP-SC-45	2.9	LP	Center of Sparcap	Rosette
SG19-2900-LP-SC-90	2.9	LP	Center of Sparcap	Rosette
SG20-2900-LP-FP-0	2.9	LP	Mid Fore Panel	Rosette
SG21-2900-LP-FP-45	2.9	LP	Mid Fore Panel	Rosette
SG22-2900-LP-FP-90	2.9	LP	Mid Fore Panel	Rosette
SG23-3250-HP-SC	3.25	HP	Center of Sparcap	Uni
SG24-3250-LP-SC	3.25	LP	Center of Sparcap	Uni
SG25-3250-LE	3.25	LP	LE	Uni
SG26-3250-TE	3.25	LP	TE	Uni
SG27-3250-LP-TE	3.25	LP	TE	Uni
SG28-6300-LP-AP-0	6.3	LP	Mid Aft Panel	Rosette
SG29-6300-LP-AP-45	6.3	LP	Mid Aft Panel	Rosette
SG30-6300-LP-AP-90	6.3	LP	Mid Aft Panel	Rosette
SG31-6300-HP-LE-0	6.3	HP	LE	Rosette
SG32-6300-HP-LE-45	6.3	HP	LE	Rosette
SG33-6300-HP-LE-90	6.3	HP	LE	Rosette
SG34-6500-HP-SC	6.5	HP	Center of Sparcap	Uni
SG35-6500-LP-SC	6.5	LP	Center of Sparcap	Uni
SG36-6500-LE	6.5	LP	LE	Uni
SG37-6500-TE	6.5	LP	TE	Uni
SG38-9000-LP-AP-0	9	LP	Mid Aft Panel	Rosette
SG39-9000-LP-AP-45	9	LP	Mid Aft Panel	Rosette
SG40-9000-LP-AP-90	9	LP	Mid Aft Panel	Rosette
SG41-9750-HP-SC	9.75	HP	Center of Sparcap	Uni
SG42-9750-LP-SC	9.75	LP	Center of Sparcap	Uni
SG43-9750-LE	9.75	LP	LE	Uni

Strain Gage Name	Span	Surface	Chord Position	Type
SG44-9750-TE	9.75	LP	TE	Uni
SG45-3250-HP-TE	3.25	HP	TE	Uni

Table 8.6 provides specifications for the strain gages. For static testing, strain gage channels were zeroed before application of the first load step but after all hardware and rigging was installed on the blade (i.e. zeroed with tare weight). For fatigue testing, gages were periodically zeroed at mean load during calibration pulls (blade with load saddles and UREX installed).

Table 8.6. Strain Gage Specifications

Type	Manufacturer	Model
Single element Strain Gage	Vishay	WK-06-250BG-350
Rosette Strain Gage	Vishay	WK-06-250RA-350

8.4-Temperature and Humidity

Ambient temperature and relative humidity were measured during the test. Measurements were taken near the blade root. Table 8.7 provides specifications for the temperature and relative humidity sensor.

Table 8.7. Temperature and Humidity Sensor Specifications

Type	Manufacturer	Model	Serial
Temperature Humidity	Omega	HX93BV2	1603050

8.5-Accelerometers

Accelerometers were mounted to the blade during fatigue testing. Each accelerometer measured acceleration in both flap and edge (lead-lag) directions. Table 8.8 provides a list of the accelerometers locations used during fatigue testing. Accelerometers were mounted to the top surface of the blade.

Table 8.8. Accelerometer Specifications

EDAS Channel Name	Manufacturer	Model	Serial	Position
Accel1Flap	SDI	2470-002	3441	Root HP
Accel1LeadLag	SDI	2470-002	3441	Root HP
Accel2Flap	SDI	2460-005	1242	4.6 m UREX N
Accel2LeadLag	SDI	2460-005	1242	4.6 m UREX N
Accel3Flap	SDI	2470-005	3105	4.6 m UREX S
Accel3LeadLag	SDI	2470-005	3105	4.6 m UREX S

EDAS Channel Name	Manufacturer	Model	Serial	Position
Accel4Flap	SDI	2460-005	1341	4.7 m TE
Accel4LeadLag	SDI	2460-005	1341	4.7 m TE
Accel5Flap	SDI	2470-005	3106	4.7 m LE
Accel5LeadLag	SDI	2470-005	3106	4.7 m LE
Accel6Flap	SDI	2460-010	1340	9.75 m TE
Accel6LeadLag	SDI	2460-010	1340	9.75 m TE
Accel7Flap	SDI	2470-005	2073	9.75 m LE
Accel7LeadLag	SDI	2470-005	2073	9.75 m LE

8.6 - Data Acquisition

The Ethercat Data Acquisition System (EDAS) was used for static and fatigue testing. The EDAS is based on National Instruments (NI) Ethercat PXI technology combined with custom NREL developed LabVIEW coded software (software version 120120). All channels were scanned at 1000 Hz and recorded as time series data at 100 Hz. For fatigue testing, data was also collected as peak/valley data pairs, recording the maximum and minimum values for each cycle of every channel.

8.7-Property Testing Instrumentation

A Chatillon crane scale was used to measure weight for the mass and CG balance. A 2-inch wide poly sling was used to lift the blade. A digital protractor was used to measure the inclination of the root face of the blade during the mass and CG balance. Table 8.9 provides specifications on the instruments used for weight and balance measurements.

Table 8.9. Property Testing Instrumentation Specifications

Type	Manufacturer	Model	Serial
Crane Scale	Chatillon	RDWT-2000	41998
Digital Protractor	Mitutoyo	PRO 3600	950-316

Instrumentation used for modal testing is provided in a separate report [2].

9-APPLIED TEST LOADING

9.1 – Static Proof Load Cases

Each proof load case was performed by applying the external loads of ballast weight and crane load. For each load case the loads were applied in three load ramps, at approximately 25%, 50%, and 100% of the target load.

9.2 – Fatigue Test Loading

Fatigue test moments were applied by operating the UREX actuators at the system's natural frequency. The mean test moment was created by the static weight of the blade and saddles, including the weight of the UREX system. Moment amplitude was maintained by using dual-mode feedback for UREX actuator amplitude control.

Periodically, a static load was applied to the blade at the 10.85 m saddle. Strain to moment sensitivities of select strain gages were then be used to calculate the applied bending moment under dynamic cycling through strain gage measurements.

9.3 – Ultimate Static Load Case

Loads were applied to the 10.85 m station saddle through a two-part rigging line connected to an electric winch. The initial ramp to 75% of anticipated failure moment was performed with the load cell beneath the load saddle. The load cell was moved to winch line during the load to failure.

10-TESTING AND RESULTS

10.1-Property Testing

Weight and CG measurements of the blade were performed with a single point lift prior to installing test instrumentation. A polyester lifting sling was choked around the blade at the center of gravity location. The lift was conducted with the blade positioned such that the trailing edge (TE) was up, towards the laboratory ceiling, and the leading edge (LE) was down, towards the laboratory floor. The sling position was adjusted along the span of the blade until the root face of the blade was vertical. The weight was measured with crane scale and the CG distance was measured with a tape measure from the root face of the blade to the center of the sling along the low-pressure (LP) surface. The results are presented in Table 10.1.

Table 10.1. Weight and CG

Property	Measured Values
Weight (kN)	5.08
CG Location (m)	3.630

Modal parameters were measured using free-decay and impact methods. The blade was cantilevered to the test stand in Building A-60 for modal characterization. Summary information of modal survey results is provided in Table 10.2.

Table 10.2. Modal Survey Summary Results

Mode Shape	Frequency [Hz]	Damping [% of Critical Damping]
1st Flat	2.19	0.11
1st Edge	4.92	0.20
2nd Flat	7.06	0.14
3rd Flat	14.5	0.16
2nd Edge	18.1	0.23
Flap / Torsion	24.0	0.20
1st Torsion	26.6	0.19

10.2-Static Proof Testing

Blade static proof load testing followed the test plan. Table 10.3 provides the 100% applied test moments for each of the static proof load cases. Appendix A provides information on how the applied loads are calculated. Figure 10.1 provides the ratio between the applied test moment to the target test moment. The applied test moment exceeded the target test moment for ratios greater than 1.

Table 10.3. Applied Test Loads for Static Proof Load Cases

	Maximum Flapwise		Minimum Flapwise		Maximum Edgewise		Minimum Edgewise	
Spanwise Station [m]	Target Test Moment [kN-m]	Applied Test Moment [kN-m]	Target Test Moment [kN-m]	Applied Test Moment [kN-m]	Target Test Moment [kN-m]	Applied Test Moment [kN-m]	Target Test Moment [kN-m]	Applied Test Moment [kN-m]
0	224.90	222.51	195.80	192.28	166.80	169.64	159.40	163.19
0.87	197.20	197.68	168.00	167.64	145.20	148.57	136.50	141.42
1.82	171.70	171.24	139.30	141.39	124.20	126.22	112.60	118.32
2.6	149.90	149.80	117.00	120.11	106.40	108.14	95.10	99.62
3.48	126.50	125.96	93.90	96.46	87.50	88.10	77.20	78.88
4.44	102.30	100.35	72.90	71.05	69.00	66.63	59.10	56.64
5.46	77.90	79.02	53.10	53.74	52.10	51.58	43.30	42.71
5.98	68.20	68.82	44.30	45.96	44.20	44.76	36.20	36.64
7.02	48.60	48.63	30.20	30.60	30.80	31.34	24.70	24.73
8.05	32.60	32.52	19.30	19.31	20.40	20.77	15.60	15.82
9.05	21.00	20.80	11.40	12.31	12.60	13.25	9.10	10.07
9.52	15.50	15.36	8.50	9.08	9.70	9.78	6.80	7.43
10.4	8.70	5.28	4.50	3.16	5.00	3.40	3.70	2.60
11.53	3.20	0.07	1.20	0.07	1.40	0.07	1.00	0.07
12.37	0.30	0.01	0.20	0.01	0.20	0.01	0.10	0.01
12.99	0.00	0.00	0.00	0.00	0.00	0.00	0.00	0.00

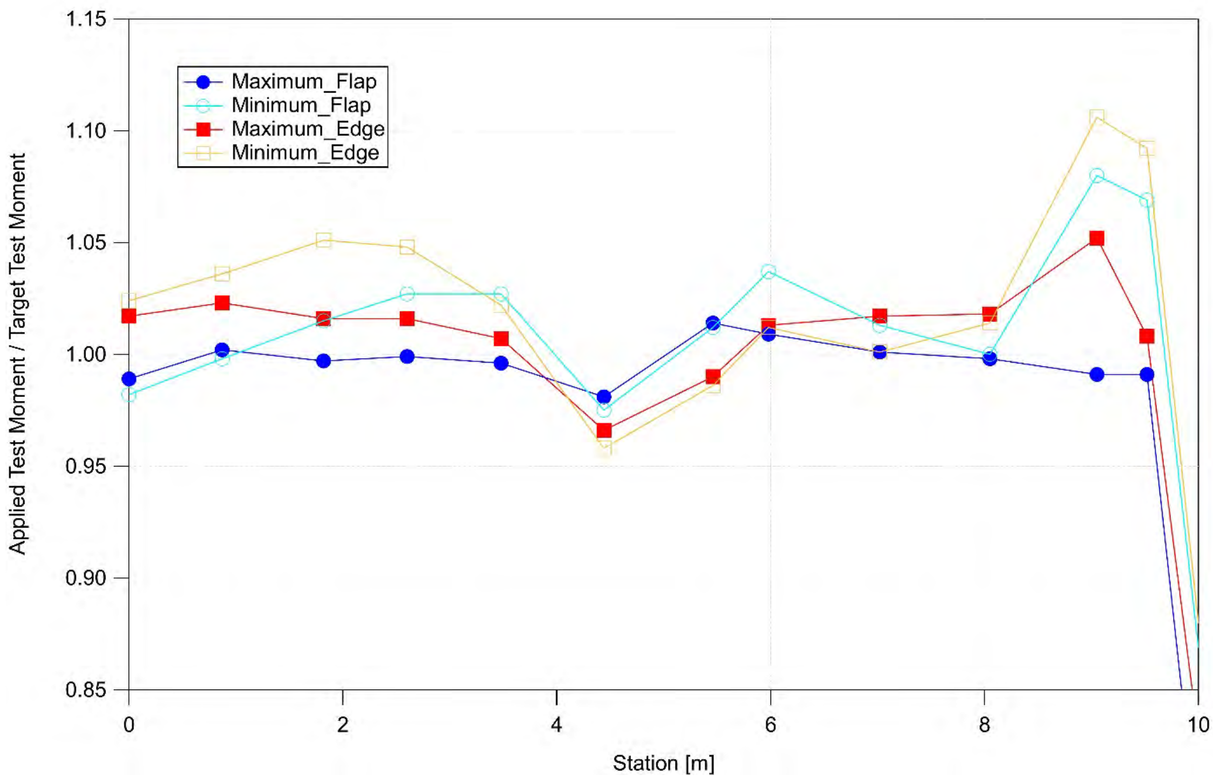

Figure 10.1. Static Proof Load Testing Applied to Target Load Ratio

Appendix B through Appendix E provide data charts for the 100% load ramps for each of the static proof load cases.

The blade sustained each of the proof load cases without evidence of damage or apparent changes in physical shape.

10.3-Flapwise Fatigue Loading

Testing was performed in attended operation, where staff was always present during loading. The test was stopped in the evening and restarted in the morning.

Table 10.4 provides the strain to moment sensitivities of gages located on the spar caps or root that were used to monitor applied moment. These sensitivities were calculated during calibration pulls performed periodically during testing. The sensitivity is the linear curve-fit slope of the strain versus applied moment curve.

Table 10.4. Strain to Moment Sensitivities

Strain Gage Information		Strain to Moment Sensitivity (kN m)				
Strain Gage Name	Strain Gage Span Location [m] \ Cal Pull Date	2017.12.04	2017.12.27	2018.01.05	2018.01.12	2018.01.19
SG01-200-LP0	0.2	0.4667	0.4623	0.4584	0.4557	0.4569
SG05-200-HP180	0.2	0.4935	0.4718	0.4730	0.4732	0.4669
SG23-3250-HP-SC	3.25	0.0444	0.0438	0.0440	0.0442	0.0439
SG24-3250-LP-SC	3.25	0.0490	0.0477	0.0481	0.0483	0.0477
SG34-6500-HP-SC	6.5	0.0229	0.0225	0.0226	0.0227	0.0225
SG35-6500-LP-SC	6.5	0.0242	0.0236	0.0237	0.0239	0.0237
SG41-9750-HP-SC	9.75	0.0076	0.0073	0.0073	0.0073	0.0073
SG42-9750-LP-SC	9.75	0.0083	0.0078	0.0079	0.0079	0.0079

Figure 10.2 compares the target 1 million cycle DEL with DEL's calculated from the applied fatigue test load. Appendix F provides the equations used to calculate the applied test DEL. An inverse slope parameter of 12 is used for this calculation. The low-pressure surface gages provided higher estimates of applied DEL, with an excepting being at the 0.2 m station. The DEL at the 0.2 m station is approximately 15% below the target DEL. Including moments in the lead-lag direction, the DEL at the 0.2 m station is approximately 8% below the target DEL.

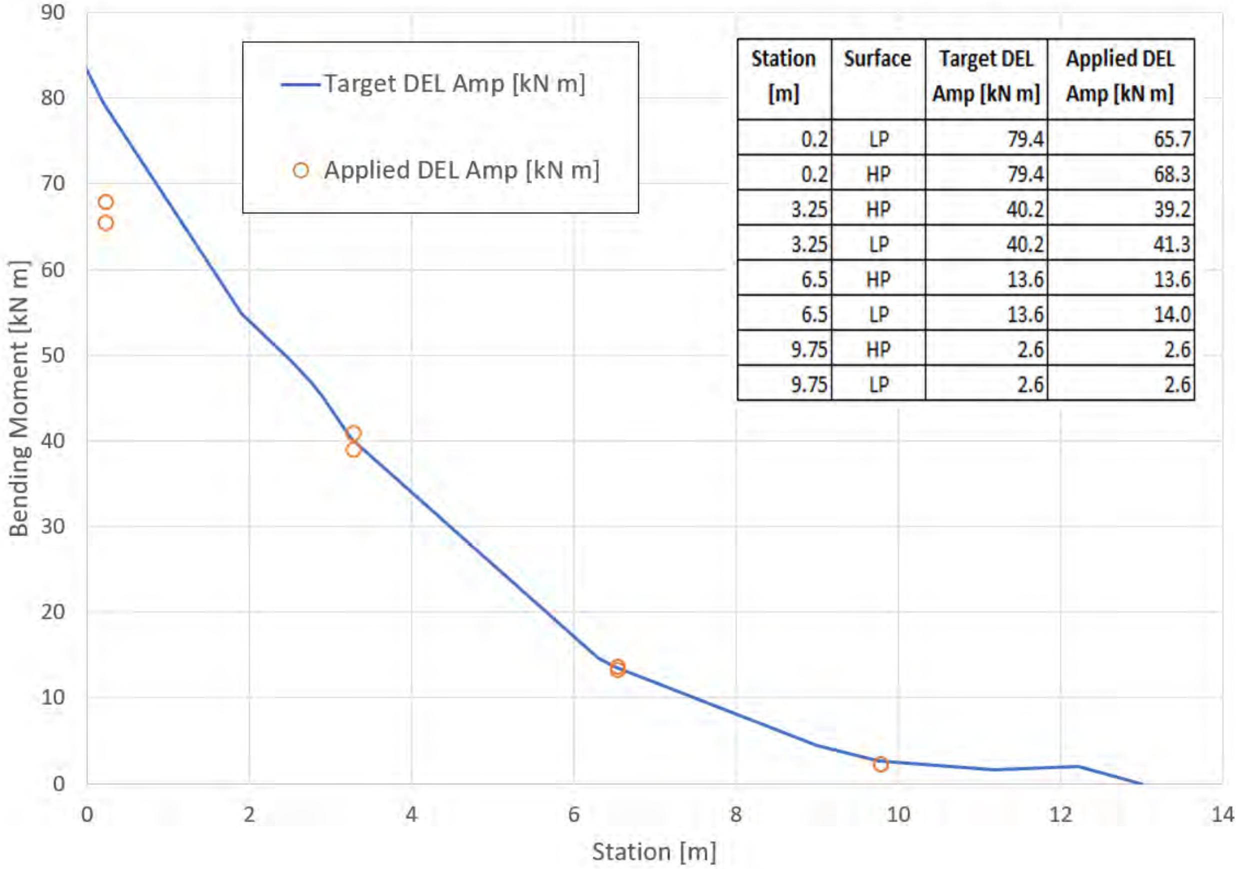

Station [m]	Surface	Target DEL Amp [kN m]	Applied DEL Amp [kN m]
0.2	LP	79.4	65.7
0.2	HP	79.4	68.3
3.25	HP	40.2	39.2
3.25	LP	40.2	41.3
6.5	HP	13.6	13.6
6.5	LP	13.6	14.0
9.75	HP	2.6	2.6
9.75	LP	2.6	2.6

Figure 10.2. Target and Applied DEL's

Appendix G provides data charts for the flapwise fatigue test. Data in these charts have been averaged in blocks of 50 cycles. Data collected during startup and shutdown (low amplitude response) have been filtered from charted data. Taking a snapshot of operating data, Table 10.5 provides data ranges (peak-to-peak) at a cycle count of 1 million cycles.

Table 10.5. Data ranges at the 1-million cycle mark

Channel Name	Range @ 1e6 Cycles	Units	Channel Name	Range @ 1e6 Cycles	Units
LVDT-S	83.4	mm	SG14-2500-HP-AP-90	459	ue
Temperature (Average Value)	20.5	C	SG15-2750-HP-TE	609	ue
Humidity (Average Value)	11.0	% RH	SG16-2750-TE	551	ue
LDT	1.86	mm	SG17-2900-LP-SC-0	2057	ue
A-Tip-Flap	8.111	g	SG18-2900-LP-SC-45	654	ue
A-Tip-LeadLag	1.892	g	SG19-2900-LP-SC-90	511	ue
A-4700TE-Flap	0.804	g	SG20-2900-LP-FP-0	1308	ue

Channel Name	Range @ 1e6 Cycles	Units	Channel Name	Range @ 1e6 Cycles	Units
A-4700TE-LeadLag	0.260	g	SG21-2900-LP-FP-45	616	ue
A-9750TE-Flap	4.357	g	SG22-2900-LP-FP-90	608	ue
A-9750TE-LeadLag	1.315	g	SG23-3250-HP-SC	1801	ue
A-9750LE-Flap	4.333	g	SG24-3250-LP-SC	1741	ue
A-9750LE-LeadLag	1.248	g	SG25-3250-LE	212	ue
A-4600UREXSouth-Flap	1.498	g	SG26-3250-TE	615	ue
A-4600UREXSouth-LeadLag	1.014	g	SG27-3250-LP-TE	546	ue
A-4700LE-Flap	0.842	g	SG28-6300-LP-AP-0	645	ue
A-4700LE-LeadLag	0.246	g	SG29-6300-LP-AP-45	302	ue
A-4600UREXNorth-Flap	0.853	g	SG30-6300-LP-AP-90	376	ue
A-4600UREXNorth-LeadLag	0.278	g	SG31-6300-HP-LE-0	129	ue
A-Root-Flap	0.002	g	SG32-6300-HP-LE-45	57	ue
A-Root-LeadLag	0.004	g	SG33-6300-HP-LE-90	133	ue
SG01-200-LP0	290	ue	SG34-6500-HP-SC	1221	ue
SG02-200-LP45	247	ue	SG35-6500-LP-SC	1197	ue
SG03-200-LP90	52	ue	SG36-6500-LE	108	ue
SG04-200-LP135	157	ue	SG37-6500-TE	534	ue
SG05-200-HP180	295	ue	SG38-9000-LP-AP-0	345	ue
SG06-200-HP225	270	ue	SG39-9000-LP-AP-45	193	ue
SG07-200-HP270	57	ue	SG40-9000-LP-AP-90	175	ue
SG08-200-HP315	151	ue	SG41-9750-HP-SC	716	ue
SG09-1900-HP-AP-0	279	ue	SG42-9750-LP-SC	673	ue
SG10-1900-HP-AP-45	106	ue	SG43-9750-LE	124	ue
SG11-1900-HP-AP-90	230	ue	SG44-9750-TE	247	ue
SG12-2500-HP-AP-0	618	ue	SG45-3250-HP-TE	669	ue
SG13-2500-HP-AP-45	93	ue	SG46-2750-LP-TE	487	ue

A ‘Clicking’ noise was noted around the 2.9 m station early in testing but diminished as the test progressed. Beyond the initial strain drift at the 2.9 m station (SG 17, SG18, and SG19) no abnormal behavior was observed in strain or acceleration data.

10.4-Ultimate Positive Flapwise Static Load

The 75% (of maximum flap proof) and load to failure were the final structural loads applied to the blade. During the ramp to failure the load cell was between the winch and turning blocks. The turning blocks add friction that reduces the applied load reading. From this, strain to moment sensitivities were used to estimate the applied test load at the time of failure. The blade failed near the 2.9 m station. Reviewing video, the skin and shear web on the low-pressure surface was observed to buckle prior to failure. The applied test bending moment at the 2.9 m station when the blade failed catastrophically was 228.7 kN m. Table 10.5 provides the strain to load sensitivities used to calculate the applied test bending moment at the time of failure. Figure 10.3 provides the applied test bending moment at failure, as calculated using strain to load sensitivities.

Table 10.5. Strain to Moment Sensitivities for Ultimate Static Flapwise Moment Calculation

Strain Gage	Station [m]	Strain to Load sensitivity [kN / ue]	Strain Offset [ue]	Strain at Failure [ue]	Moment at Failure [kN m]
SG23-3250-HP-SC	3.25	0.003457	1566	4970	214.4
SG24-3250-LP-SC	3.25	-0.00318	-1437	-4342	214.4
SG34-6500-HP-SC	6.5	0.003826	690	4361	100.2
SG35-6500-LP-SC	6.5	-0.00373	-668	-4214	100.2

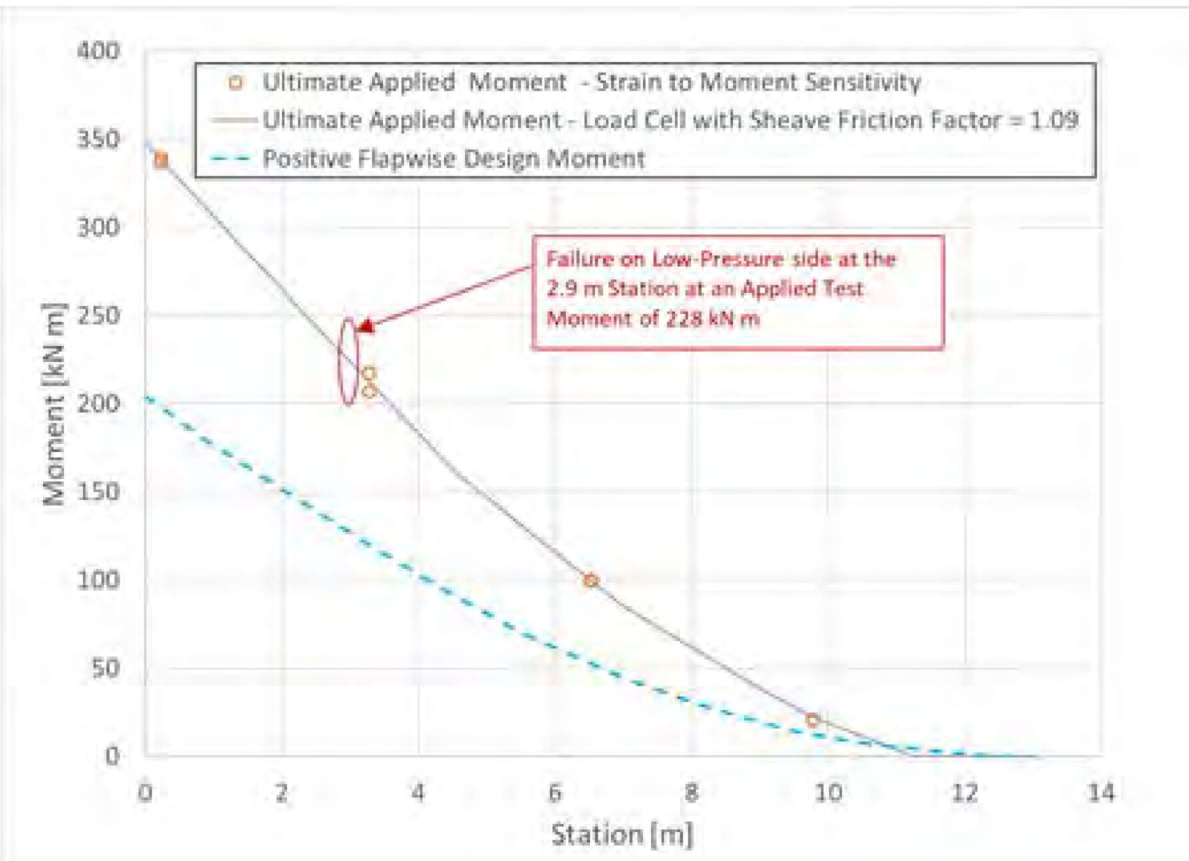

Figure 10.3. Applied Flapwise Static Moment at Failure

Figure 10.4 shows the low-pressure surface of the blade just before and after failure. The light-colored area in the photo on the left is centered near the 2.9 m station. Video will more clearly show this area was bulging out prior to failure

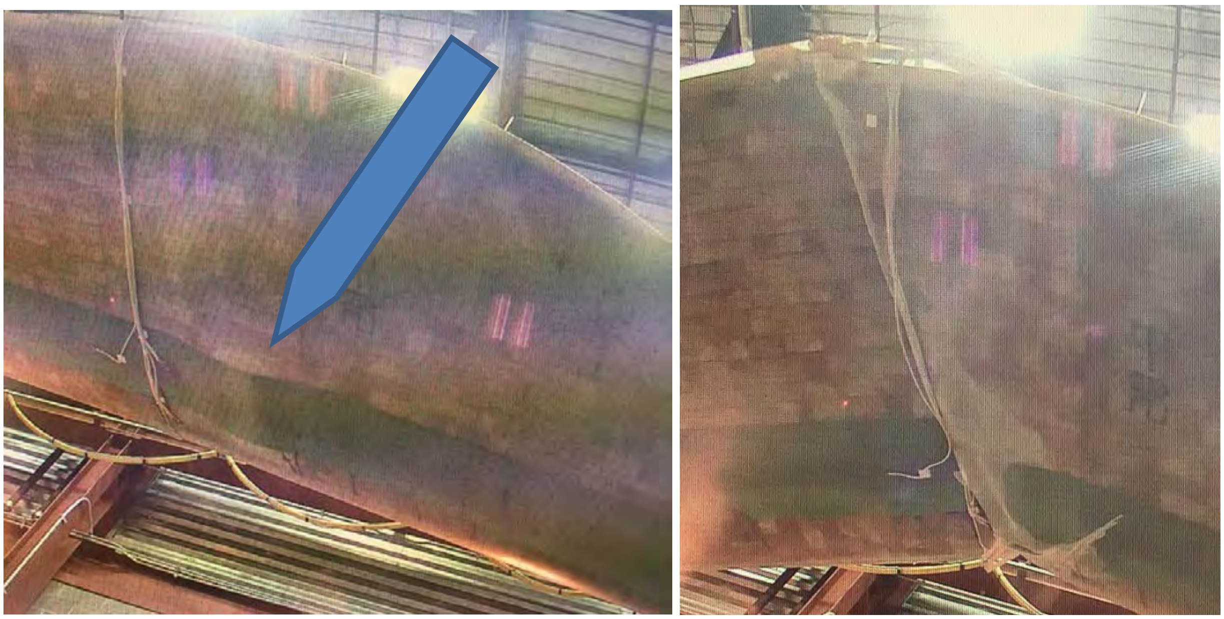

Figure 10.4. Low-pressure Blade Surface Before and After Failure

Appendix H provides data charts for the ultimate positive flapwise static test.

11-SECTION WEIGHT BALANCE

Following the completion of structural testing and the failure of the blade during the ultimate static load case the blade was sectioned into 13 sections along the length of the blade, each section was approximately 1 meter in length. The CG of each section was determined by balancing the section on a length of angle iron. The weight of the sections was measured by placing the sections on a platform scale. Table 9.1 provides data collected during blade sectioning. At several locations noted in Table 11.1, the aluminum bar of the Lightning Protection System (LPS) was observed to be broken.

Table 11.1. Blade Section Weight Balance Summary

Section #	Nominal Section Start [mm]	Nominal Section End [mm]	Section Length at LE [mm]	Section Length at TE [mm]	Chord Length at root side [mm]	Section CG from root end along spar cap [mm]	Mass [kg]	Notes
1	0	1000	994	1014	584	323	138.2	
2	1000	2000	992	1107	812	518	55.4	center cracked / delamination on LP side
3	2000	3000	996	996	1361	486	50.8	LE/center splintered
4	3000	4000	897	890	1465	427	41	trailing edge split, center broken, detached
5	4000	5000	1093	1100	1382	536	46.5	trailing edge split, Aluminum (LPS) broken
6	5000	6000	1002	997	1244	496	37.5	
7	6000	7000	999	1005	1106	489	32.9	Lightning Protection System (LPS) Aluminum bar broken at mid span
8	7000	8000	996	1000	980	484	29.5	
9	8000	9000	996	994	879	497	25.9	
10	9000	10000	999	1014	790	487	22	
11	10000	11000	994	988	702	483	18	
12	11000	12000	997	1002	619	478	13.7	Added expanding foam to secure LPS. Great Stuff foam weight of 16 oz [0.45 kg]
13	12000	13000	1018		483	441	8.7	Length measured along center of spar cap. A small amount of added foam in this section

12-MEASUREMENT UNCERTAINTITY

Table 12.1 provides uncertainty estimates for the recorded measurements with a 95% level of confidence (coverage factor k = 2).

Table 12.1. Uncertainty Budget

Instrument	Manufacturer	Model No.	Estimate of the Measurand	Expanded Uncertainty	Effective degrees of freedom (v_{eff})
Temperature	Omega	HX93*	20 °C	1.0 °C	>1E+03
Humidity	Omega	HX93*	50 %RH	8.0 %RH	57
Load Cell	MTS	661.20E-02	--	0.2 %RD	>1E+03
String Pot	Unimeasure	HX-PA-*	--	0.5 %RD	>1E+03
Strain Gage Element	Vishay	WK-06-250BG-350 WK-06-250RA-350	1000 ue	3.0 %RD	>1E+03
Torque wrench	*	*	--	10 %RD	>1E+03
Crane Scale	Chatillon	*	--	0.5 %RD	>1E+03
Tape measure	*	*	--	0.3 %RD	>1E+03

* = various manufacturers/models

%RD = percent reading

%RH = percent relative humidity

13-EXCEPTIONS FROM STANDARD PRACTICE

13.1-Deviations from the Test Plans

1. Modified weight of the UREX saddle and the number of UREX's employed for fatigue testing.

2. LVDT initially recording in inches

13.2-Deviations from the IEC 61400-23 Standard

1. The inside of the blade was not inspected between static and fatigue test programs

13.3-Deviations from the NREL Quality Assurance Program

1. The lifting strap used to hoist the blade was used in a choked configuration during weight balancing, the internal procedure calls for the lifting strap to be used in a basket configuration.

14-REFERENCES

1. Airfoil profile data. MS Excel file 'NRT Airfoil Points (180222).xlsx', and 'all sections and spar cap Combined tabdelim (180222).txt'. Sent on 22 February 2018 to Josh Paquette from Scott Hughes.
2. NREL Test Report. Sandia NRT Blade-0 Laboratory Modal Survey. May 1, 2018
3. NREL Report. Blade Sectioning and Weight Balancing of the SNL NRT Blade 0 Sections.
4. Interagency Agreement. SNL Standard Purchase Order 1793182.
5. IEC, Wind turbines—Part23:: Full-scale structural testing of rotor blades, IEC, 2014.
6. http://www.a2la.org/scopepdf/1239-01.pdf
7. Safe Operating Procedures, No. 515009412, *Conducting Structural Tests at the NWTC.*
8. NREL Static Test Plan. Laboratory Maximum Flapwise Static Testing of the Sandia National Rotor Testbed 13-meter Wind Turbine Blade. 30 June 2017.
9. NREL Static Test Plan. Laboratory Minimum Flapwise, and Maximum and Minimum Edgewise, Static Testing of the Sandia National Rotor Testbed 13-meter Wind Turbine Blade. 7 August 2017.
10. NREL Fatigue Test Plan. Laboratory Flapwise Fatigue Testing of the Sandia National Rotor Testbed 13-meter Wind Turbine Blade. 5 December 2017.
11. NREL Static Test Plan. Laboratory Ultimate Flapwise Static Testing of the Sandia National Rotor Testbed 13-meter Wind Turbine Blade. 29 January 2018.

15-LIST OF APPENDICIES

Appendix A – Applied Test Moment Calculation
Appendix B – Data Charts for Maximum Flapwise Proof Loading
Appendix C – Data Charts for Minimum Flapwise Proof Loading
Appendix D – Data Charts for Maximum Edge Proof Loading
Appendix E – Data Charts for Minimum Edge Proof Loading
Appendix F – Fatigue Damage Equivalent Load Calculation
Appendix G – Data Charts for Flapwise Fatigue Loading
Appendix H – Data Charts for Ultimate Positive Flapwise Loading
Appendix I – Test Photographs

APPENDIX A- Applied Test Moment Calculation for Static Proof Load Cases

This appendix provides parameters and equations used to calculate the Applied Test Moment (ATM). The ATM includes tare loads and external loads. For all static test load cases, the applied test loads were acting with gravity, being applied downward toward the laboratory floor. Tare load at each load station includes all weight suspended by the blade from load saddle to load cell. This includes saddles, rigging hardware like chains, shackles, spreader bar, and the weight of the load cell. In addition to the tare loads from rigging equipment and the external loads, the self-weight of the blade creates an additional bending moment. External loads were applied by hanging ballast weights or applying loads with the overhead crane. External loads were measured by the inboard and outboard load cells. The ATM is calculated by summing the contributions from rigging tare, blade self-weight tare, and the external load. Figure A-1 provides a schematic of the dimension used to calculate the ATM.

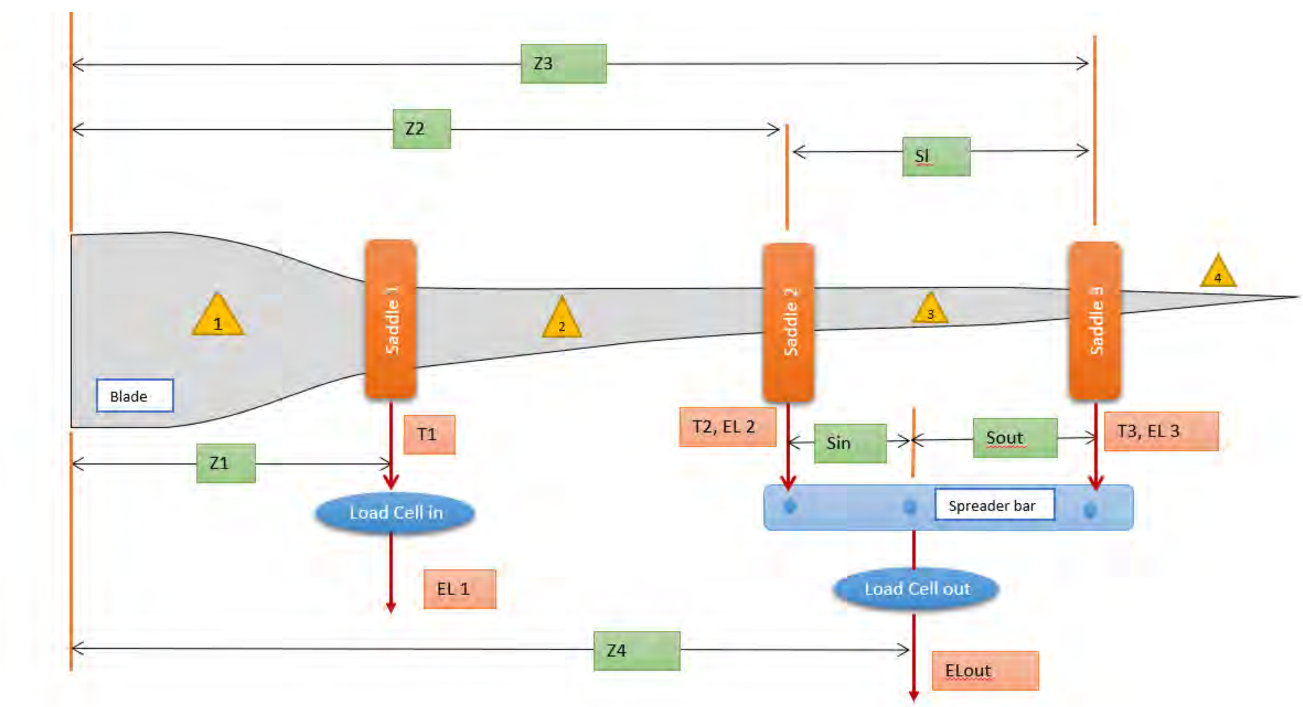

Figure A-1 – Dimensions used for calculating the Applied Test Moment

In addition to the load saddles, a spreader bar was used to apply loads at the 7.55 m and 10.85 m stations by dividing the outboard external load of the overhead crane (reacted through turning blocks to pull down towards the laboratory floor). The tare weight of the spreader bar was taken to be evenly distributed between the 7.55 m and 10.85 m stations. The center of gravity of the spreader bar is offset from the center of the beam as the reaction point hardware connecting to the external winch line was not always positioned at the center of the beam. This difference in the center of gravity of the spreader bar is considered negligible. The weight of instrumentation and cables placed on the blade for strain gages and accelerometers was not included in tare weight values. Table A-1 provides dimensions and rigging tare weights.

Table A-1 – Test setup geometry and rigging tare weights

<table>
<tr><th>Load Case</th><th>Z1 [m]</th><th>Z2 [m]</th><th>Z3 [m]</th><th>Z4 [m]</th><th>T1 [N]</th><th>T2 [N]</th><th>T3 [N]</th><th>Sl [m]</th><th>Sin [m]</th><th>Sout [m]</th><th>EL 2 [fraction of EL out]</th><th>EL 3 [Fraction of EL out]</th></tr>
<tr><td>Maximum Flap</td><td rowspan="4">4.6</td><td rowspan="4">7.55</td><td rowspan="4">10.85</td><td>9.679</td><td>1923.9</td><td>1896.1</td><td>1555.8</td><td rowspan="4">3.299</td><td>2.129</td><td>1.170</td><td>0.355</td><td>0.645</td></tr>
<tr><td>Minimum Flap</td><td>9.120</td><td>1923.9</td><td>1896.1</td><td>1555.8</td><td>1.570</td><td>1.729</td><td>0.524</td><td>0.476</td></tr>
<tr><td>Maximum Edge</td><td>9.679</td><td>2012.8</td><td>1896.1</td><td>1555.8</td><td>2.129</td><td>1.170</td><td>0.355</td><td>0.645</td></tr>
<tr><td>Minimum Edge</td><td>9.279</td><td>1923.9</td><td>1896.1</td><td>1555.8</td><td>1.729</td><td>1.570</td><td>0.476</td><td>0.524</td></tr>
</table>

Viariable Description	
Z1	Distance from root to Saddle 1
Z2	Distance from root to Saddle 2
Z3	Distance from root to Saddle 3
Z4	Distance from root to effective outboard load station
T1	Tare load at Saddle 1
T2	Tare load at Saddle 2
T3	Tare load at Saddle 3
Sl	Spreader length
Sin	Distance between Saddle 2 and external outboard load station
Sout	Distance between external outboard load station and Saddle 3
EL 2	Fraction of external outboard load applied at Saddle 2
EL 3	Fraction of external outboard load applied at Saddle 3

The tare moment created by the self-weight of the blade was estimated based on mass per unit length data provided in the design document and then scaled by the root bending moment calculated by laboratory mass balance measurements performed prior to structural testing. To calculate self-weight bending moment, the blade was discretized into sections between the stations given in the design information document. The CG of each of these sections was calculated as the center of a trapezoid with lengths equal to the design mass per unit at the section end points. For most sections, the sectional CG calculated as a trapezoid is very close to taking the section CG as the midpoint of the section. As the design mass per unit length did not include the weight of the steel root inserts, a mass of 22 kg was added at the z=0.1 m station, where (z) is the distance from the root face of the blade. For a measured blade weight of 5.08 kN and CG 3.63 m from root, the calculated root bending moment due to blade self-weight is 18.44 kN. This result is more conservative relative to the weight and CG measured during the post mortem as less self-weight moment is included in the applied test load. Table A-2 provides the bending moment from blade self-weight based on design information and the estimated bending moment based from blade self-weight scaled to the as-measured CG and mass of the blade. Values for estimated self-weight bending moment (M_z^{SW}) are used for reporting.

Table A-2 – Design and estimated as-built blade self-weight bending moment.

Spanwise Station [m]	Self-weight Bending Moment from Design Information [N m]	Estimated Self Weight Bending Moment based on measured Weight and CG [N m]
0.000	20657.901	18440.000
0.125	20000.801	17853.449
0.250	19406.843	17323.260
0.670	17654.259	15758.839
0.850	16958.791	15138.039
1.525	14492.652	12936.673
2.200	12254.007	10938.376
2.605	11023.899	9840.337
3.482	8647.698	7719.252
4.443	6472.733	5777.799
5.458	4615.954	4120.370
6.115	3627.839	3238.342
7.023	2507.295	2238.103
7.542	1982.957	1770.060
8.054	1540.916	1375.478
8.950	929.844	830.013
9.518	638.136	569.623
10.402	311.556	278.106
11.184	132.383	118.170
11.650	65.832	58.764
12.125	23.767	21.215
12.460	7.548	6.738
12.738	1.247	1.113
12.865	0.202	0.180
12.947	0.018	0.016
13.000	0.000	0.000

Creating a spline fit of the information in Table A-2, Table A-3 provides the estimated blade self-weight bending moment at saddle and strain gage locations. These values are used for reporting moment versus strain.

Table A-3 – Design and estimated as-built blade self-weight bending moment at select blade stations.

Station [m]	Estimated Self-Weight Bending Moment based on Measured Weight and CG [N m]
0.000	18440
0.200	17529
1.900	11801
2.500	10118
2.750	9466
2.900	9088
3.250	8247
4.000	6625
4.600	5496
6.300	3015
6.500	2785
7.000	2261
9.000	805
9.700	499
9.750	480
11.250	108

Given the geometry and values of rigging tare and blade self-weight moments provided above, the ATM can be calculated by including the external loads measured during testing. The external loads applied to Saddle 2 and Saddle 3 by the outboard external load is calculated with the following equations.

$$EL_2 = EL_{out}\left(\frac{S_L - S_{in}}{S_L}\right)$$
$$EL_3 = EL_{out}\left(\frac{S_{in}}{S_L}\right)$$

Between the root of the blade and Saddle 1 (Section 1) the Applied Test Moment is then calculated as:

$$ATM_{Section\ 1} = M_z^{SW} + \{(T_1 + EL_1) * (Z_1 - z)\} + \{(T_2 + EL_2) * (Z_2 - z)\} + \{(T_3 + EL_3) * (Z_3 - z)\}$$

Again, (z) is the distance from the root of the blade where the ATM is calculated. Between Saddle 1 and Saddle 2 (Section 2) the Applied Test Moment is calculated as:

$$ATM_{Section\ 2} = M_z^{SW} + \{(T_2 + EL_2) * (Z_2 - z)\} + \{(T_3 + EL_3) * (Z_3 - z)\}$$

Between Saddle 2 and Saddle 3 (Section 3) the Applied Test Moment is calculated as:

$$ATM_{Section\ 3} = M_z^{SW} + \{(T_3 + EL_3) * (Z_3 - z)\}$$

Outboard of Saddle 3 (Section 4) the Applied Test Moment is simply the moment due to blade self-weight, given as:

$$ATM_{Section\ 4} = M_z^{SW}$$

APPENDIX B – Maximum Flap Charts

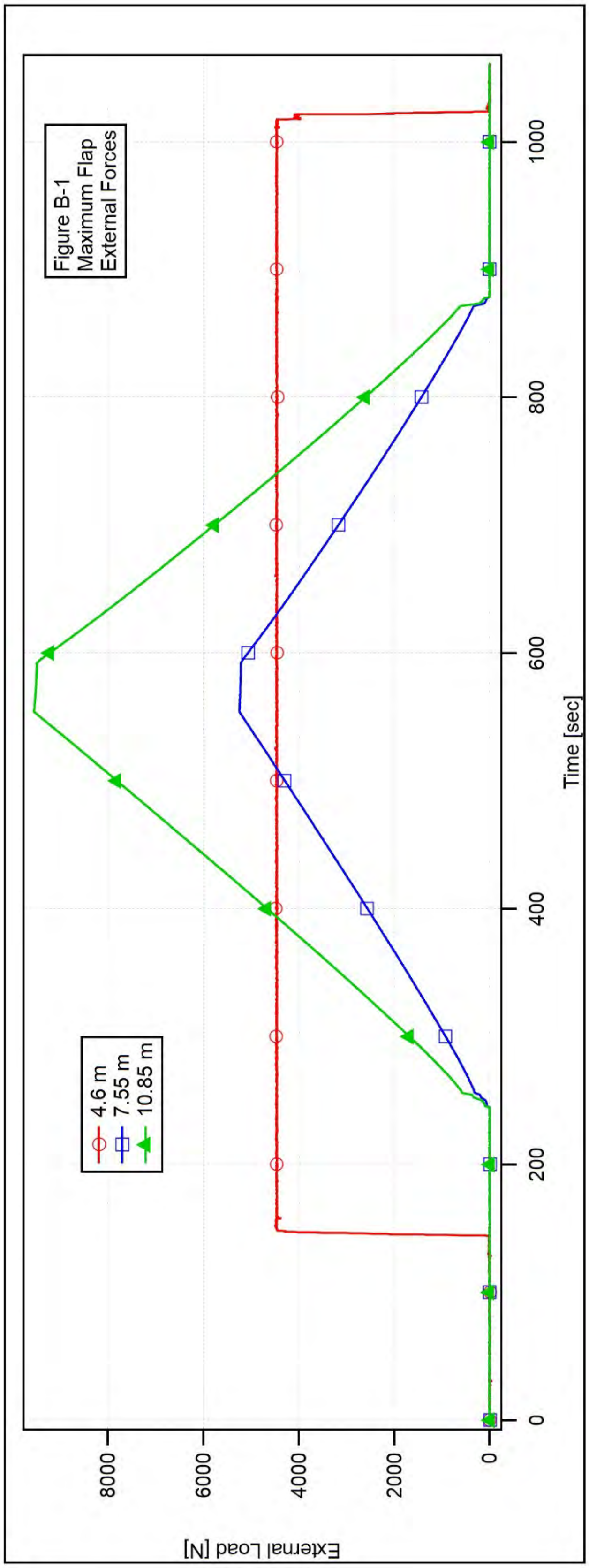

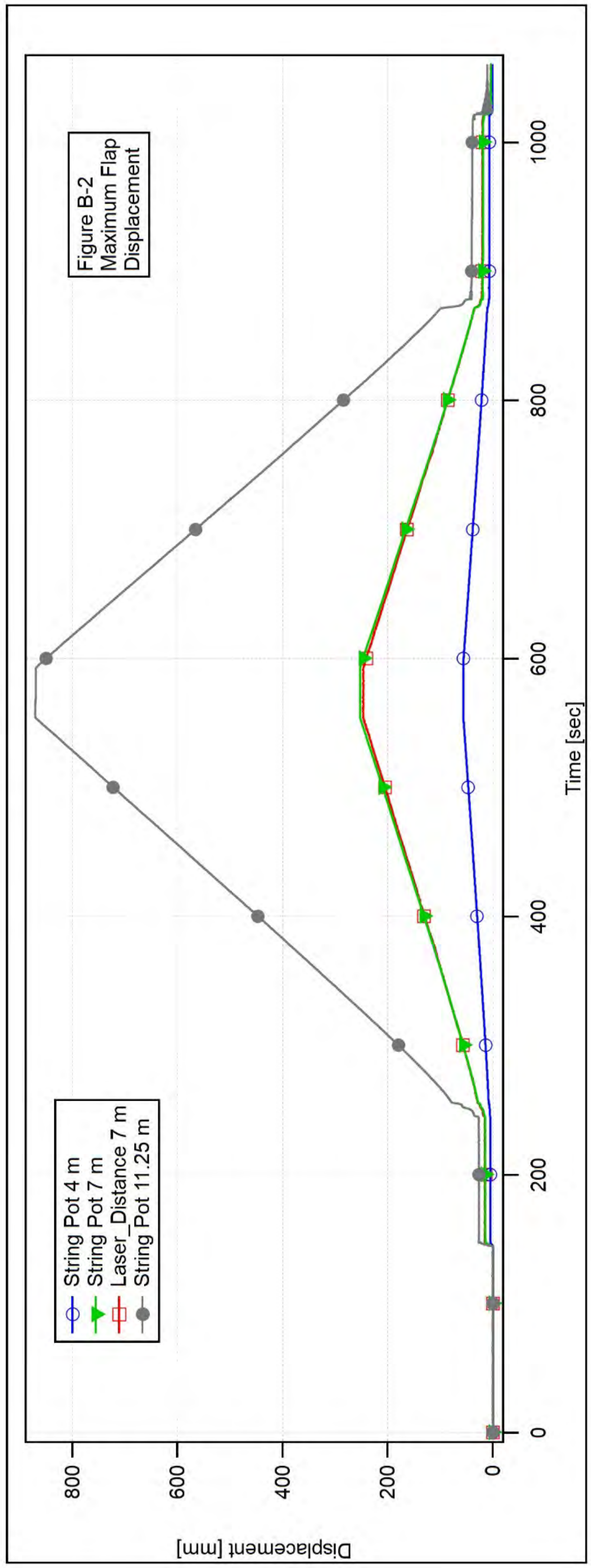

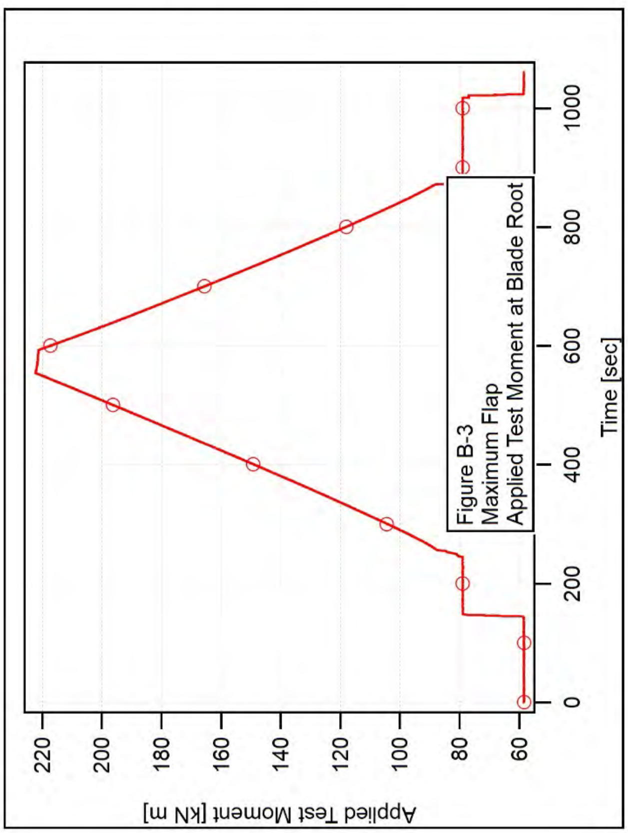
Figure B-3
Maximum Flap
Applied Test Moment at Blade Root
Applied Test Moment [kN m]
Time [sec]

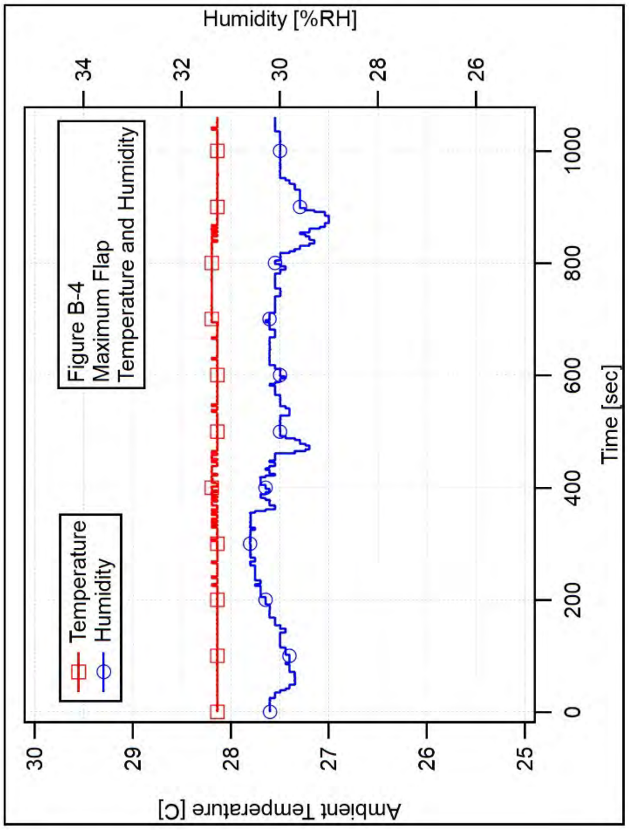
Figure B-4
Maximum Flap
Temperature and Humidity
Temperature
Humidity
Ambient Temperature [C]
Humidity [%RH]
Time [sec]

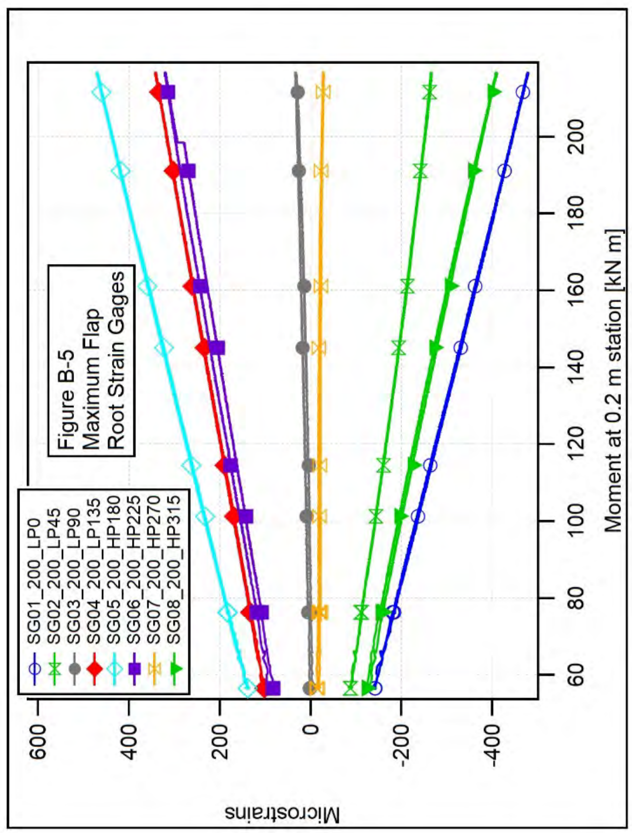
Figure B-5
Maximum Flap
Root Strain Gages
SG01_200_LP0
SG02_200_LP45
SG03_200_LP90
SG04_200_LP135
SG05_200_HP180
SG06_200_HP225
SG07_200_HP270
SG08_200_HP315
Microstrains
Moment at 0.2 m station [kN m]

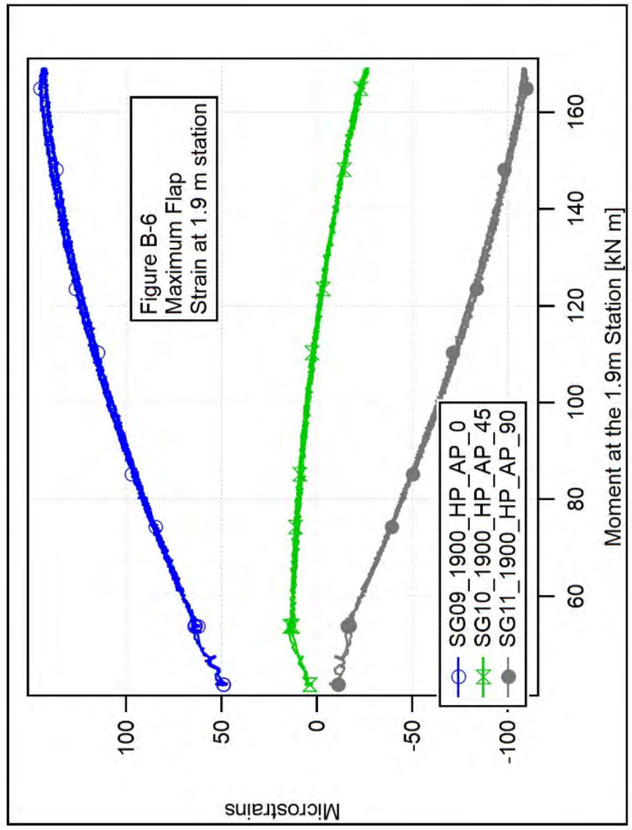
Figure B-6
Maximum Flap
Strain at 1.9 m station
SG09_1900_HP_AP_0
SG10_1900_HP_AP_45
SG11_1900_HP_AP_90
Microstrains
Moment at the 1.9m Station [kN m]

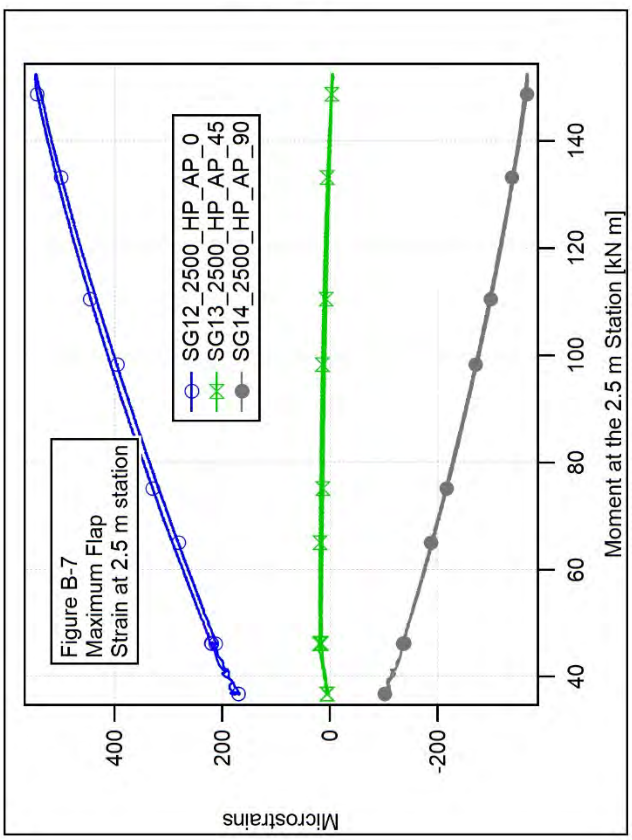
Figure B-7
Maximum Flap
Strain at 2.5 m station
SG12_2500_HP_AP_0
SG13_2500_HP_AP_45
SG14_2500_HP_AP_90
Microstrains
Moment at the 2.5 m Station [kN m]

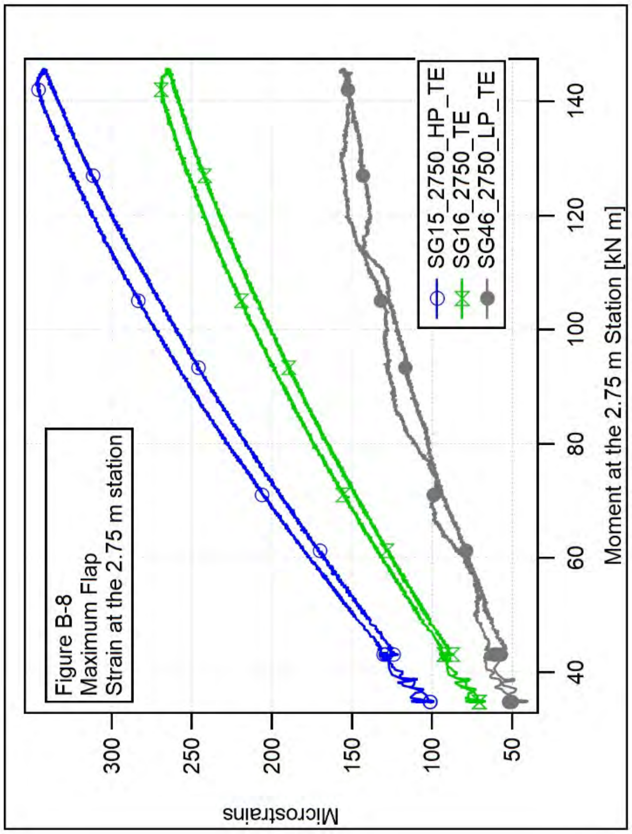
Figure B-8
Maximum Flap
Strain at the 2.75 m station
SG15_2750_HP_TE
SG16_2750_TE
SG46_2750_LP_TE
Microstrains
Moment at the 2.75 m Station [kN m]

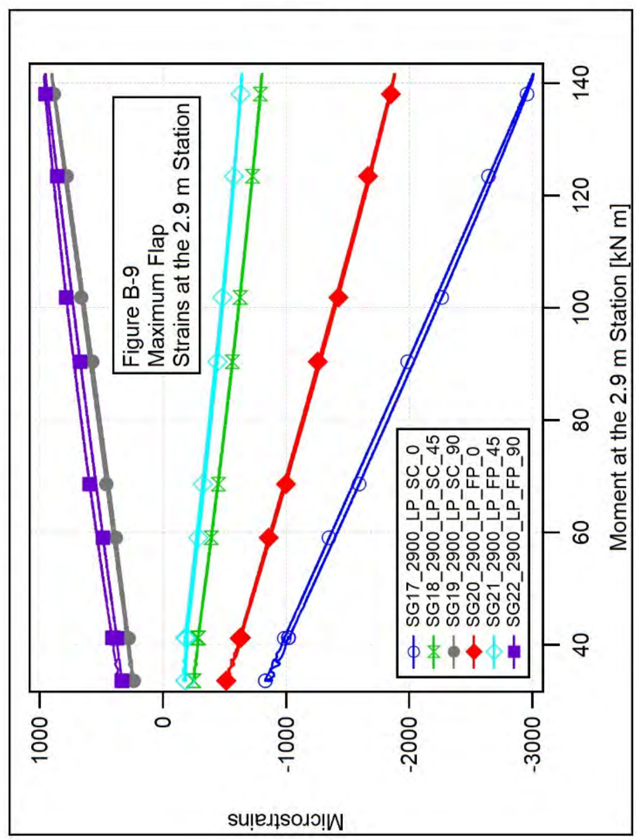
Figure B-9
Maximum Flap
Strains at the 2.9 m Station
SG17_2900_LP_SC_0
SG18_2900_LP_SC_45
SG19_2900_LP_SC_90
SG20_2900_LP_FP_0
SG21_2900_LP_FP_45
SG22_2900_LP_FP_90
Microstrains
Moment at the 2.9 m Station [kN m]

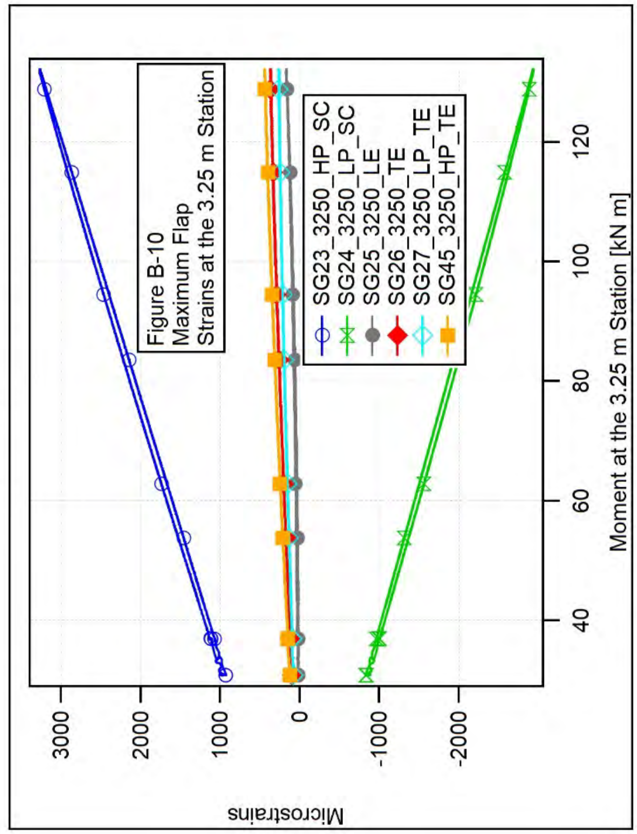
Figure B-10
Maximum Flap
Strains at the 3.25 m Station
SG23_3250_HP_SC
SG24_3250_LP_SC
SG25_3250_LE
SG26_3250_TE
SG27_3250_LP_TE
SG45_3250_HP_TE
Microstrains
Moment at the 3.25 m Station [kN m]

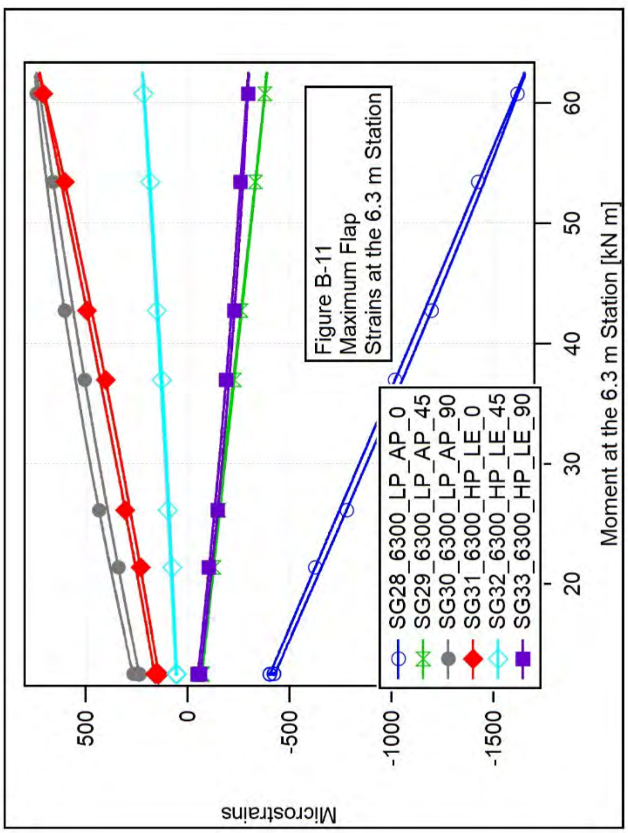
Figure B-11
Maximum Flap
Strains at the 6.3 m Station
SG28_6300_LP_AP_0
SG29_6300_LP_AP_45
SG30_6300_LP_AP_90
SG31_6300_HP_LE_0
SG32_6300_HP_LE_45
SG33_6300_HP_LE_90
Microstrains
Moment at the 6.3 m Station [kN m]

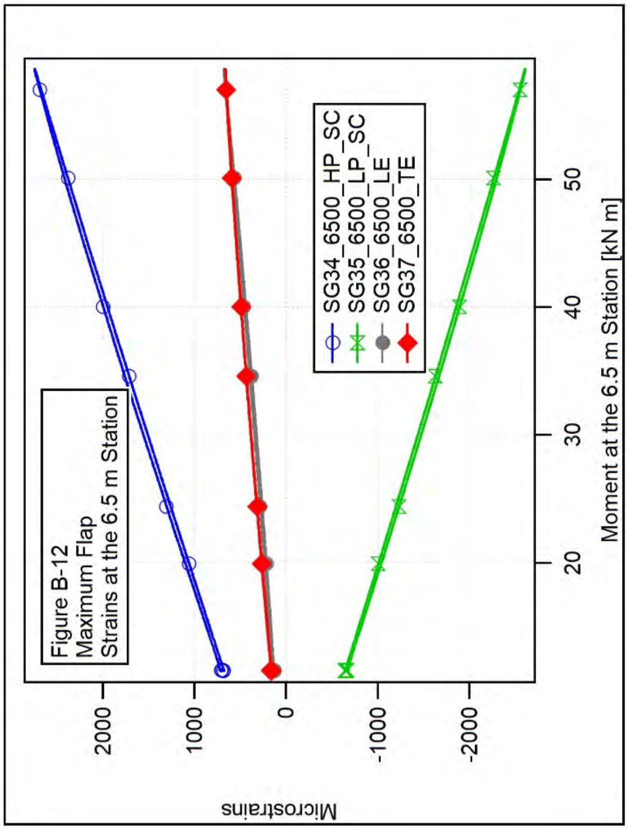
Figure B-12
Maximum Flap
Strains at the 6.5 m Station
SG34_6500_HP_SC
SG35_6500_LP_SC
SG36_6500_LE
SG37_6500_TE
Microstrains
Moment at the 6.5 m Station [kN m]

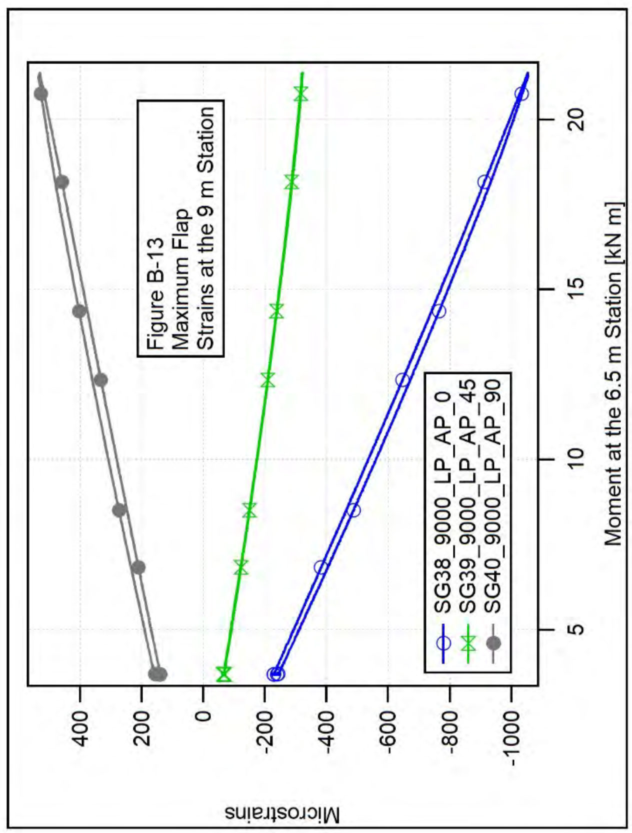
Figure B-13
Maximum Flap
Strains at the 9 m Station
SG38_9000_LP_AP_0
SG39_9000_LP_AP_45
SG40_9000_LP_AP_90
Microstrains
Moment at the 6.5 m Station [kN m]

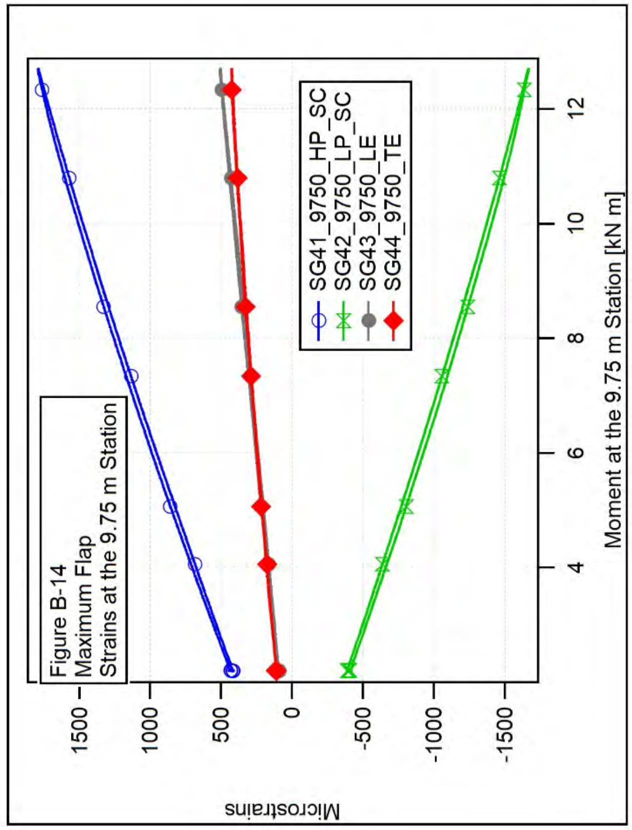
Figure B-14
Maximum Flap
Strains at the 9.75 m Station
SG41_9750_HP_SC
SG42_9750_LP_SC
SG43_9750_LE
SG44_9750_TE
Microstrains
Moment at the 9.75 m Station [kN m]

APPENDIX C – Minimum Flap Charts

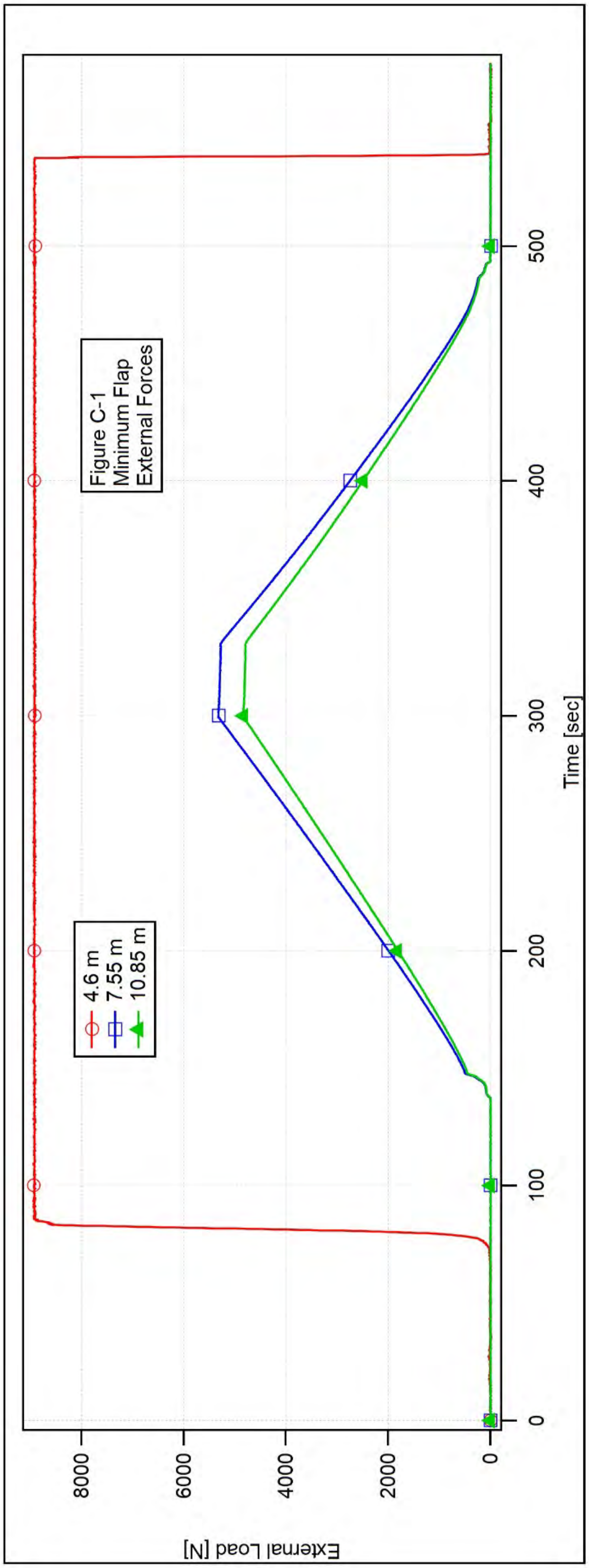

Figure C-1
Minimum Flap
External Forces

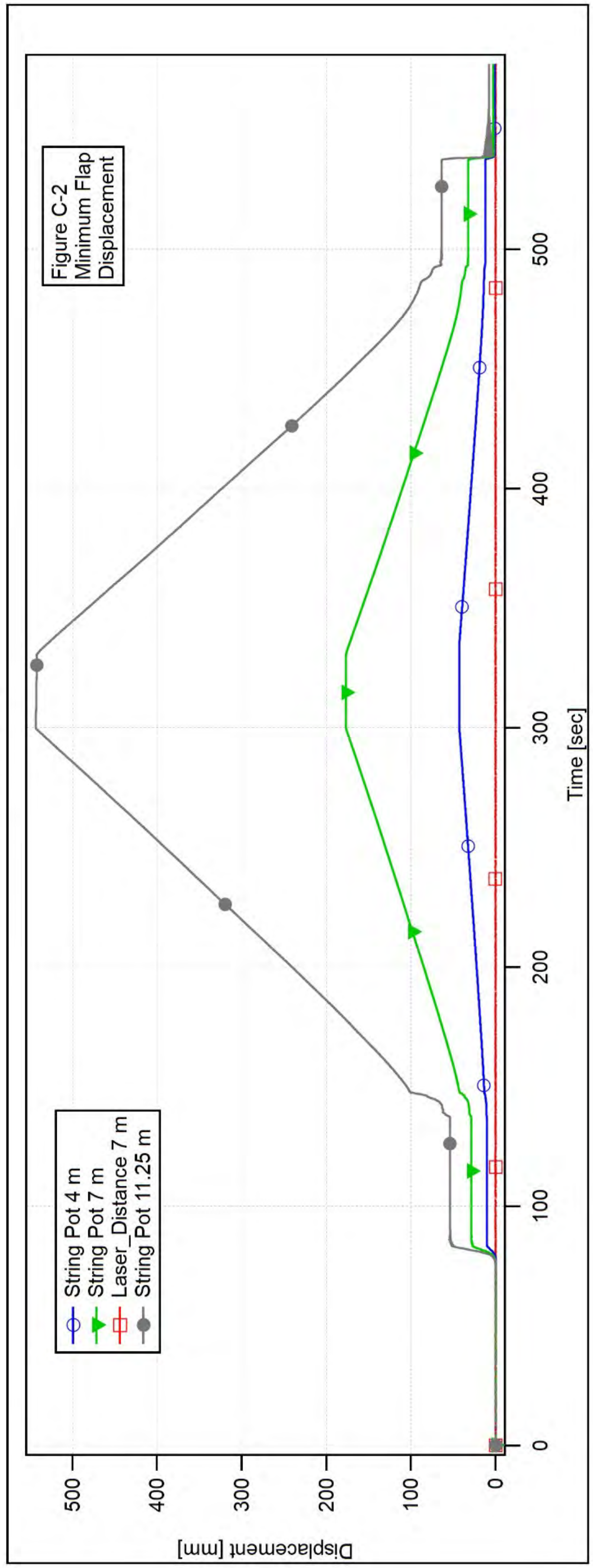

Figure C-2
Minimum Flap
Displacement

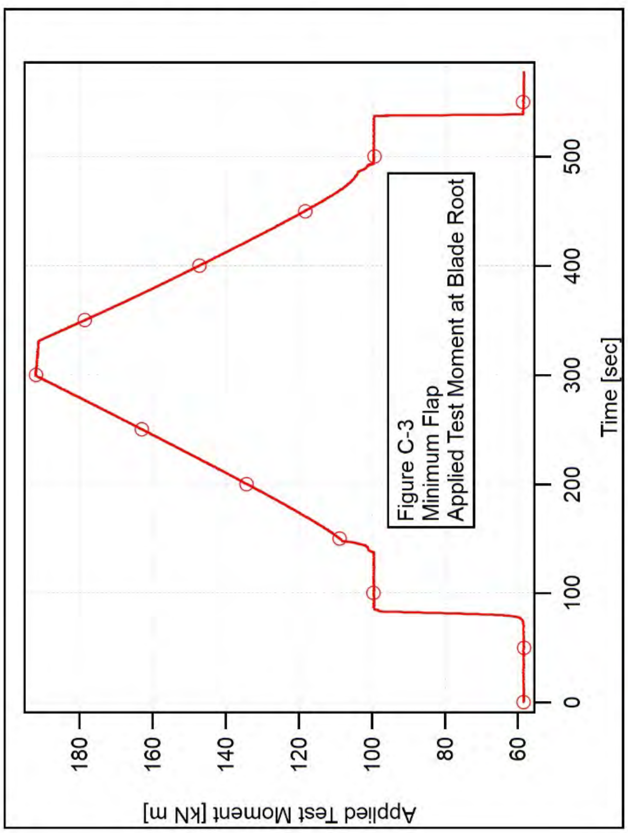

Figure C-3
Minimum Flap
Applied Test Moment at Blade Root

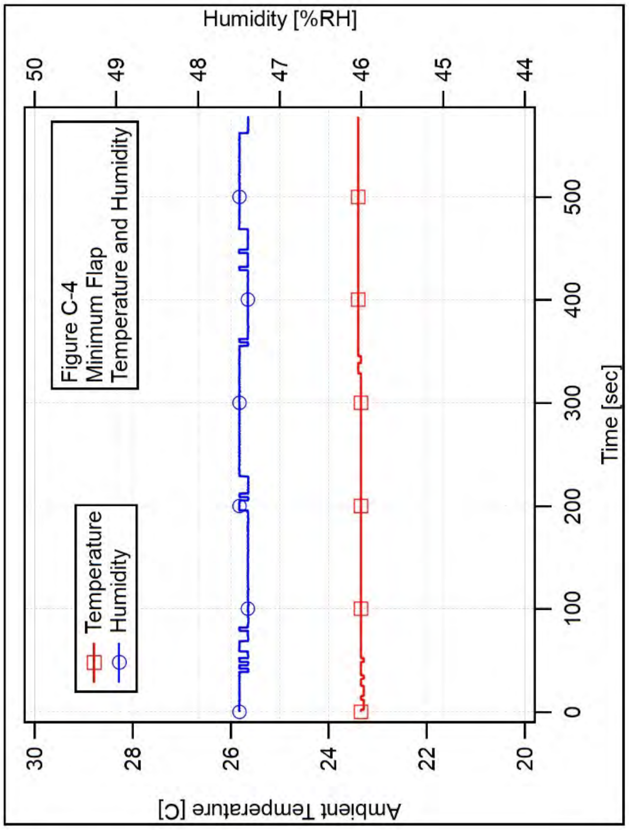

Figure C-4
Minimum Flap
Temperature and Humidity

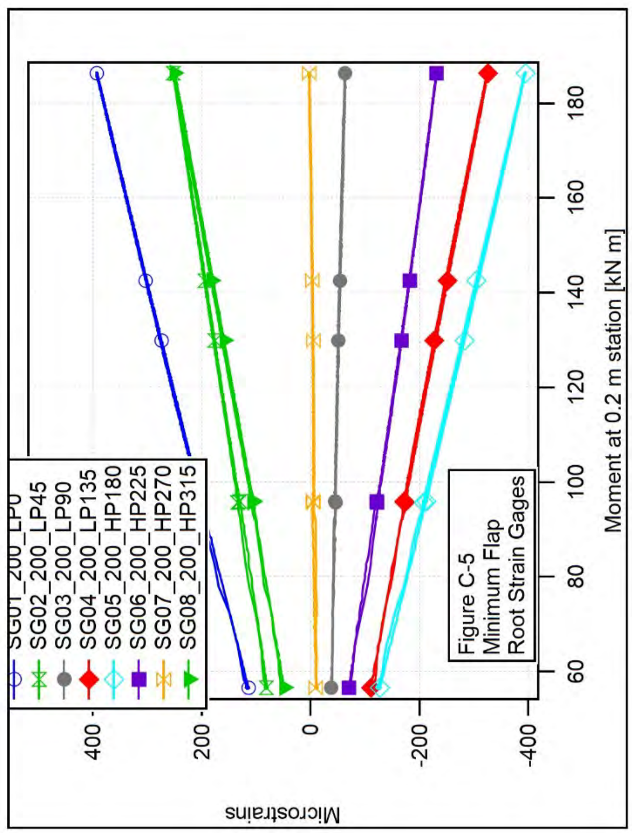

Figure C-5
Minimum Flap
Root Strain Gages

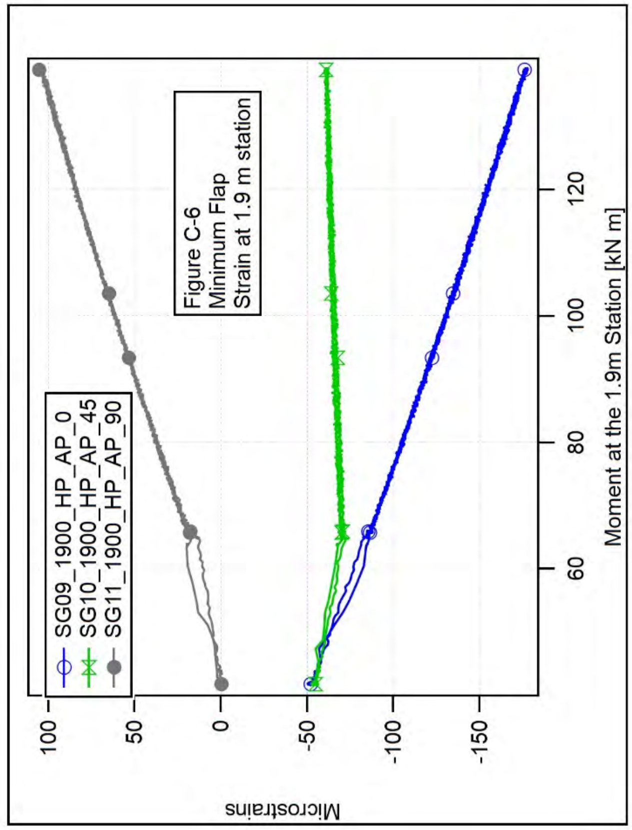

Figure C-6
Minimum Flap
Strain at 1.9 m station

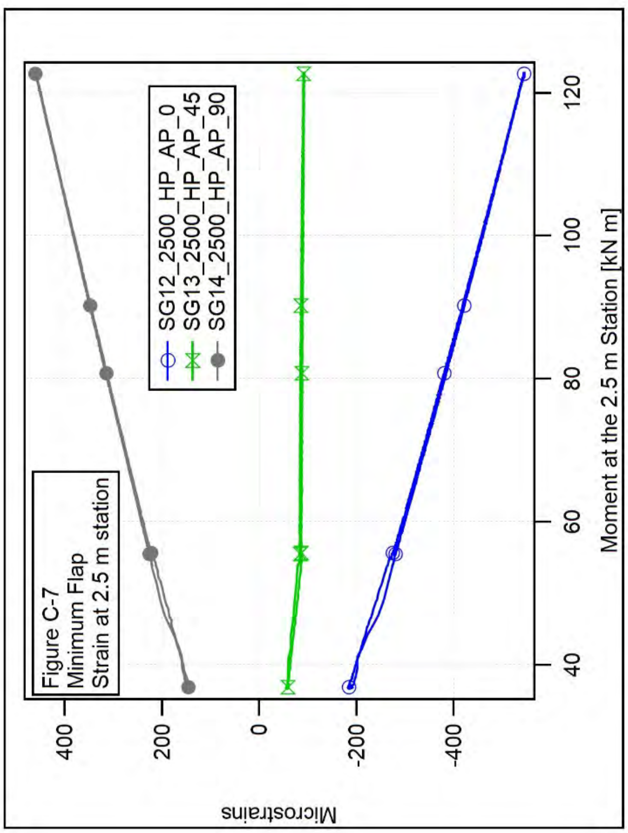
Figure C-7
Minimum Flap
Strain at 2.5 m station
SG12_2500_HP_AP_0
SG13_2500_HP_AP_45
SG14_2500_HP_AP_90
Microstrains
Moment at the 2.5 m Station [kN m]
400
200
0
-200
-400
40
60
80
100
120

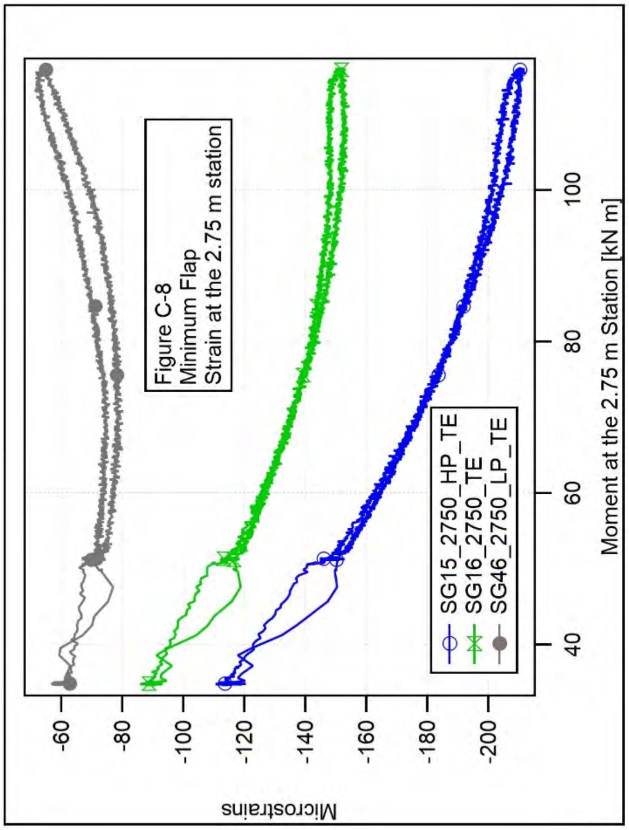
Figure C-8
Minimum Flap
Strain at the 2.75 m station
SG15_2750_HP_TE
SG16_2750_TE
SG46_2750_LP_TE
Microstrains
Moment at the 2.75 m Station [kN m]
-60
-80
-100
-120
-140
-160
-180
-200
40
60
80
100

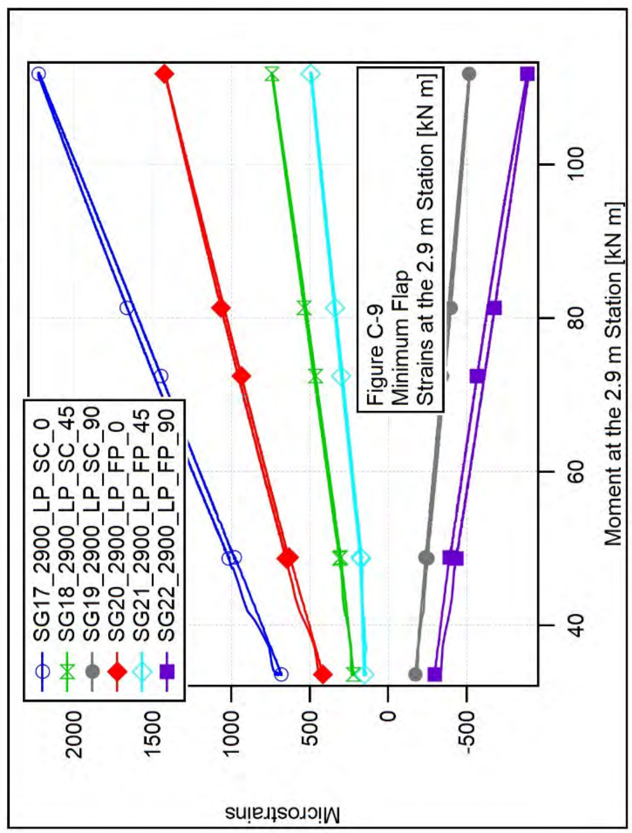
Figure C-9
Minimum Flap
Strains at the 2.9 m Station [kN m]
SG17_2900_LP_SC_0
SG18_2900_LP_SC_45
SG19_2900_LP_SC_90
SG20_2900_LP_FP_0
SG21_2900_LP_FP_45
SG22_2900_LP_FP_90
Microstrains
Moment at the 2.9 m Station [kN m]
2000
1500
1000
500
0
-500
40
60
80
100

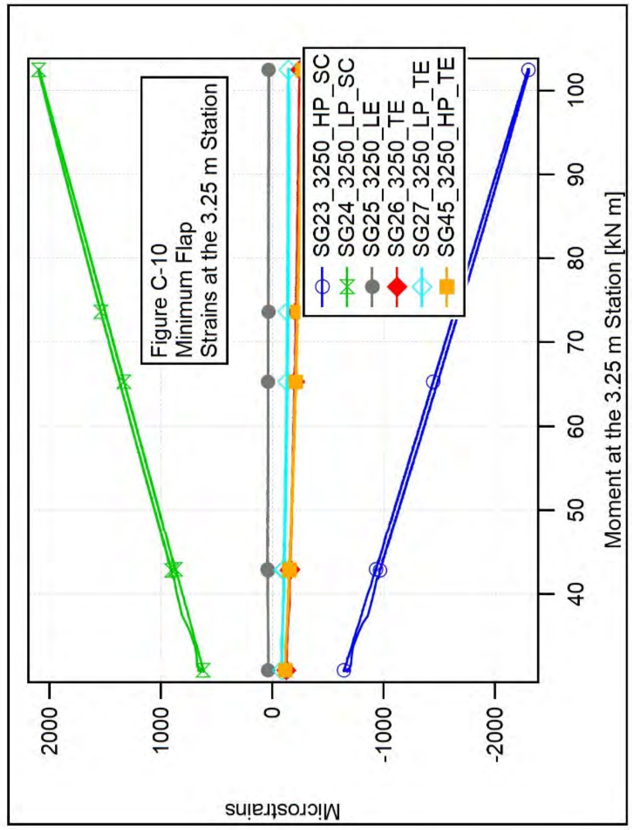
Figure C-10
Minimum Flap
Strains at the 3.25 m Station
SG23_3250_HP_SC
SG24_3250_LP_SC
SG25_3250_LE
SG26_3250_TE
SG27_3250_LP_TE
SG45_3250_HP_TE
Microstrains
Moment at the 3.25 m Station [kN m]
2000
1000
0
-1000
-2000
40
50
60
70
80
90
100

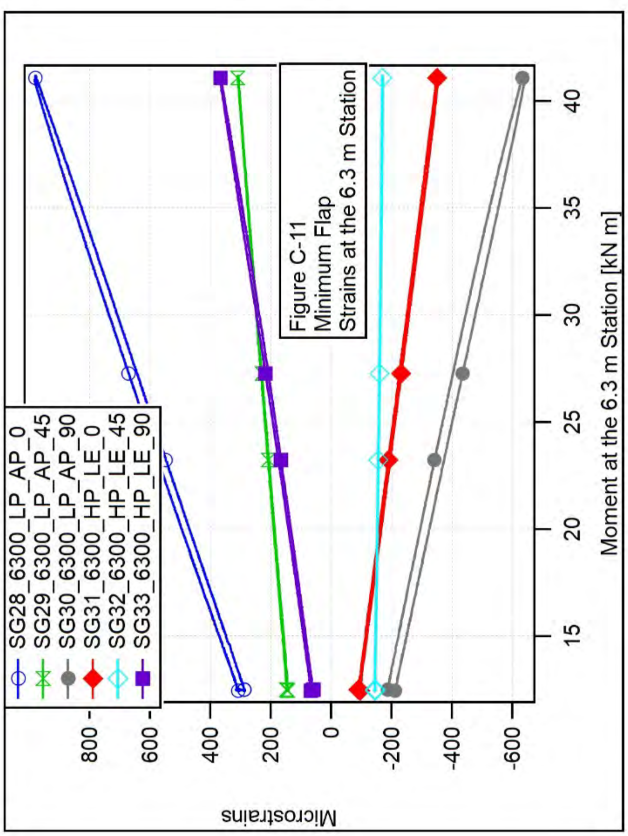

Figure C-11
Minimum Flap
Strains at the 6.3 m Station

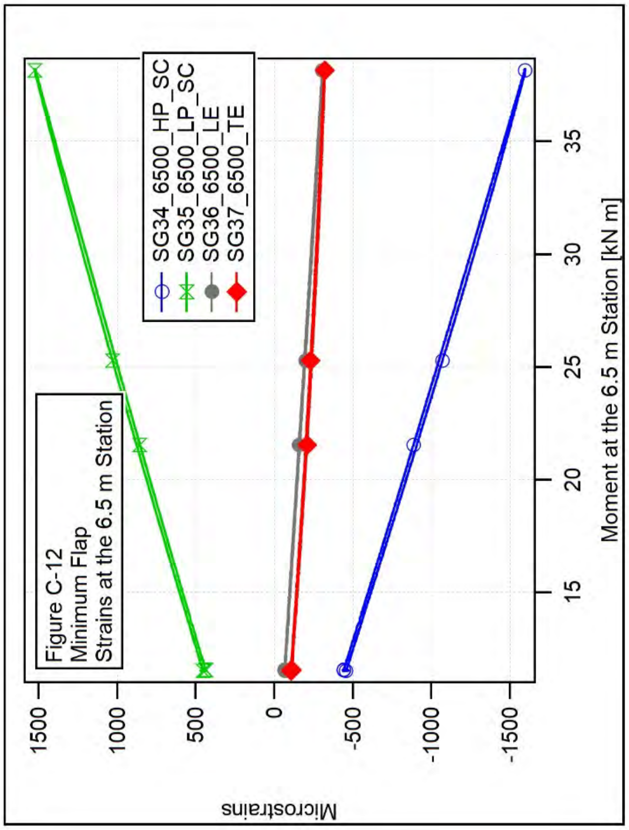

Figure C-12
Minimum Flap
Strains at the 6.5 m Station

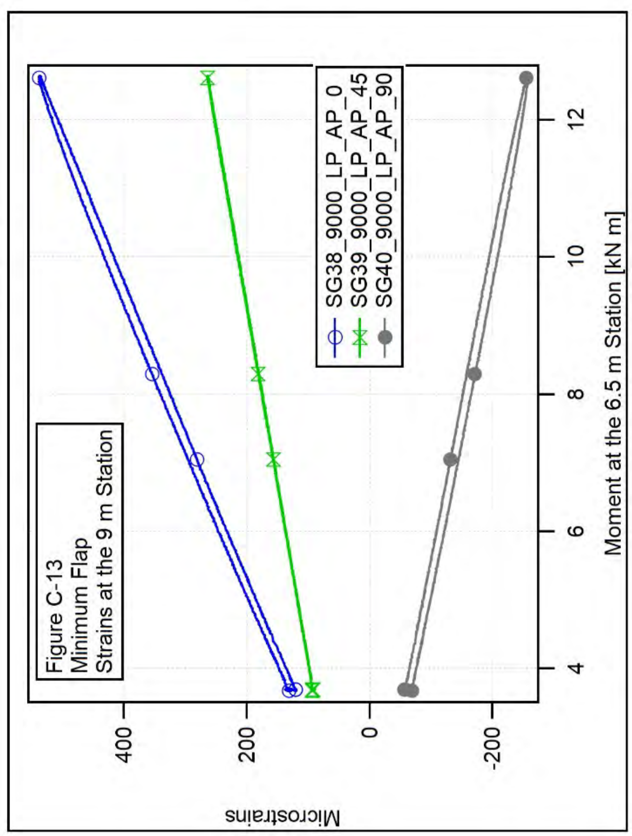

Figure C-13
Minimum Flap
Strains at the 9 m Station

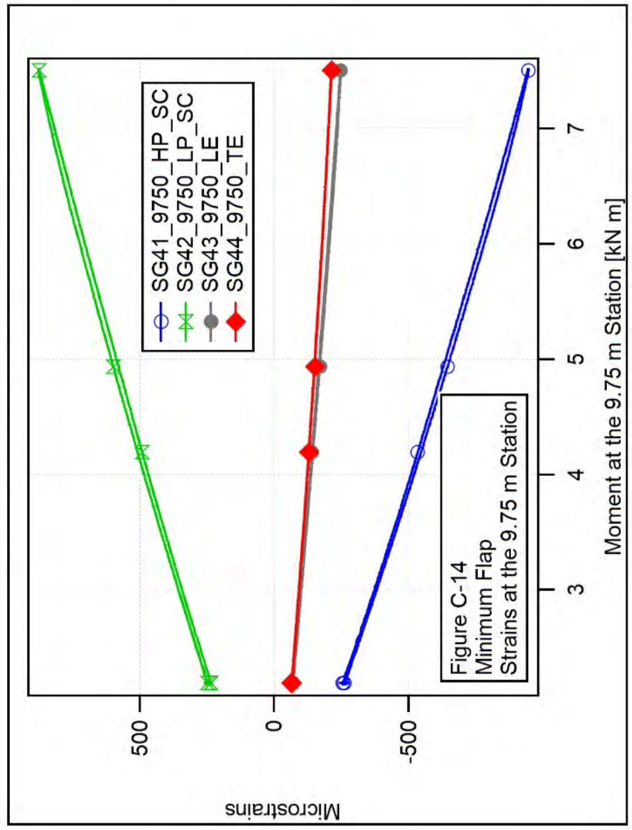

Figure C-14
Minimum Flap
Strains at the 9.75 m Station

APPENDIX D – Maximum Edge Charts

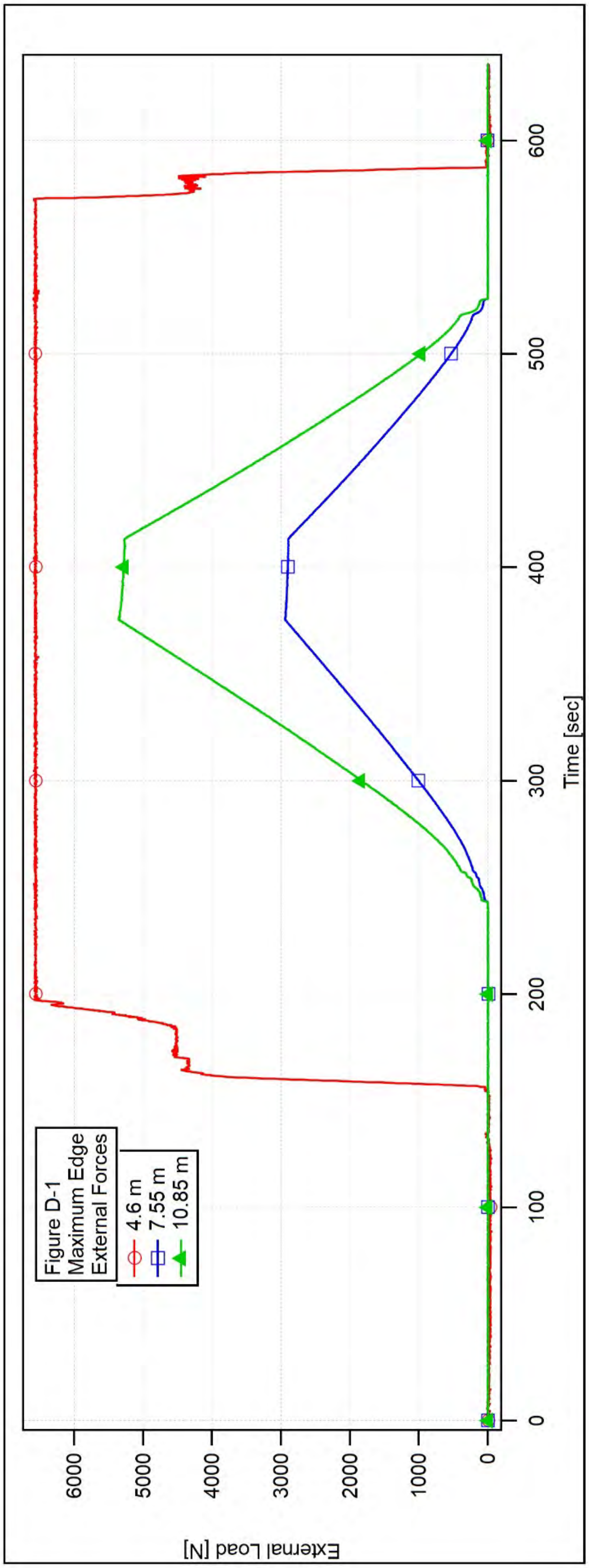

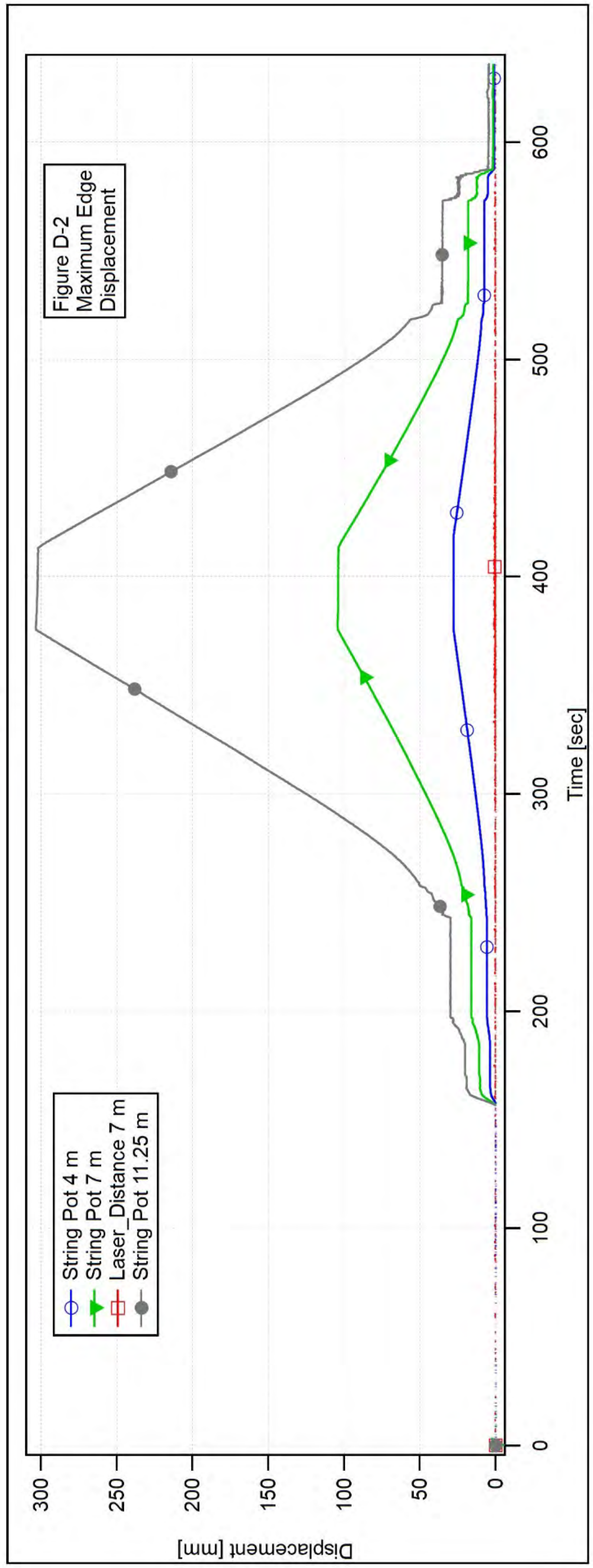

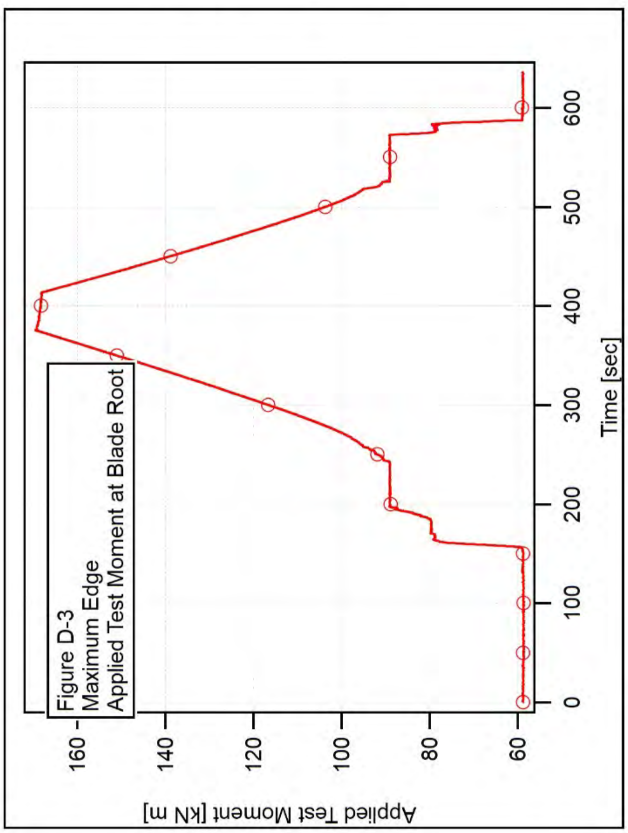
Figure D-3
Maximum Edge
Applied Test Moment at Blade Root
Applied Test Moment [kN m]
Time [sec]

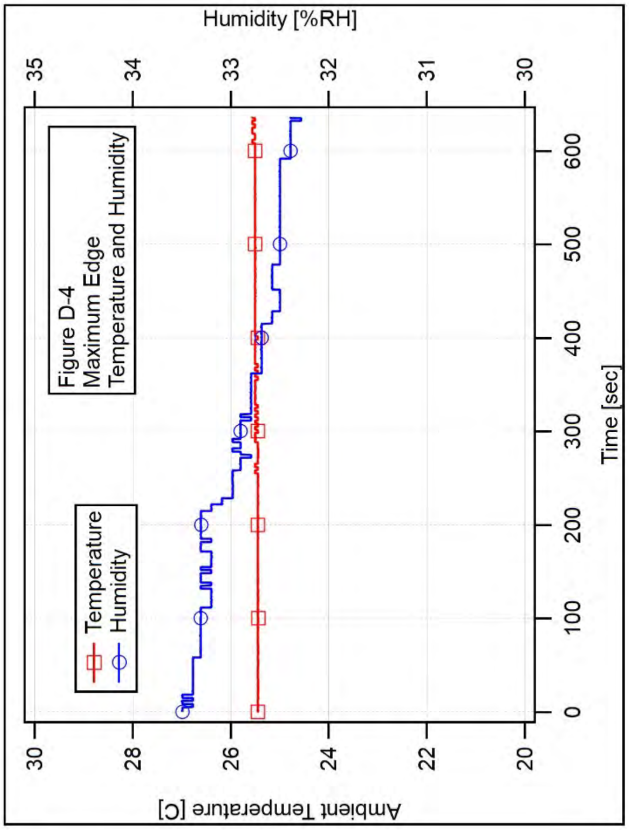
Figure D-4
Maximum Edge
Temperature and Humidity
Temperature
Humidity
Ambient Temperature [C]
Humidity [%RH]
Time [sec]

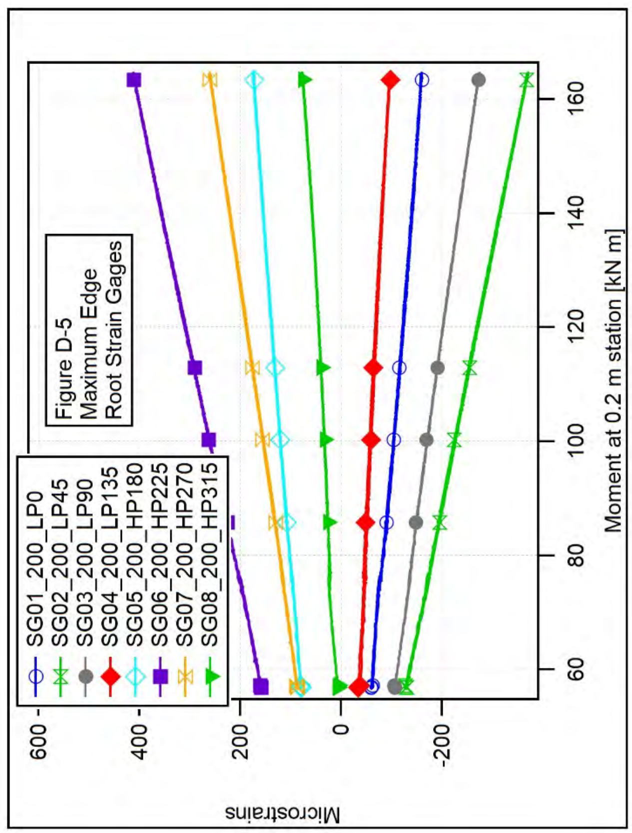
Figure D-5
Maximum Edge
Root Strain Gages
SG01_200_LP0
SG02_200_LP45
SG03_200_LP90
SG04_200_LP135
SG05_200_HP180
SG06_200_HP225
SG07_200_HP270
SG08_200_HP315
Microstrains
Moment at 0.2 m station [kN m]

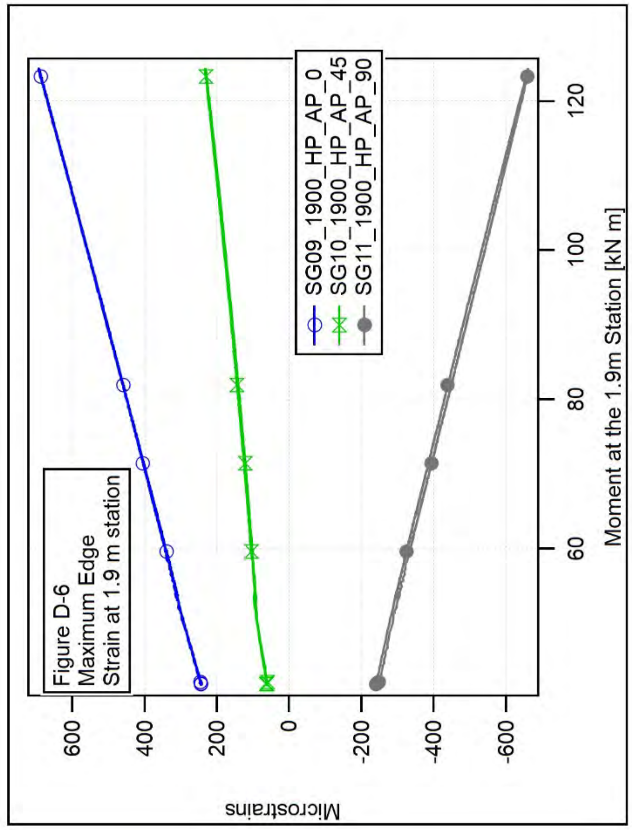
Figure D-6
Maximum Edge
Strain at 1.9 m station
SG09_1900_HP_AP_0
SG10_1900_HP_AP_45
SG11_1900_HP_AP_90
Microstrains
Moment at the 1.9m Station [kN m]

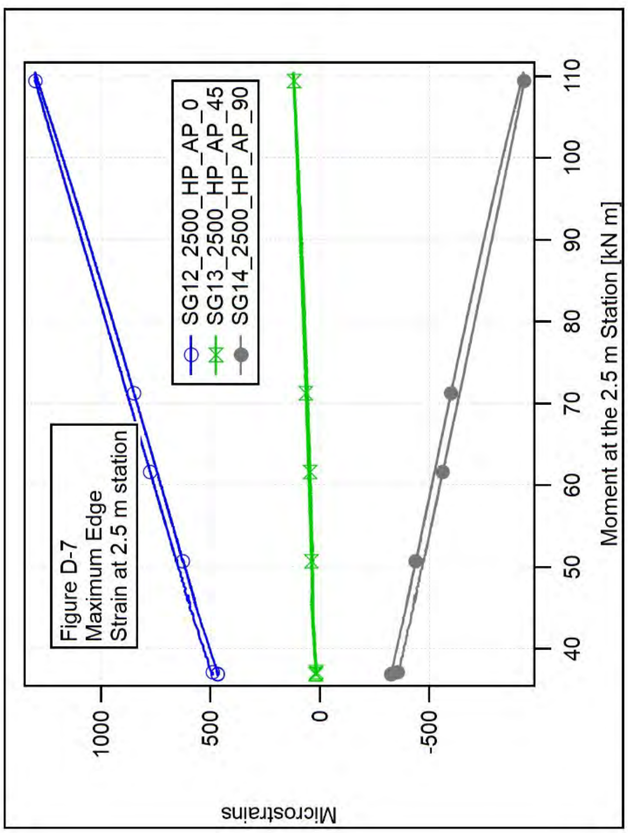
Figure D-7
Maximum Edge
Strain at 2.5 m station
SG12_2500_HP_AP_0
SG13_2500_HP_AP_45
SG14_2500_HP_AP_90
Microstrains
Moment at the 2.5 m Station [kN m]

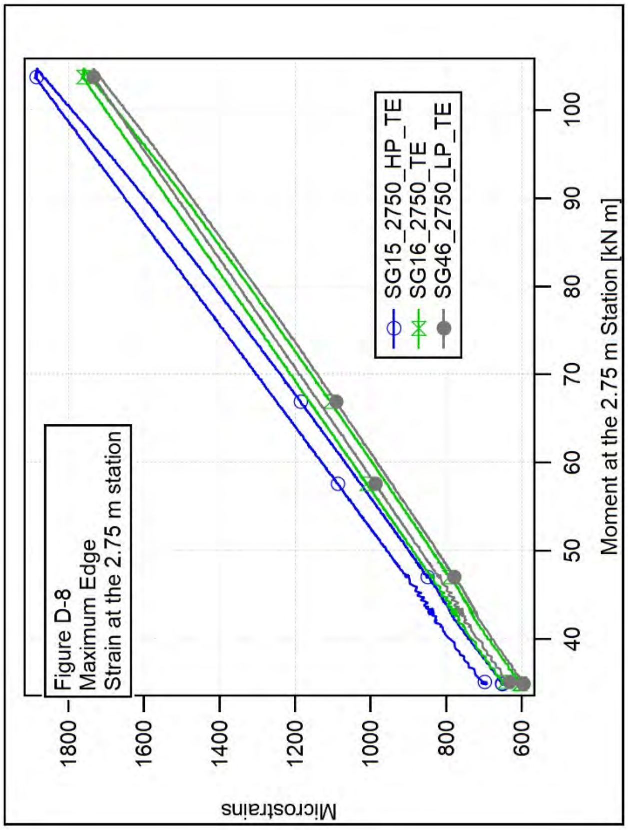
Figure D-8
Maximum Edge
Strain at the 2.75 m station
SG15_2750_HP_TE
SG16_2750_TE
SG46_2750_LP_TE
Microstrains
Moment at the 2.75 m Station [kN m]

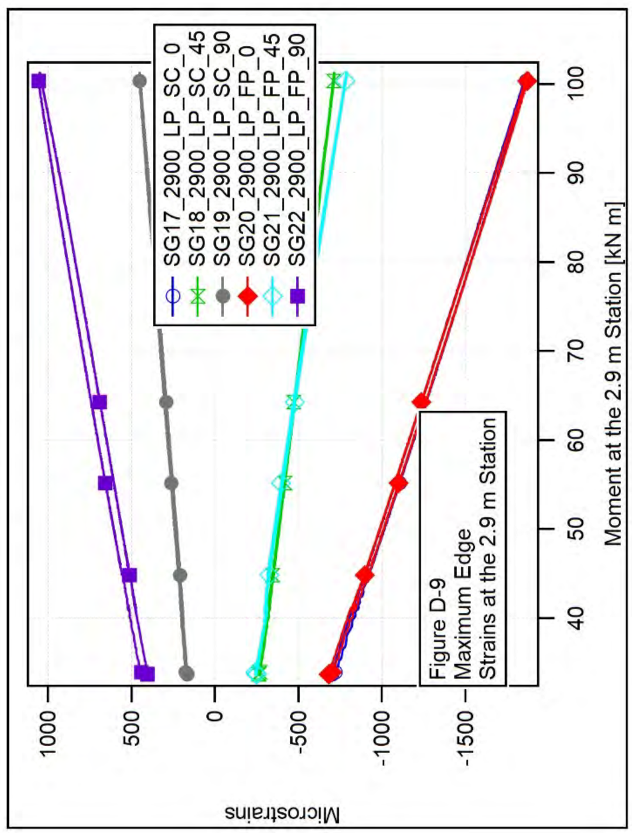
Figure D-9
Maximum Edge
Strains at the 2.9 m Station
SG17_2900_LP_SC_0
SG18_2900_LP_SC_45
SG19_2900_LP_SC_90
SG20_2900_LP_FP_0
SG21_2900_LP_FP_45
SG22_2900_LP_FP_90
Microstrains
Moment at the 2.9 m Station [kN m]

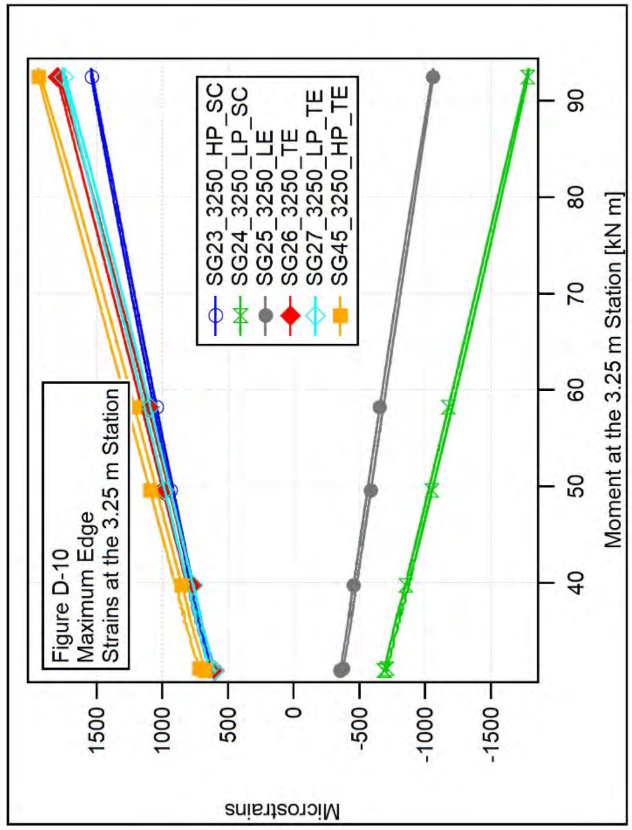
Figure D-10
Maximum Edge
Strains at the 3.25 m Station
SG23_3250_HP_SC
SG24_3250_LP_SC
SG25_3250_LE
SG26_3250_TE
SG27_3250_LP_TE
SG45_3250_HP_TE
Microstrains
Moment at the 3.25 m Station [kN m]

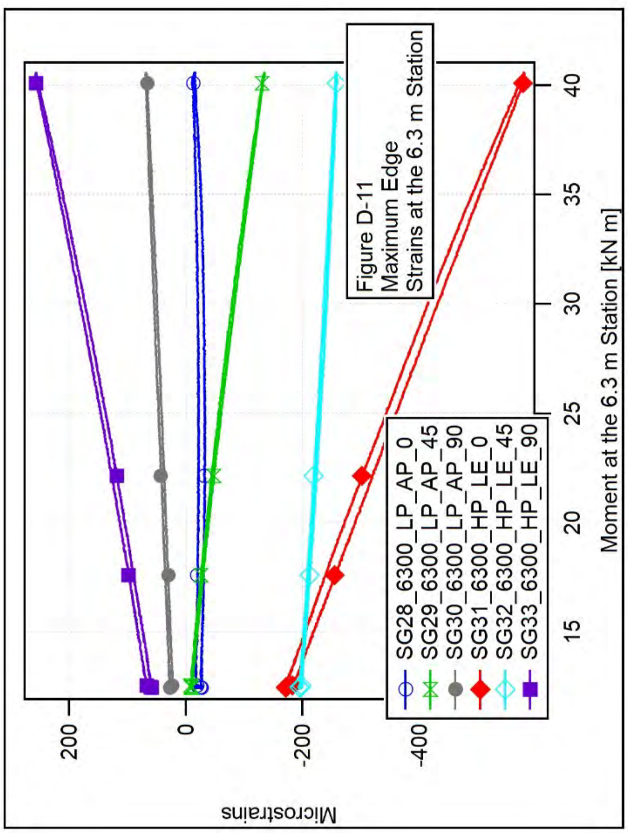
Figure D-11
Maximum Edge
Strains at the 6.3 m Station
SG28_6300_LP_AP_0
SG29_6300_LP_AP_45
SG30_6300_LP_AP_90
SG31_6300_HP_LE_0
SG32_6300_HP_LE_45
SG33_6300_HP_LE_90
Microstrains
Moment at the 6.3 m Station [kN m]

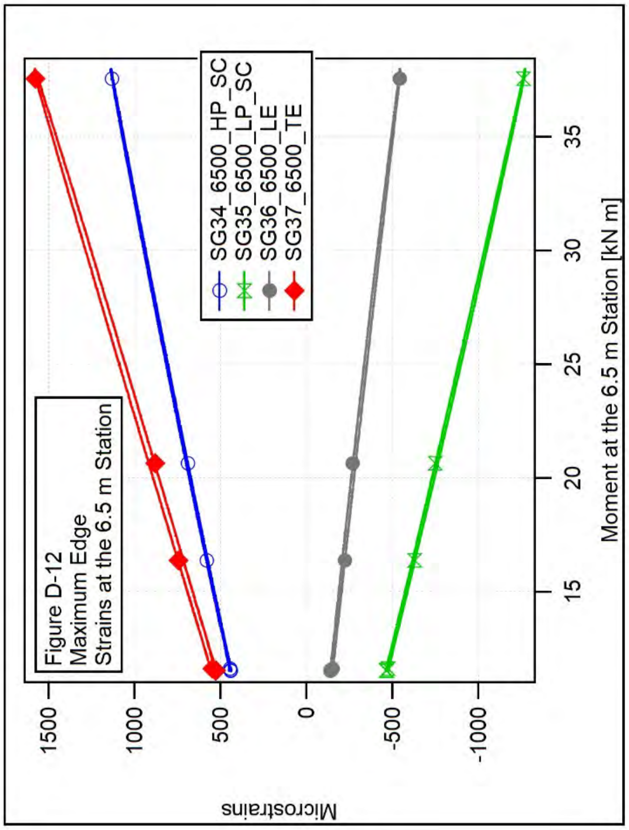
Figure D-12
Maximum Edge
Strains at the 6.5 m Station
SG34_6500_HP_SC
SG35_6500_LP_SC
SG36_6500_LE
SG37_6500_TE
Microstrains
Moment at the 6.5 m Station [kN m]

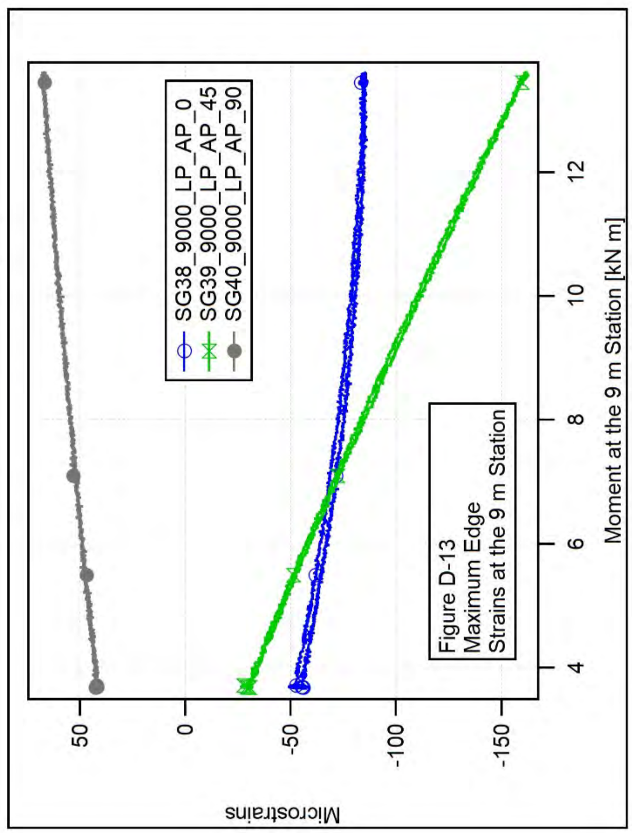
Figure D-13
Maximum Edge
Strains at the 9 m Station
SG38_9000_LP_AP_0
SG39_9000_LP_AP_45
SG40_9000_LP_AP_90
Microstrains
Moment at the 9 m Station [kN m]

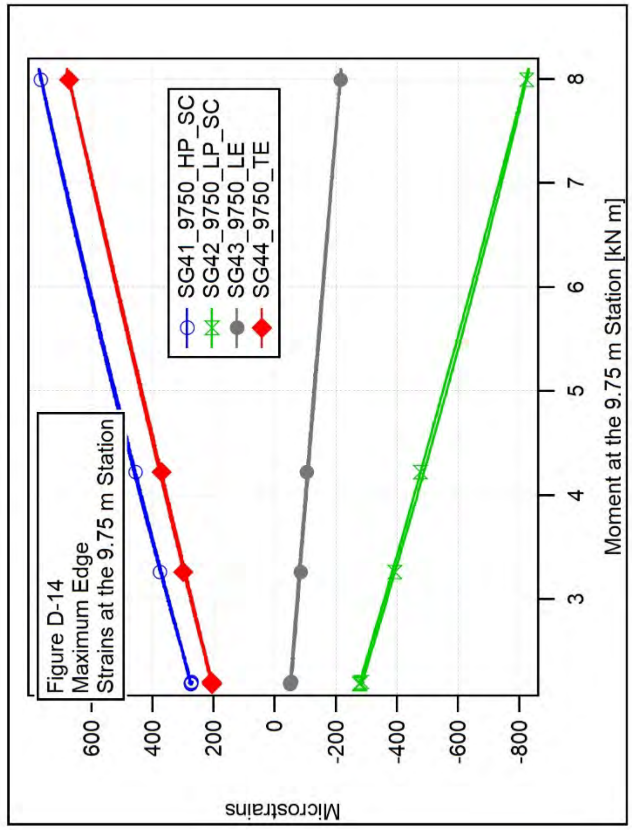
Figure D-14
Maximum Edge
Strains at the 9.75 m Station
SG41_9750_HP_SC
SG42_9750_LP_SC
SG43_9750_LE
SG44_9750_TE
Microstrains
Moment at the 9.75 m Station [kN m]

APPENDIX E – Minimum Edge Charts

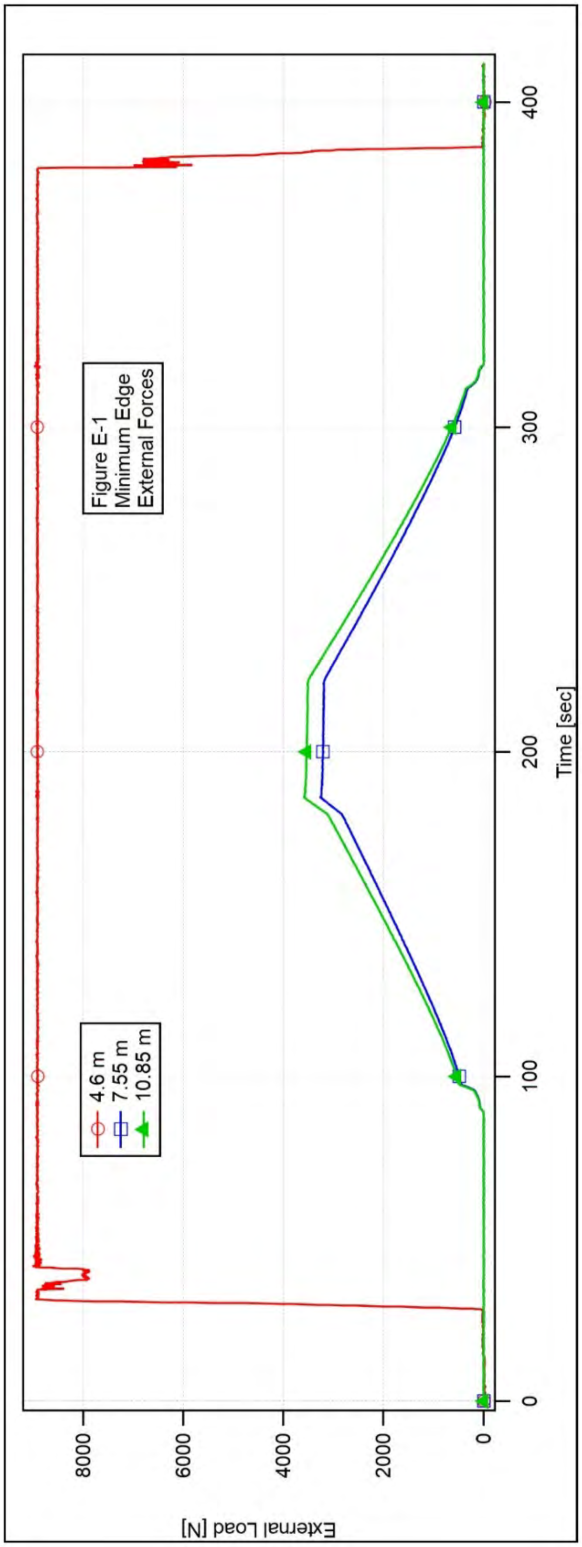

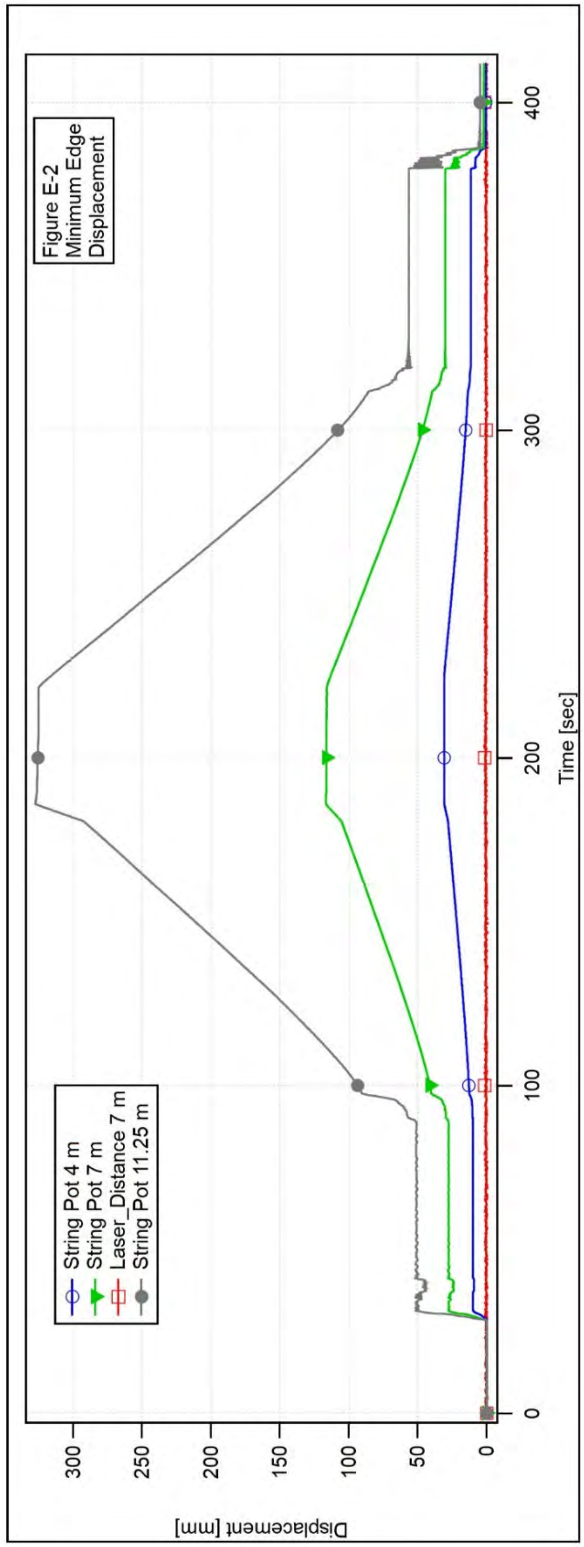

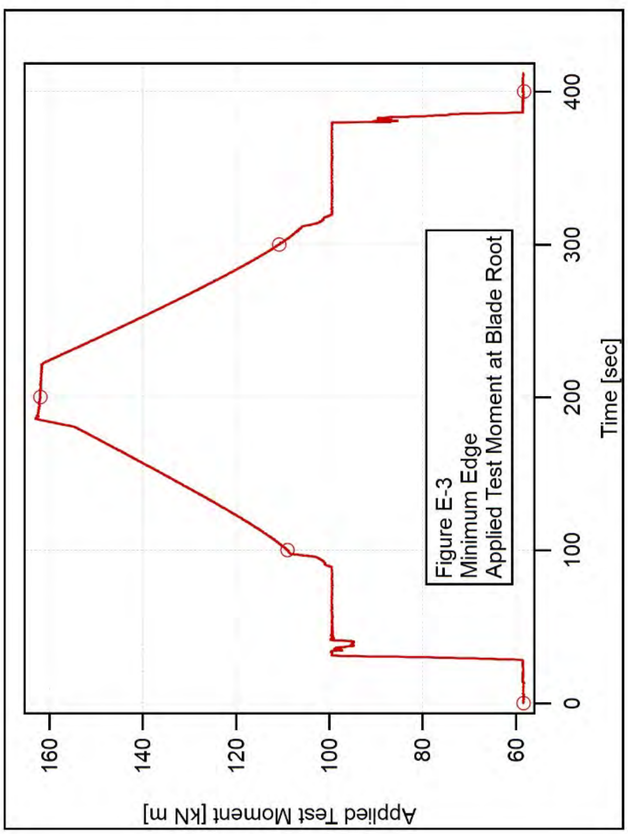
Figure E-3
Minimum Edge
Applied Test Moment at Blade Root
Applied Test Moment [kN m]
Time [sec]
60
80
100
120
140
160
0
100
200
300
400

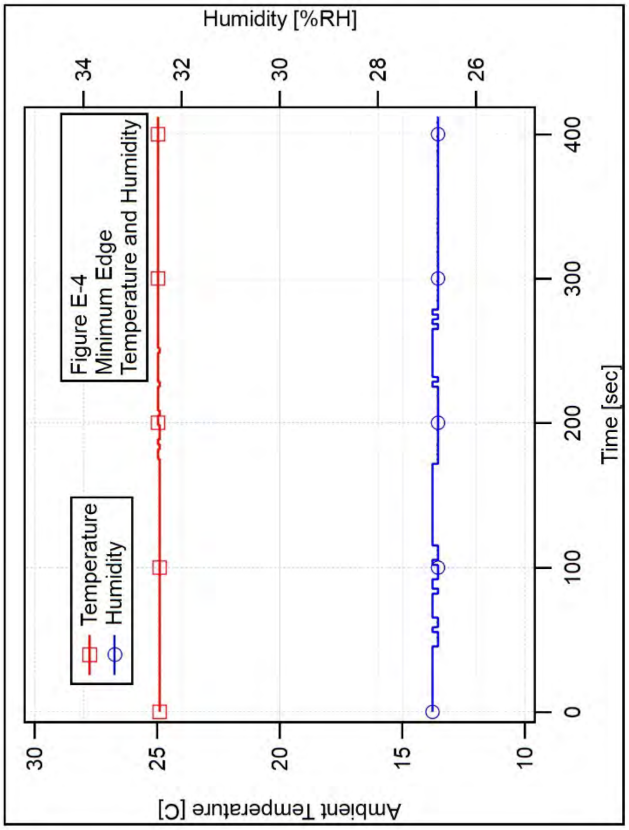
Figure E-4
Minimum Edge
Temperature and Humidity
Temperature
Humidity
Ambient Temperature [C]
Humidity [%RH]
Time [sec]
10
15
20
25
30
26
28
30
32
34
0
100
200
300
400

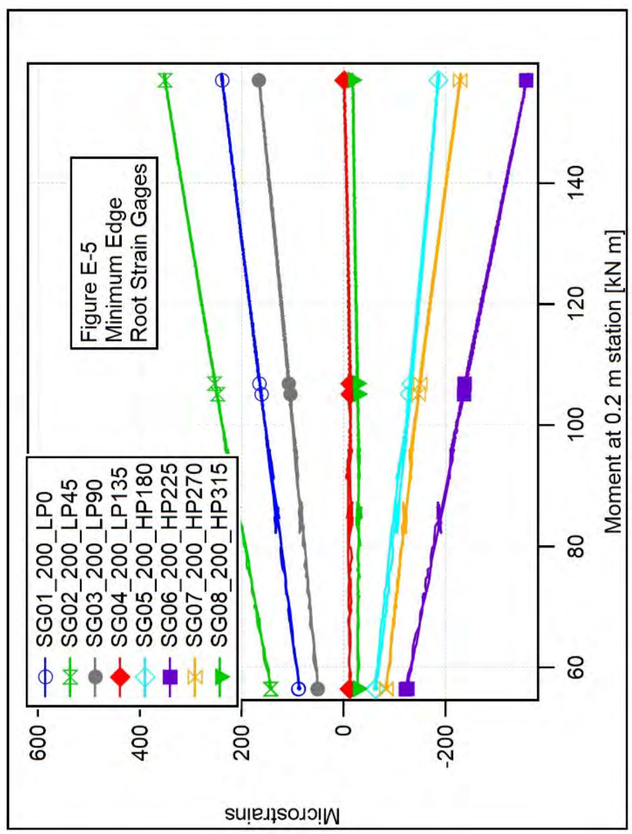
Figure E-5
Minimum Edge
Root Strain Gages
SG01_200_LP0
SG02_200_LP45
SG03_200_LP90
SG04_200_LP135
SG05_200_HP180
SG06_200_HP225
SG07_200_HP270
SG08_200_HP315
Microstrains
Moment at 0.2 m station [kN m]
-200
0
200
400
600
60
80
100
120
140

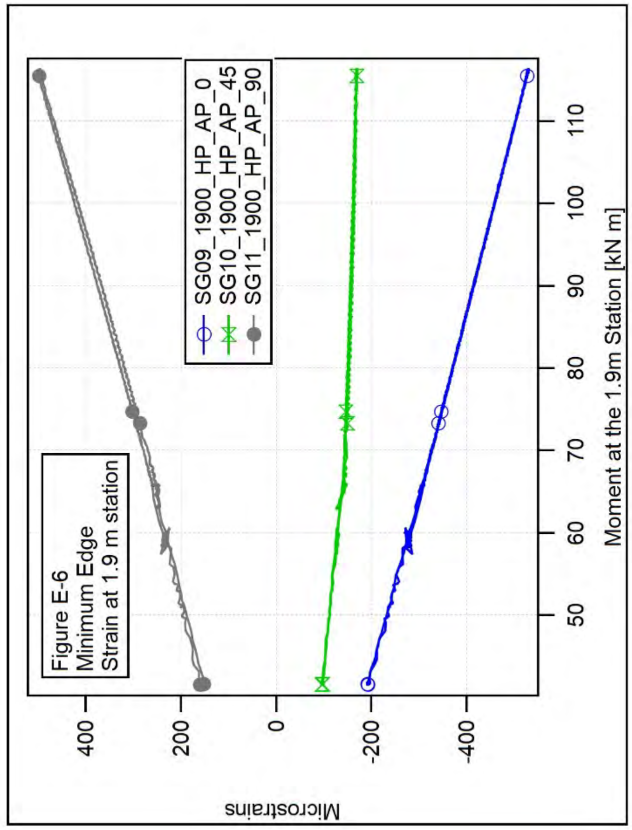
Figure E-6
Minimum Edge
Strain at 1.9 m station
SG09_1900_HP_AP_0
SG10_1900_HP_AP_45
SG11_1900_HP_AP_90
Microstrains
Moment at the 1.9m Station [kN m]
-400
-200
0
200
400
50
60
70
80
90
100
110

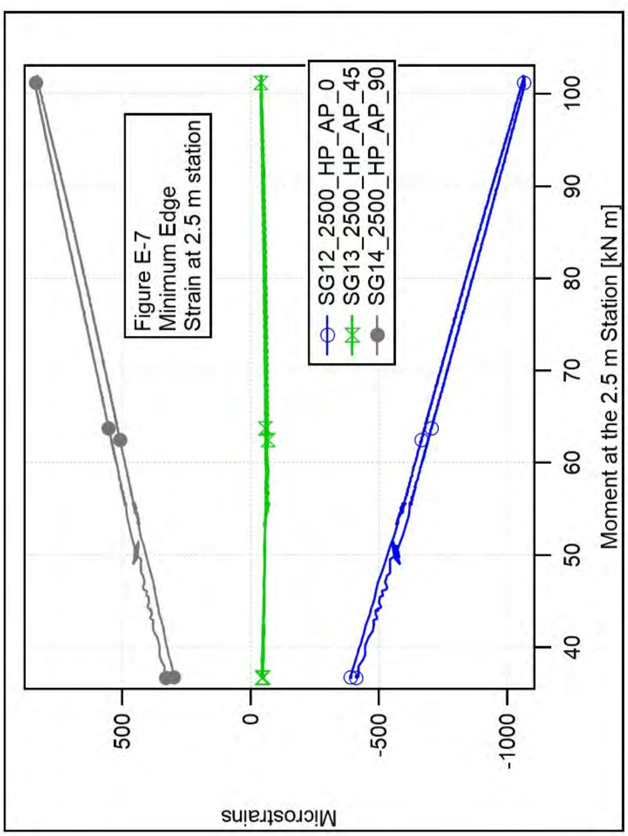
Figure E-7
Minimum Edge
Strain at 2.5 m station
SG12_2500_HP_AP_0
SG13_2500_HP_AP_45
SG14_2500_HP_AP_90
Microstrains
Moment at the 2.5 m Station [kN m]

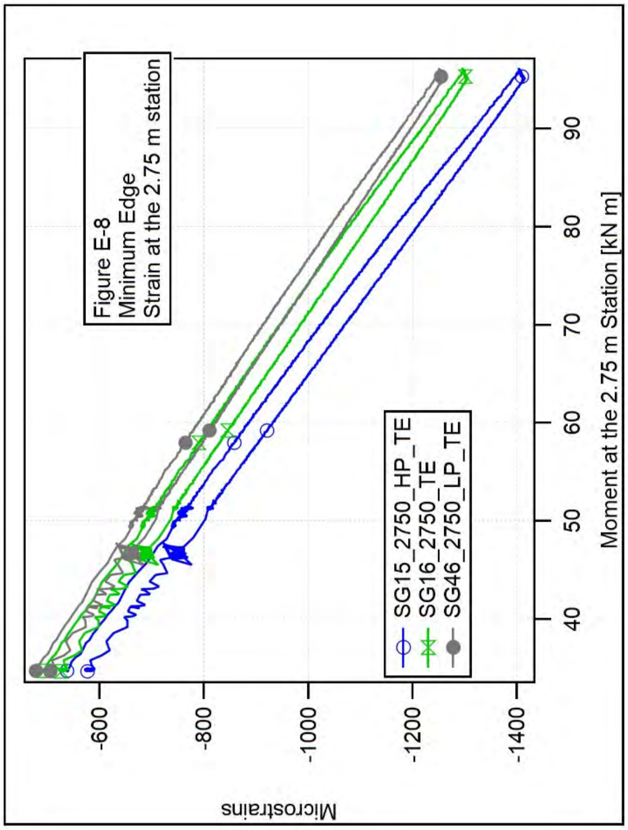
Figure E-8
Minimum Edge
Strain at the 2.75 m station
SG15_2750_HP_TE
SG16_2750_TE
SG46_2750_LP_TE
Microstrains
Moment at the 2.75 m Station [kN m]

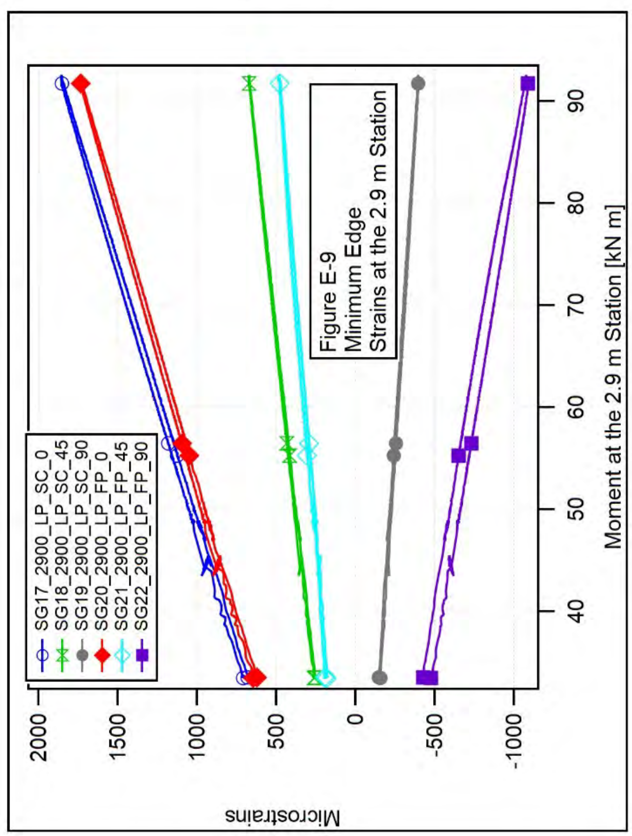
Figure E-9
Minimum Edge
Strains at the 2.9 m Station
SG17_2900_LP_SC_0
SG18_2900_LP_SC_45
SG19_2900_LP_SC_90
SG20_2900_LP_FP_0
SG21_2900_LP_FP_45
SG22_2900_LP_FP_90
Microstrains
Moment at the 2.9 m Station [kN m]

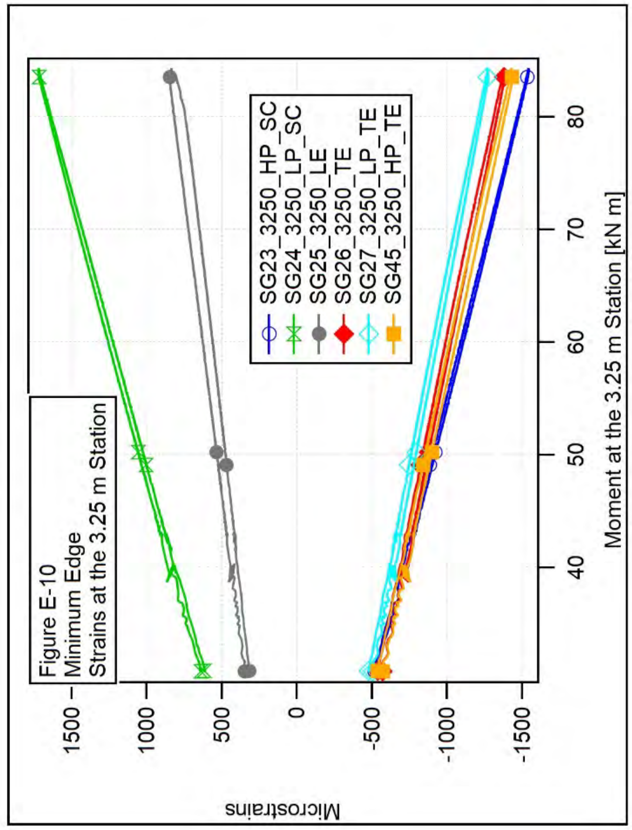
Figure E-10
Minimum Edge
Strains at the 3.25 m Station
SG23_3250_HP_SC
SG24_3250_LP_SC
SG25_3250_LE
SG26_3250_TE
SG27_3250_LP_TE
SG45_3250_HP_TE
Microstrains
Moment at the 3.25 m Station [kN m]

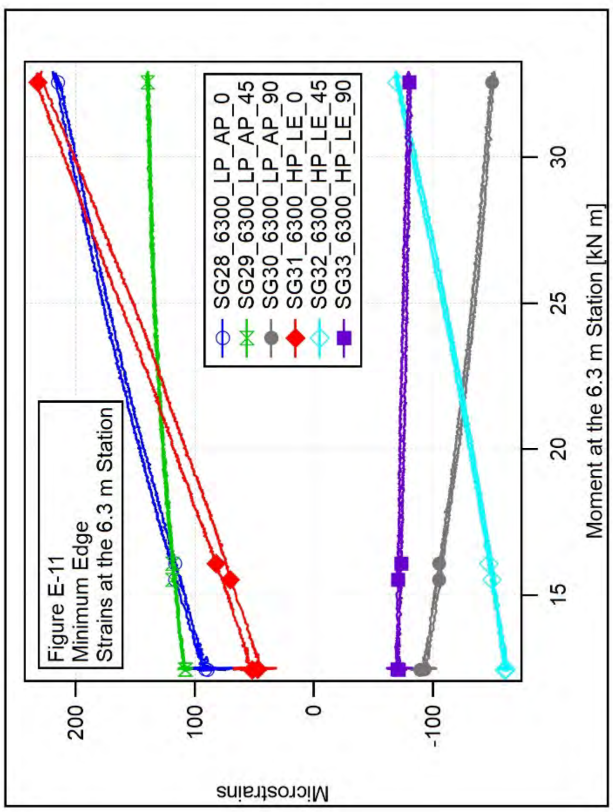
Figure E-11
Minimum Edge
Strains at the 6.3 m Station
SG28_6300_LP_AP_0
SG29_6300_LP_AP_45
SG30_6300_LP_AP_90
SG31_6300_HP_LE_0
SG32_6300_HP_LE_45
SG33_6300_HP_LE_90
Microstrains
Moment at the 6.3 m Station [kN m]

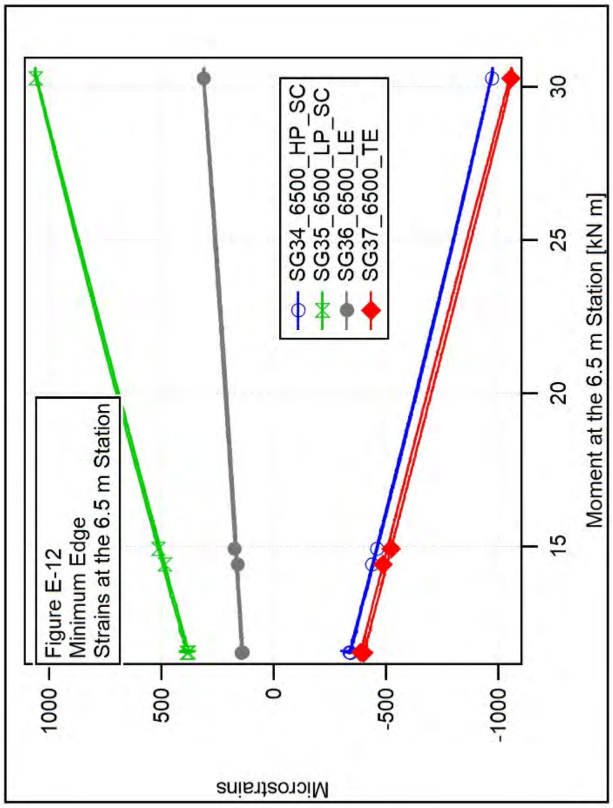
Figure E-12
Minimum Edge
Strains at the 6.5 m Station
SG34_6500_HP_SC
SG35_6500_LP_SC
SG36_6500_LE
SG37_6500_TE
Microstrains
Moment at the 6.5 m Station [kN m]

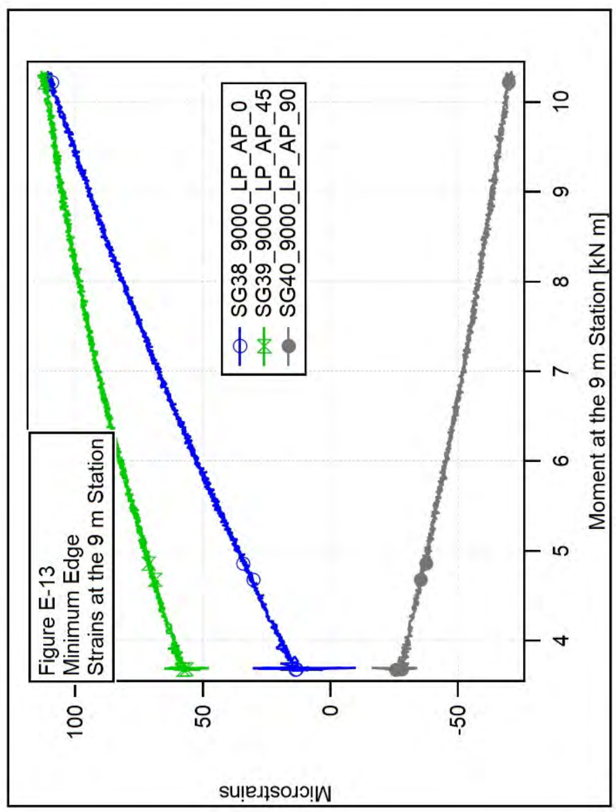
Figure E-13
Minimum Edge
Strains at the 9 m Station
SG38_9000_LP_AP_0
SG39_9000_LP_AP_45
SG40_9000_LP_AP_90
Microstrains
Moment at the 9 m Station [kN m]

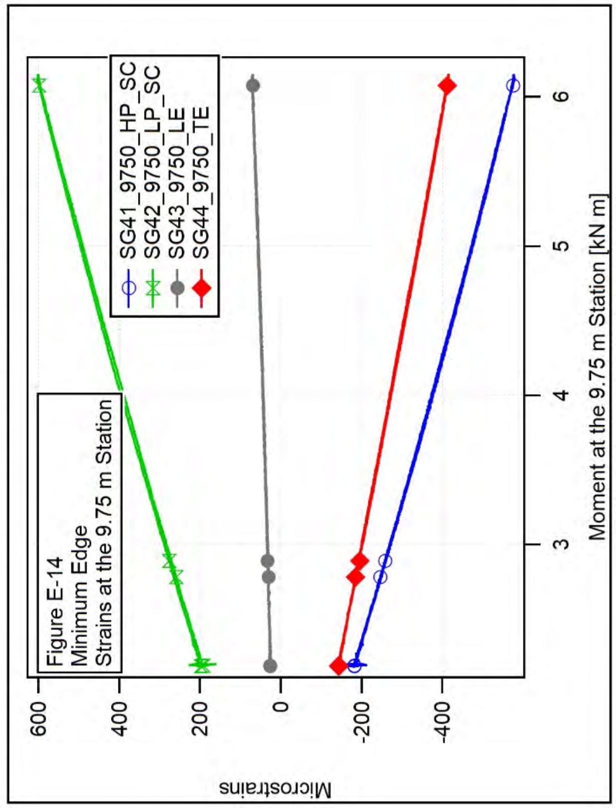
Figure E-14
Minimum Edge
Strains at the 9.75 m Station
SG41_9750_HP_SC
SG42_9750_LP_SC
SG43_9750_LE
SG44_9750_TE
Microstrains
Moment at the 9.75 m Station [kN m]

APPENDIX F- Fatigue Damage Equivalent Load Calculation

The equations used to estimate the damage equivalent load (DEL) are provided below. The DEL's were computed at five spanwise stations using the strain gages calibrated for bending moment. The DEL's are based on peak to peak strains and moments, mean effects were ignored. The equivalent damage was based on the target test cycles and target test bending moments. The complete peak-valley record of strains was used to estimate the DEL's. For reporting purposes, an inverse slope parameter (m) of 10 was used.

$$Eq.1 \quad d_i = \left(\frac{M_a}{M_u}\right)^m * \frac{N_a}{N_{eq}}$$

$$Eq.2 \quad D = \sum d_i$$

$$Eq.3 \quad DEL = M_u * D^{\frac{1}{m}}$$

Definitions for the variables in Equations 1 through 3 include:

- di – damage from binned moment range
- D – damage from all binned moment ranges
- Ma – binned moment range
- Mu – target test moment range
- Na – number of cycles in a bin
- Neq – damage equivalent cycles (Neq=1e6 used in this analysis)
- M – inverse slope parameter (m=10 used in this analysis)

APPENDIX G – Fatigue Charts

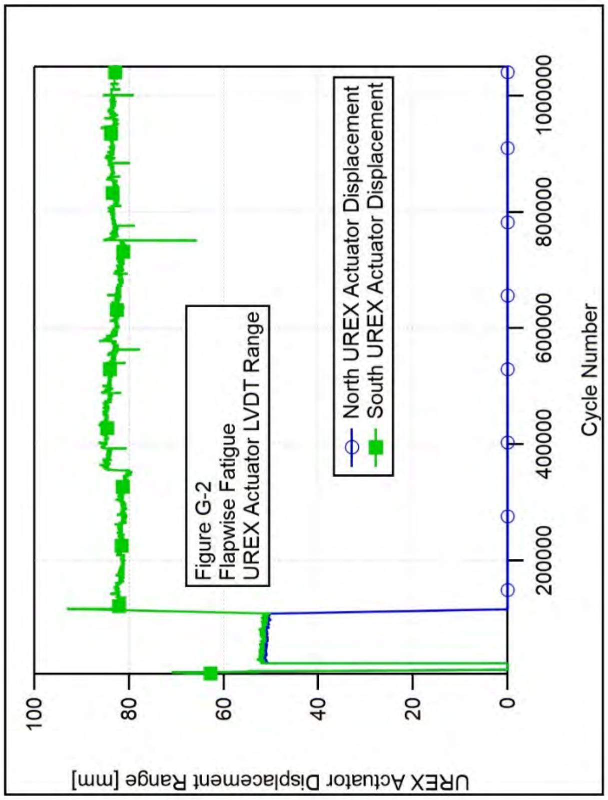

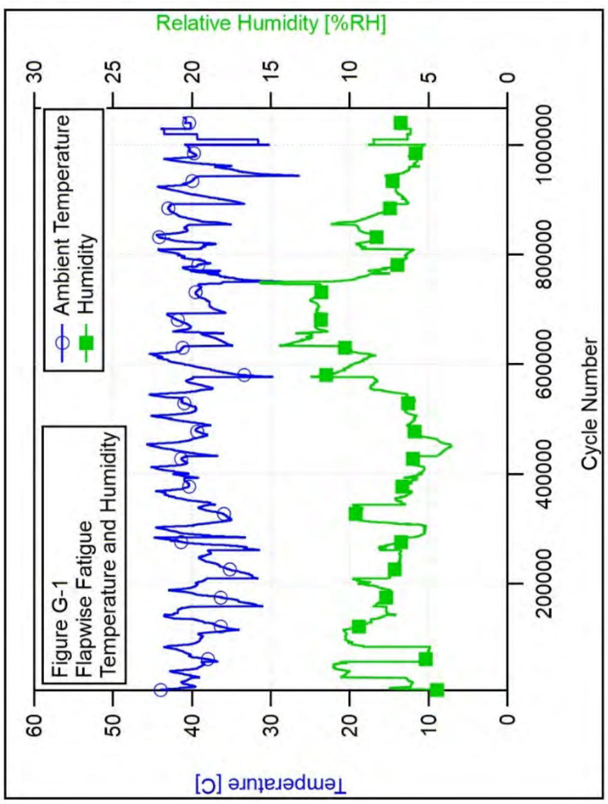

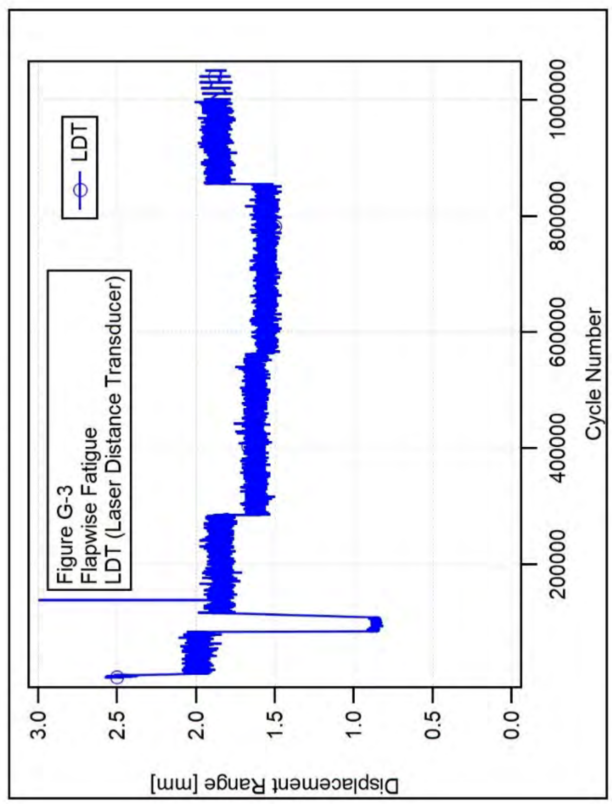

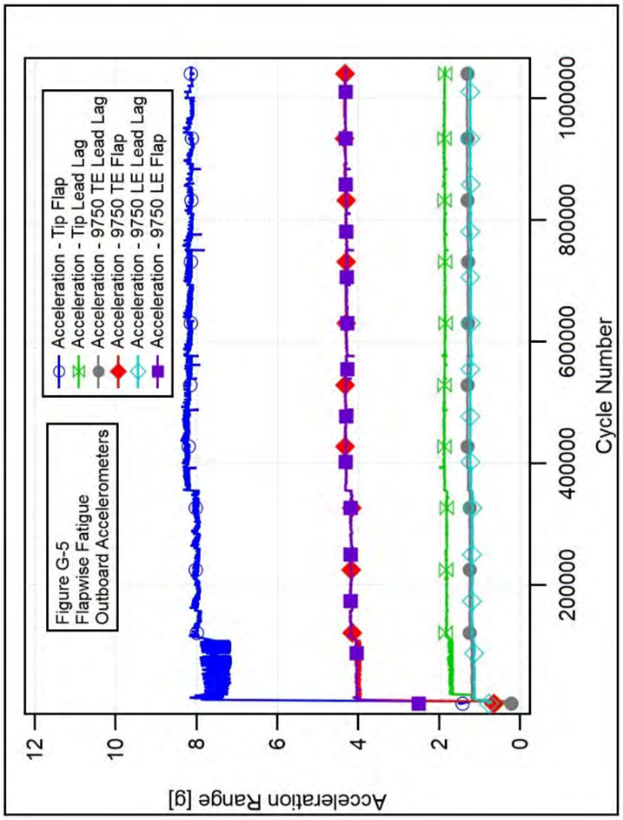
Figure G-5
Flapwise Fatigue
Outboard Accelerometers
Acceleration - Tip Flap
Acceleration - Tip Lead Lag
Acceleration - 9750 TE Lead Lag
Acceleration - 9750 TE Flap
Acceleration - 9750 LE Lead Lag
Acceleration - 9750 LE Flap
Acceleration Range [g]
Cycle Number

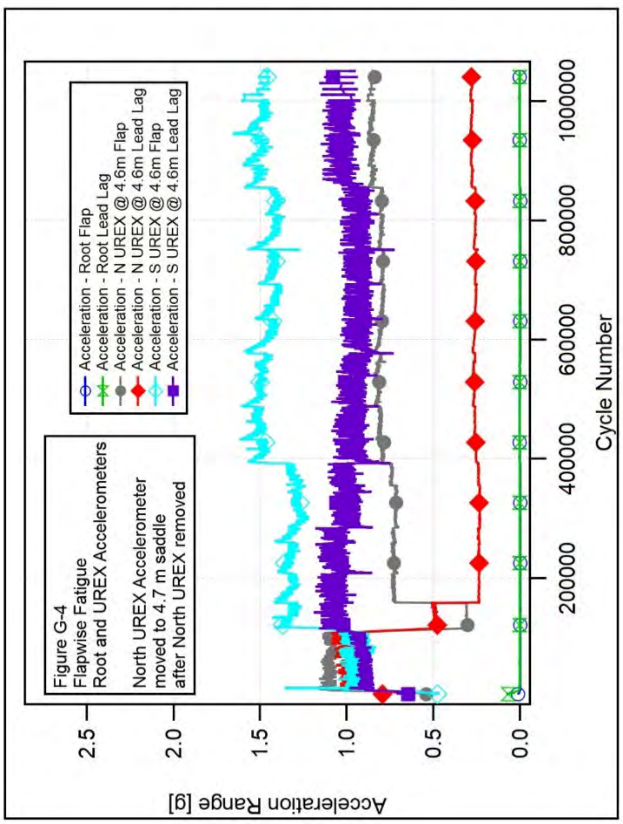
Figure G-4
Flapwise Fatigue
Root and UREX Accelerometers
North UREX Accelerometer
moved to 4.7 m saddle
after North UREX removed
Acceleration - Root Flap
Acceleration - Root Lead Lag
Acceleration - N UREX @ 4.6m Flap
Acceleration - N UREX @ 4.6m Lead Lag
Acceleration - S UREX @ 4.6m Flap
Acceleration - S UREX @ 4.6m Lead Lag
Acceleration Range [g]
Cycle Number

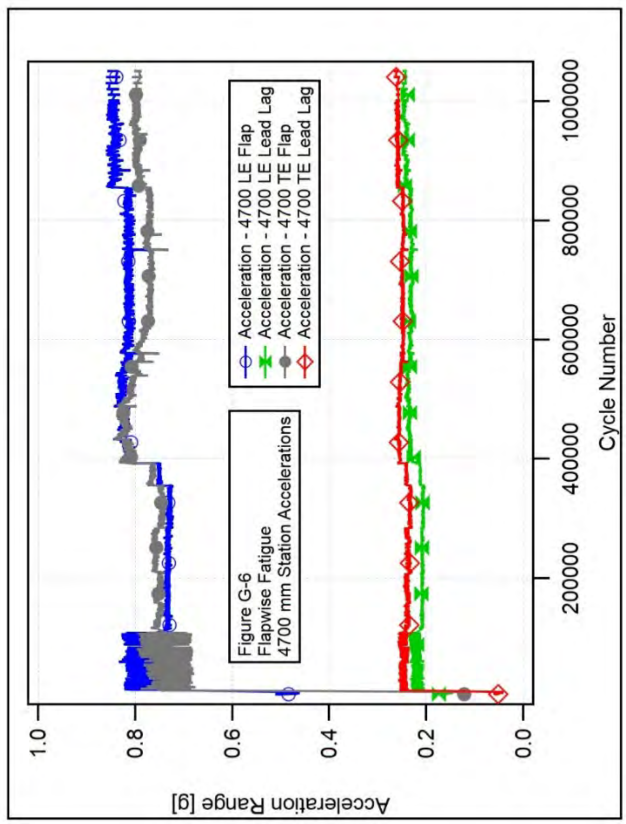
Figure G-6
Flapwise Fatigue
4700 mm Station Accelerations
Acceleration - 4700 LE Flap
Acceleration - 4700 LE Lead Lag
Acceleration - 4700 TE Flap
Acceleration - 4700 TE Lead Lag
Acceleration Range [g]
Cycle Number

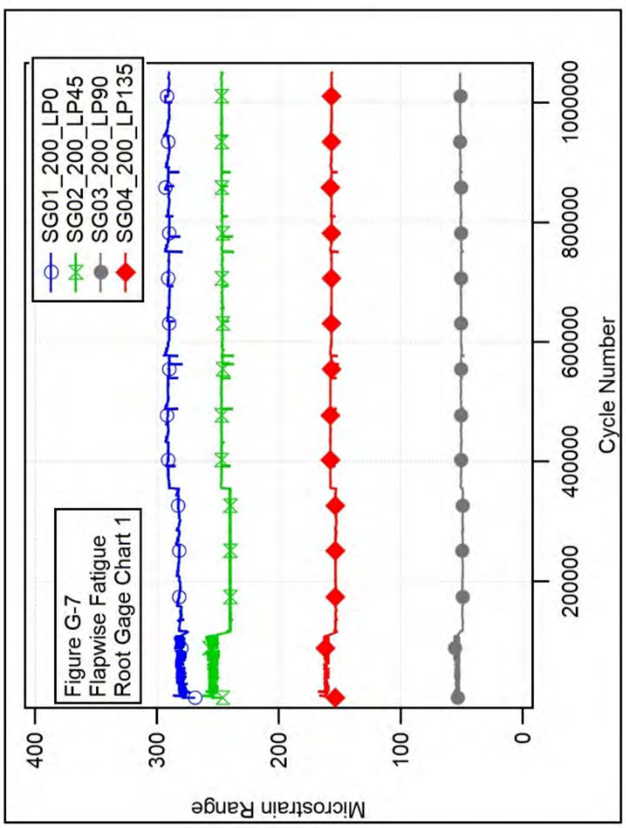
Figure G-7
Flapwise Fatigue
Root Gage Chart 1
SG01_200_LP0
SG02_200_LP45
SG03_200_LP90
SG04_200_LP135
Microstrain Range
Cycle Number
0
100
200
300
400
200000
400000
600000
800000
1000000

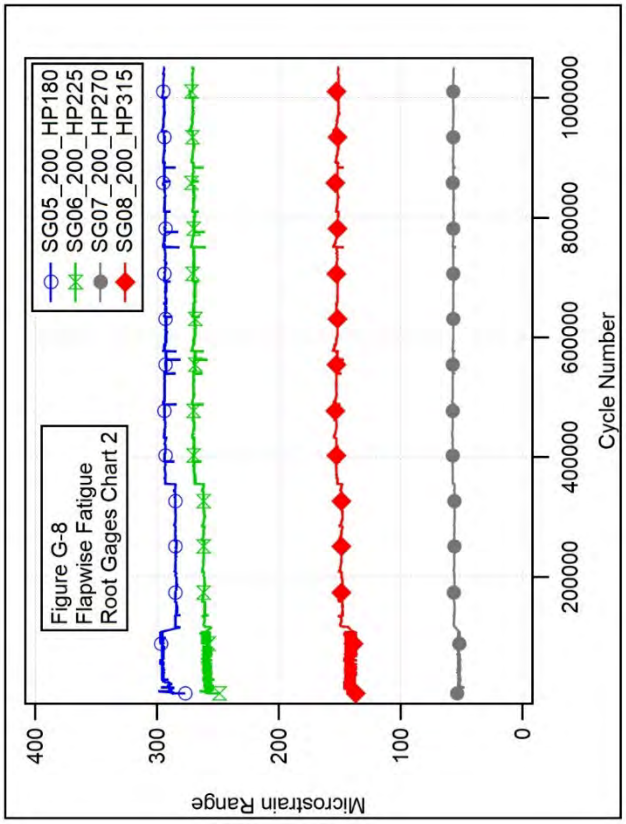
Figure G-8
Flapwise Fatigue
Root Gages Chart 2
SG05_200_HP180
SG06_200_HP225
SG07_200_HP270
SG08_200_HP315
Microstrain Range
Cycle Number
0
100
200
300
400
200000
400000
600000
800000
1000000

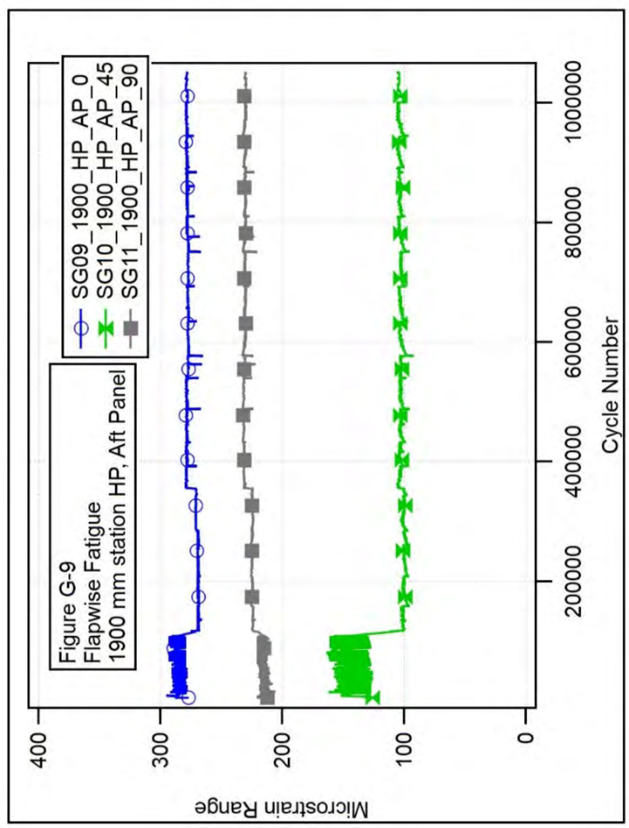
Figure G-9
Flapwise Fatigue
1900 mm station HP, Aft Panel
SG09_1900_HP_AP_0
SG10_1900_HP_AP_45
SG11_1900_HP_AP_90
Microstrain Range
Cycle Number
0
100
200
300
400
200000
400000
600000
800000
1000000

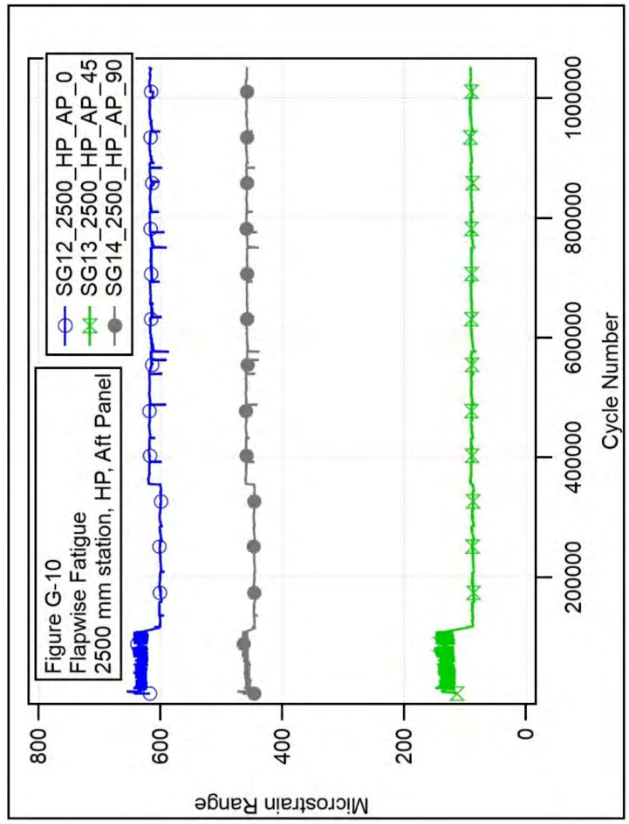
Figure G-10
Flapwise Fatigue
2500 mm station, HP, Aft Panel
SG12_2500_HP_AP_0
SG13_2500_HP_AP_45
SG14_2500_HP_AP_90
Microstrain Range
Cycle Number
0
200
400
600
800
200000
400000
600000
800000
1000000

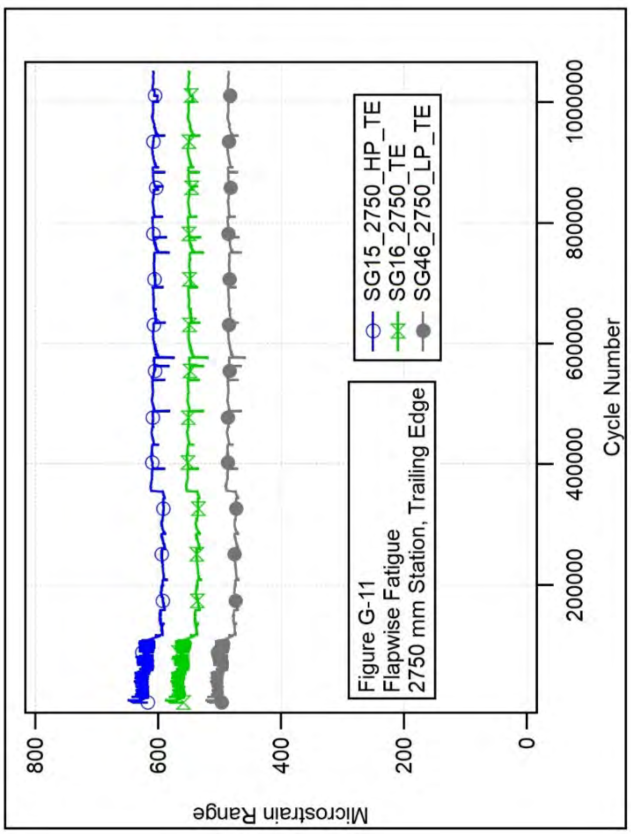
Figure G-11
Flapwise Fatigue
2750 mm Station, Trailing Edge
SG15_2750_HP_TE
SG16_2750_TE
SG46_2750_LP_TE
Microstrain Range
Cycle Number

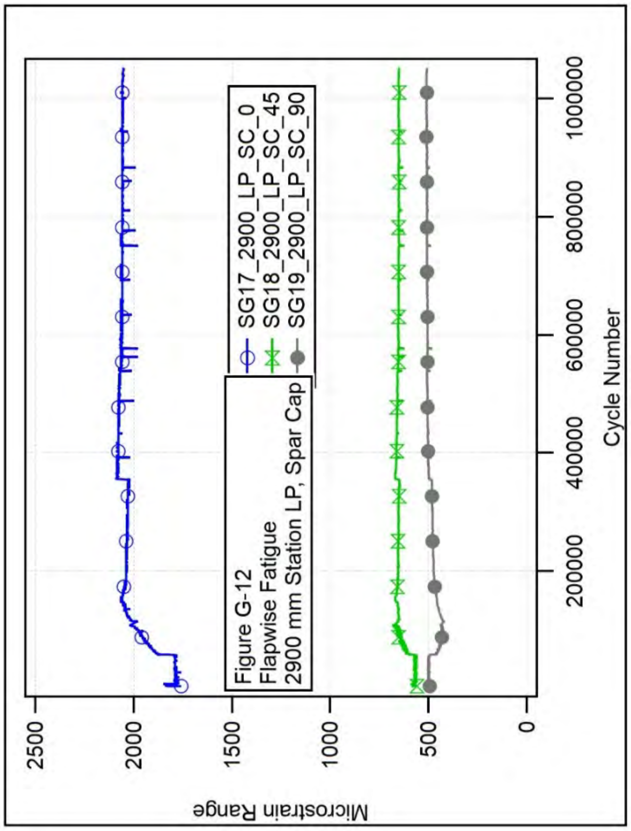
Figure G-12
Flapwise Fatigue
2900 mm Station LP, Spar Cap
SG17_2900_LP_SC_0
SG18_2900_LP_SC_45
SG19_2900_LP_SC_90
Microstrain Range
Cycle Number

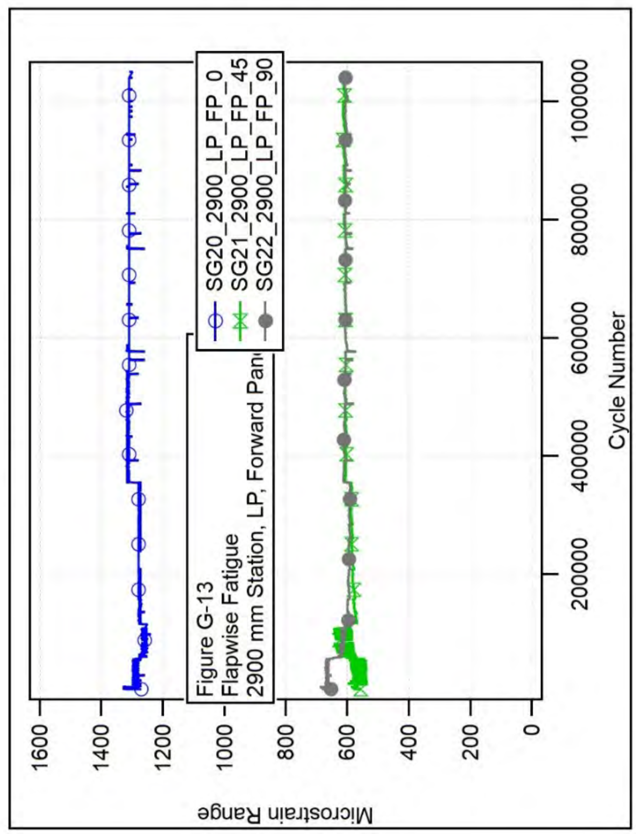
Figure G-13
Flapwise Fatigue
2900 mm Station, LP, Forward Pan
SG20_2900_LP_FP_0
SG21_2900_LP_FP_45
SG22_2900_LP_FP_90
Microstrain Range
Cycle Number

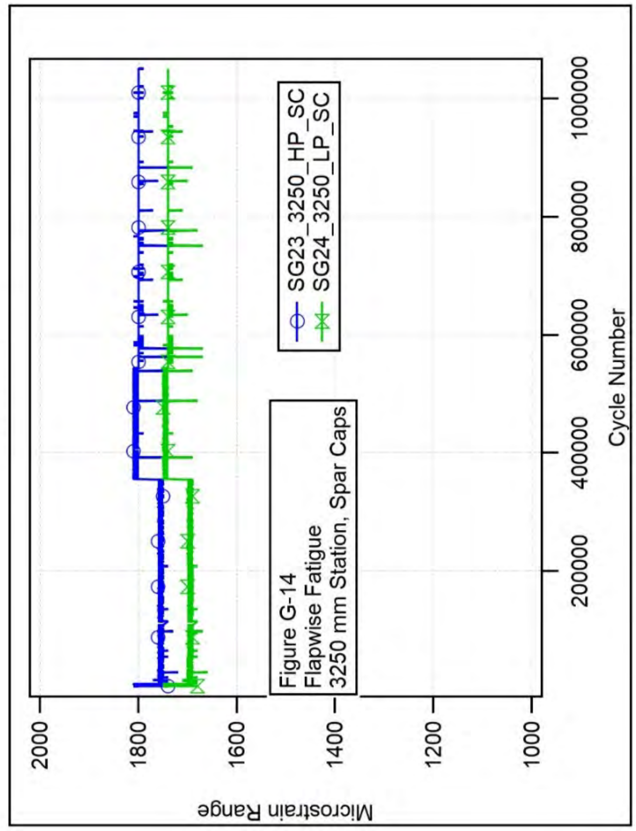
Figure G-14
Flapwise Fatigue
3250 mm Station, Spar Caps
SG23_3250_HP_SC
SG24_3250_LP_SC
Microstrain Range
Cycle Number

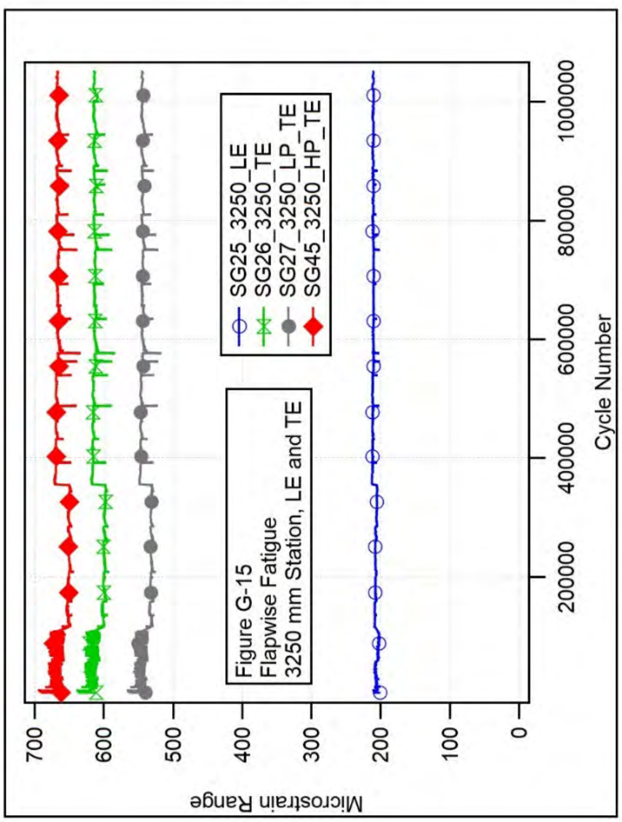
Figure G-15
Flapwise Fatigue
3250 mm Station, LE and TE
SG25_3250_LE
SG26_3250_TE
SG27_3250_LP_TE
SG45_3250_HP_TE
Microstrain Range
Cycle Number
0
100
200
300
400
500
600
700
200000
400000
600000
800000
1000000

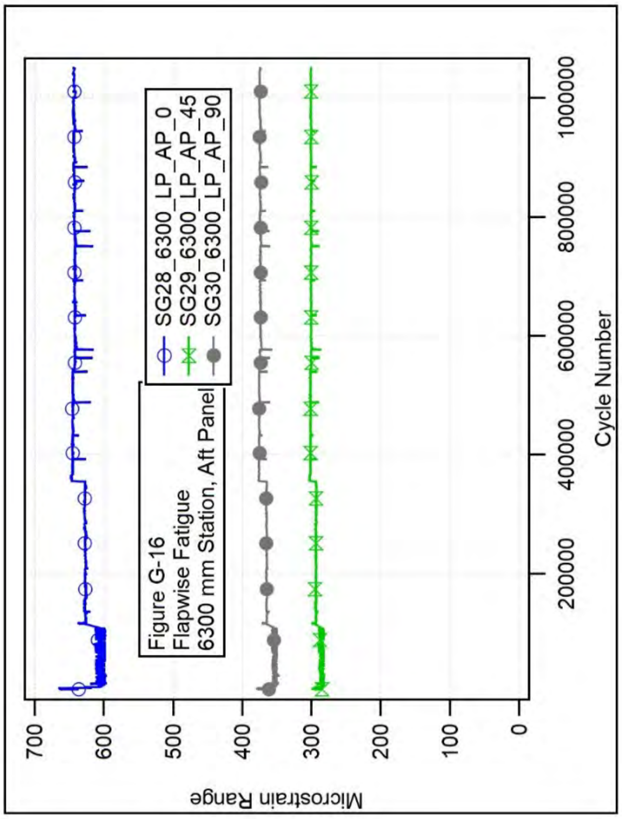
Figure G-16
Flapwise Fatigue
6300 mm Station, Aft Panel
SG28_6300_LP_AP_0
SG29_6300_LP_AP_45
SG30_6300_LP_AP_90
Microstrain Range
Cycle Number
0
100
200
300
400
500
600
700
200000
400000
600000
800000
1000000

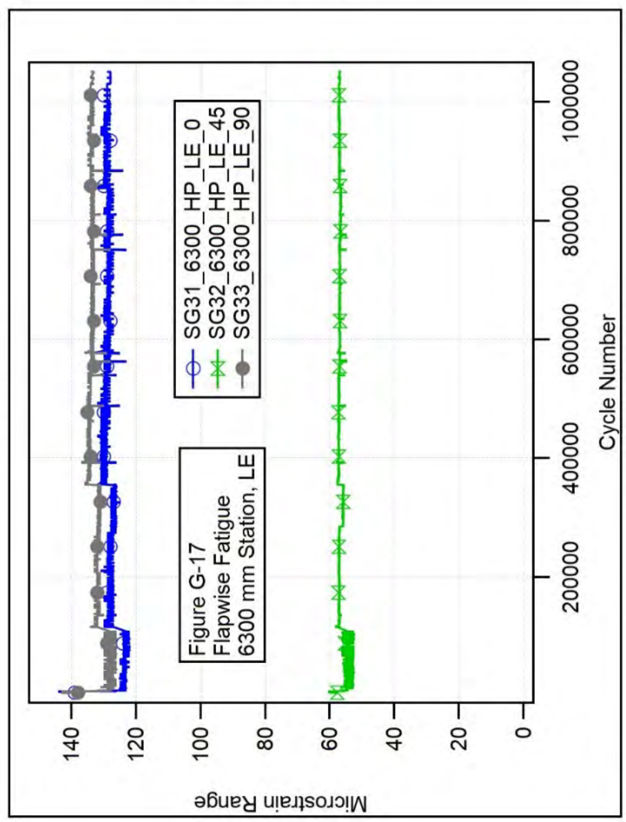
Figure G-17
Flapwise Fatigue
6300 mm Station, LE
SG31_6300_HP_LE_0
SG32_6300_HP_LE_45
SG33_6300_HP_LE_90
Microstrain Range
Cycle Number
0
20
40
60
80
100
120
140
200000
400000
600000
800000
1000000

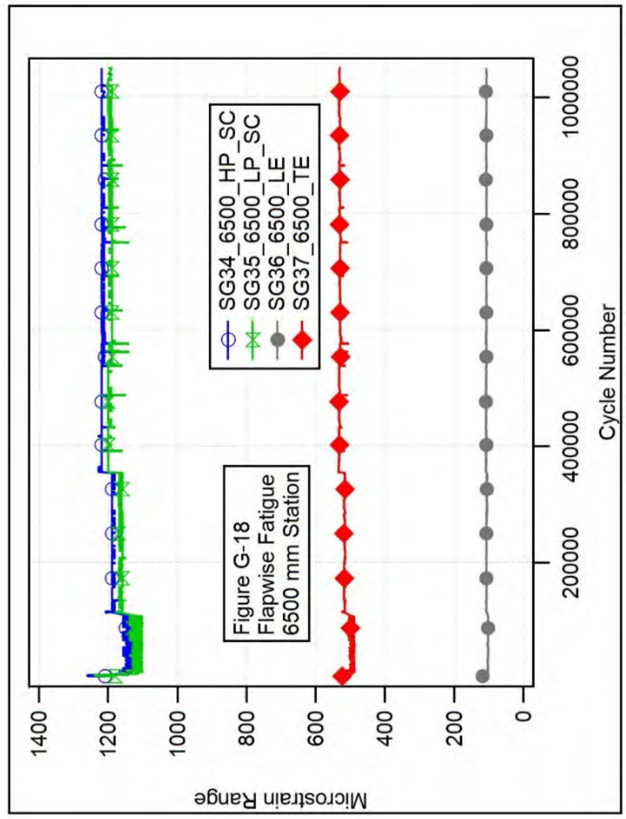
Figure G-18
Flapwise Fatigue
6500 mm Station
SG34_6500_HP_SC
SG35_6500_LP_SC
SG36_6500_LE
SG37_6500_TE
Microstrain Range
Cycle Number
0
200
400
600
800
1000
1200
1400
200000
400000
600000
800000
1000000

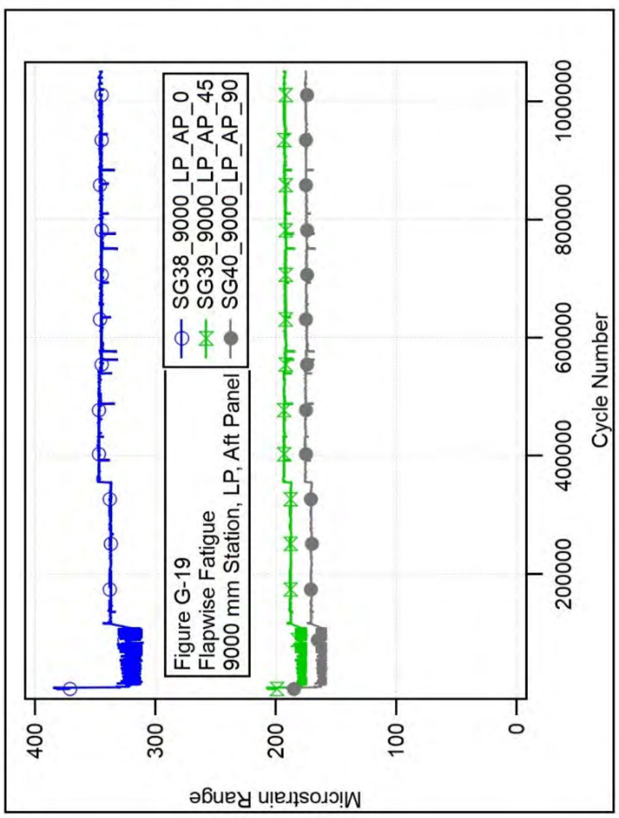
Figure G-19
Flapwise Fatigue
9000 mm Station, LP, Aft Panel
SG38_9000_LP_AP_0
SG39_9000_LP_AP_45
SG40_9000_LP_AP_90
Microstrain Range
Cycle Number
0
100
200
300
400
200000
400000
600000
800000
1000000

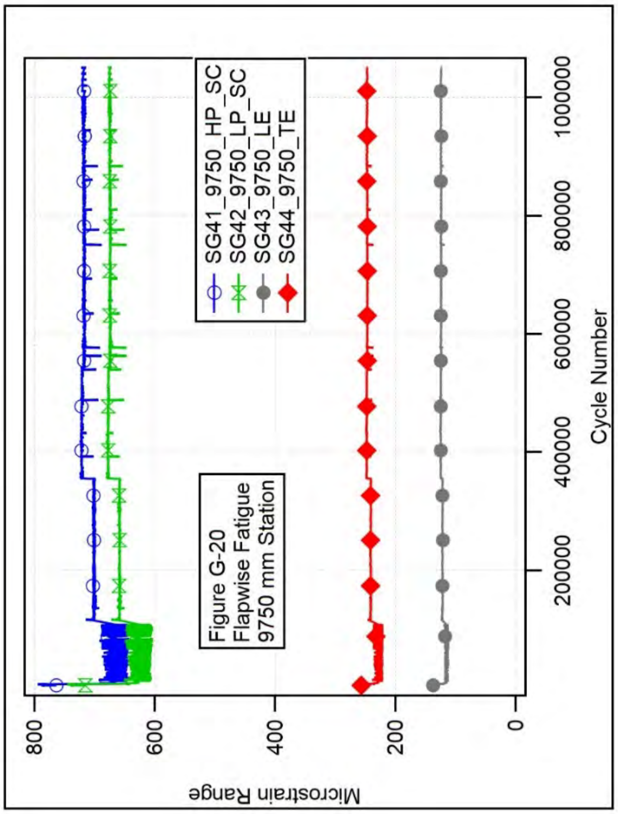
Figure G-20
Flapwise Fatigue
9750 mm Station
SG41_9750_HP_SC
SG42_9750_LP_SC
SG43_9750_LE
SG44_9750_TE
Microstrain Range
Cycle Number
0
200
400
600
800
200000
400000
600000
800000
1000000

APPENDIX H – Ultimate Flap Charts

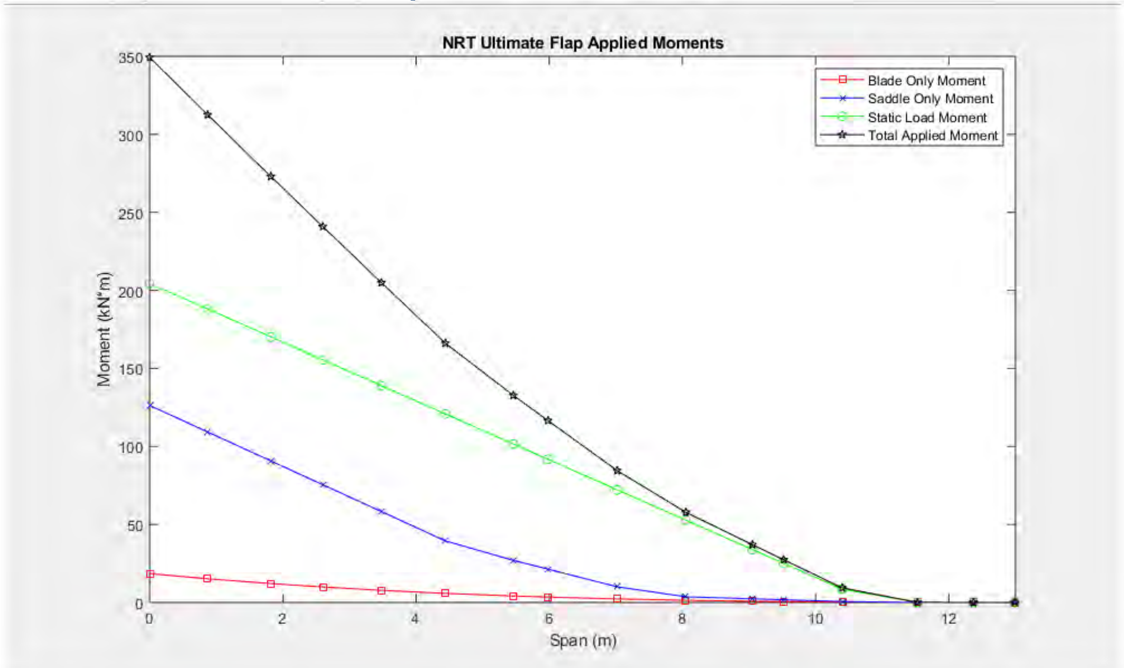

Figure H-1

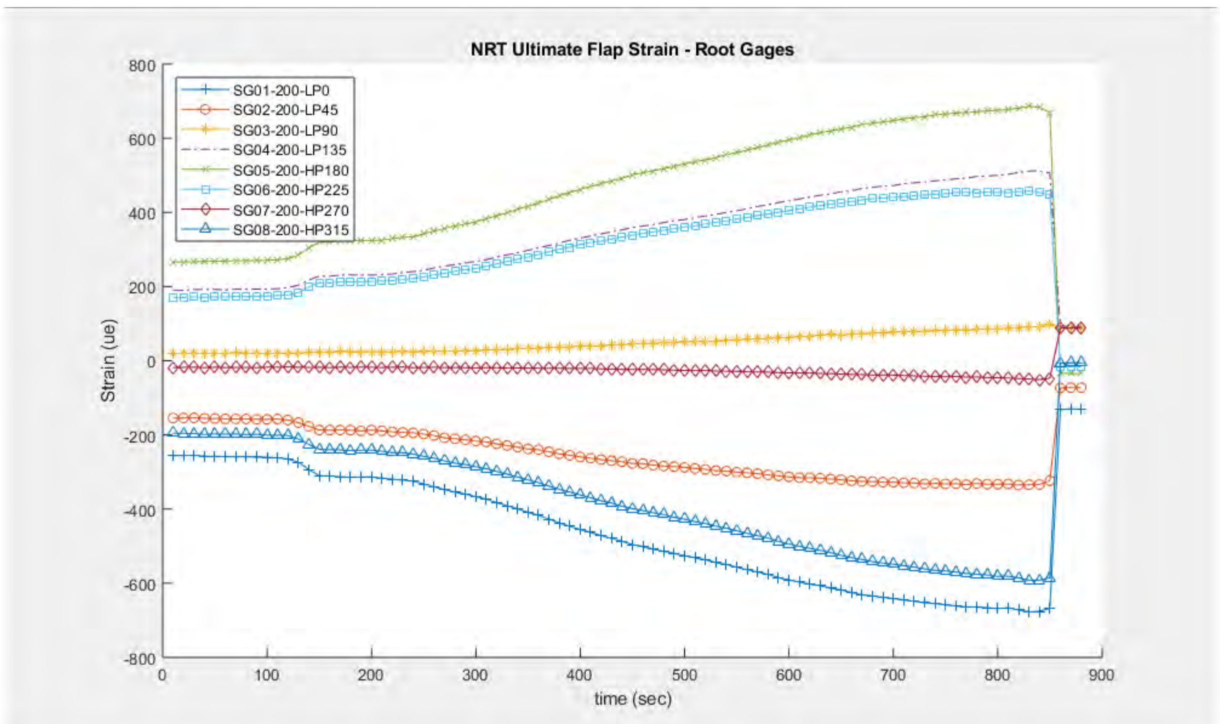

Figure H-2

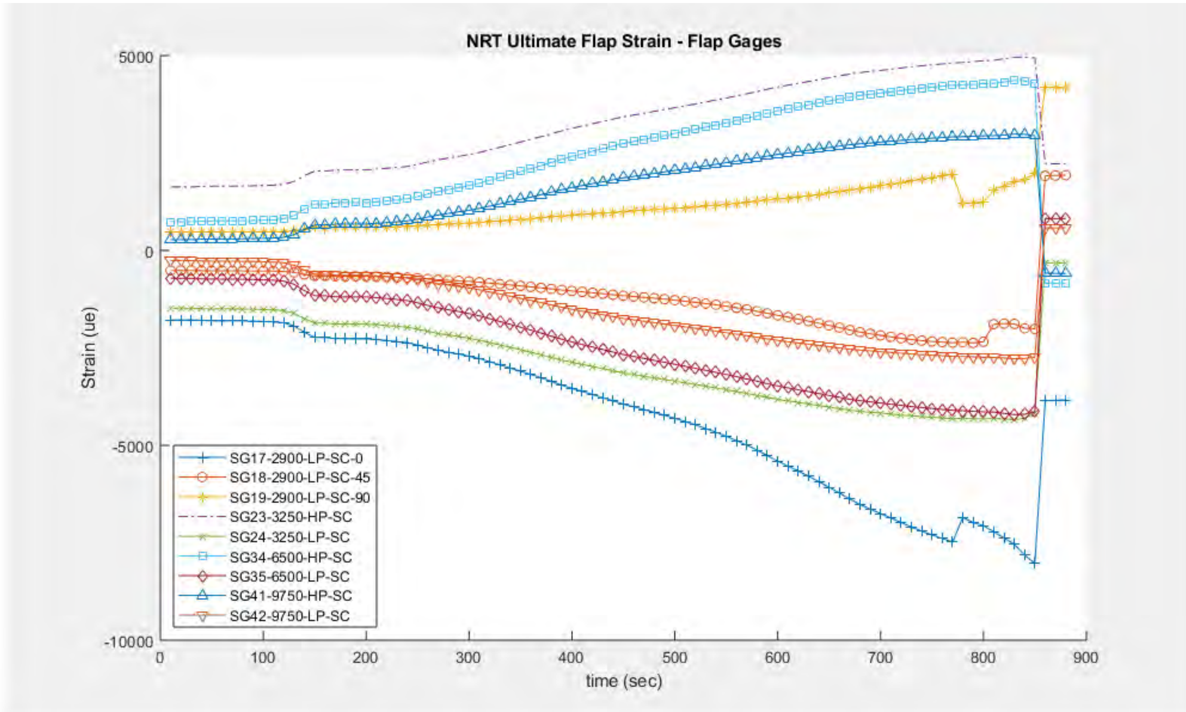

Figure H-3

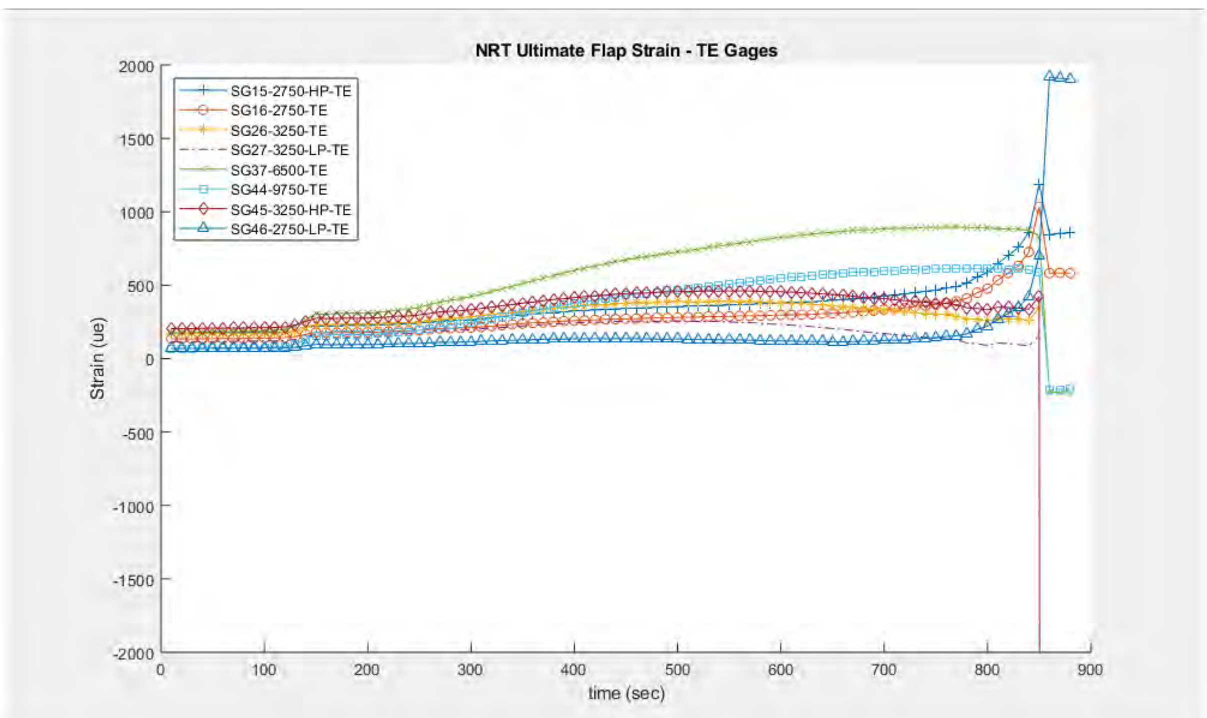

Figure H-4

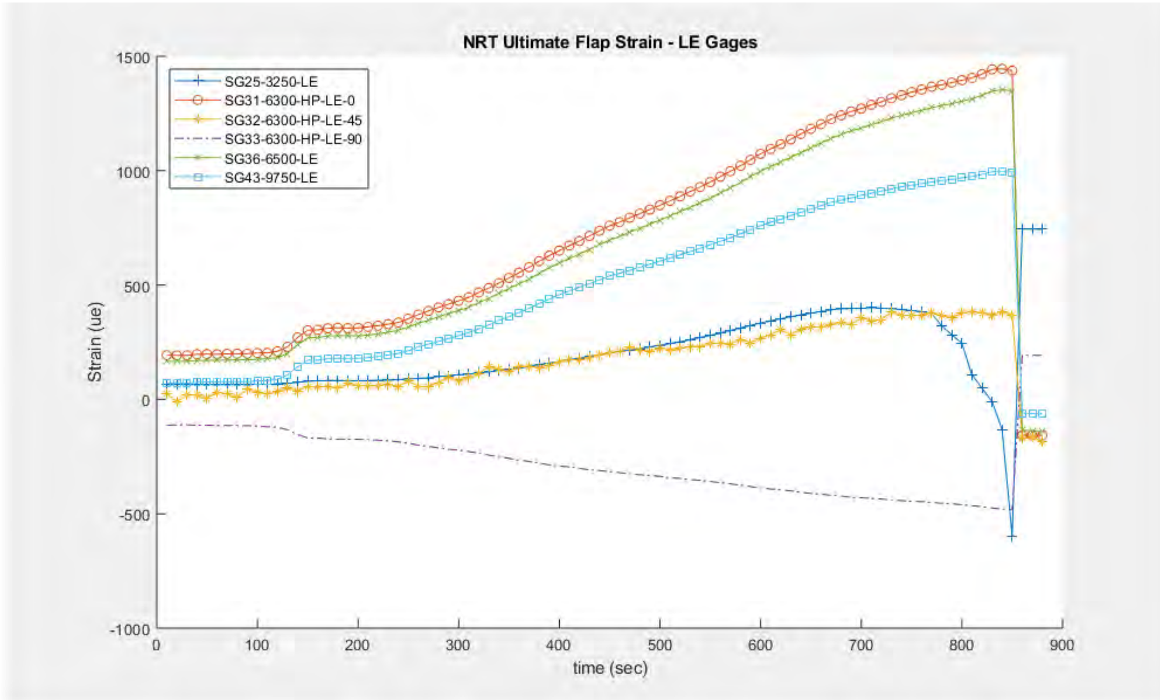

Figure H-5

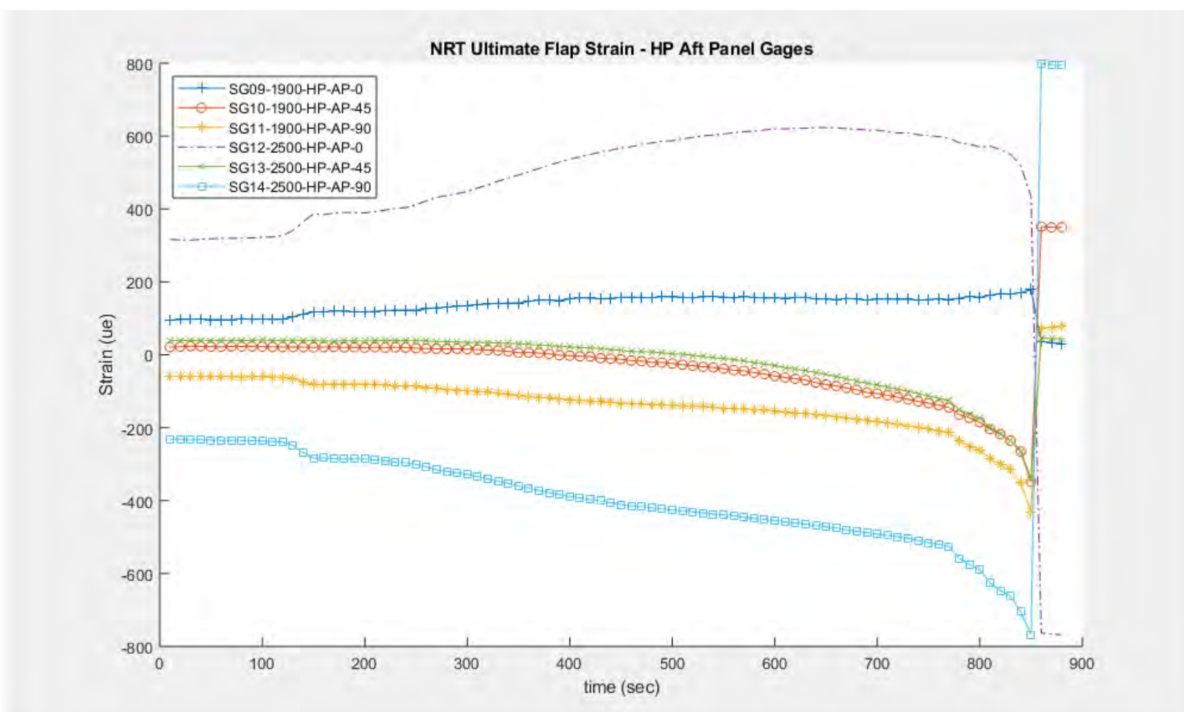

Figure H-6

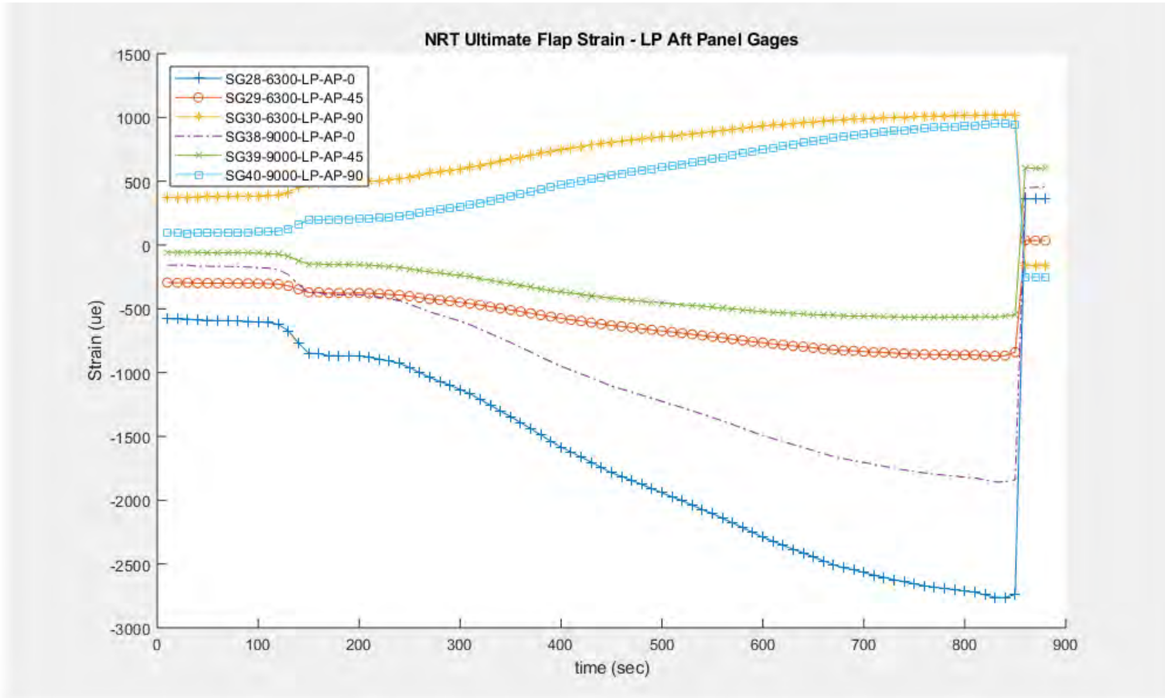

Figure H-7

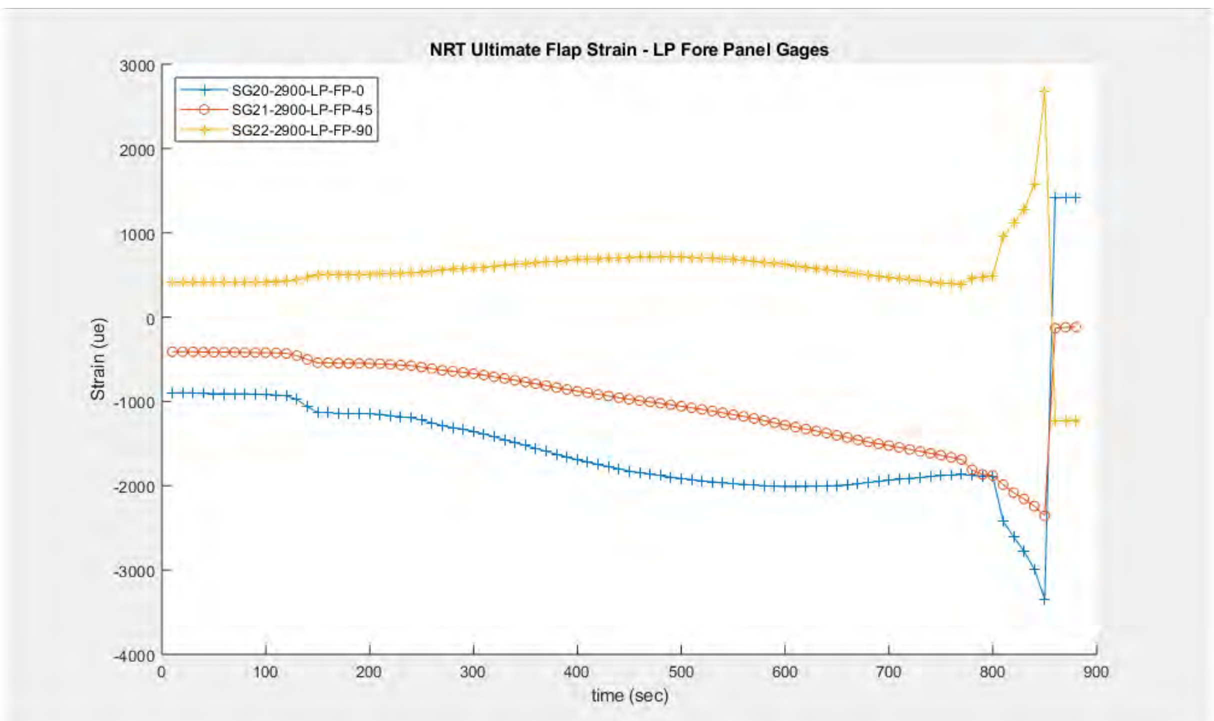

Figure H-8

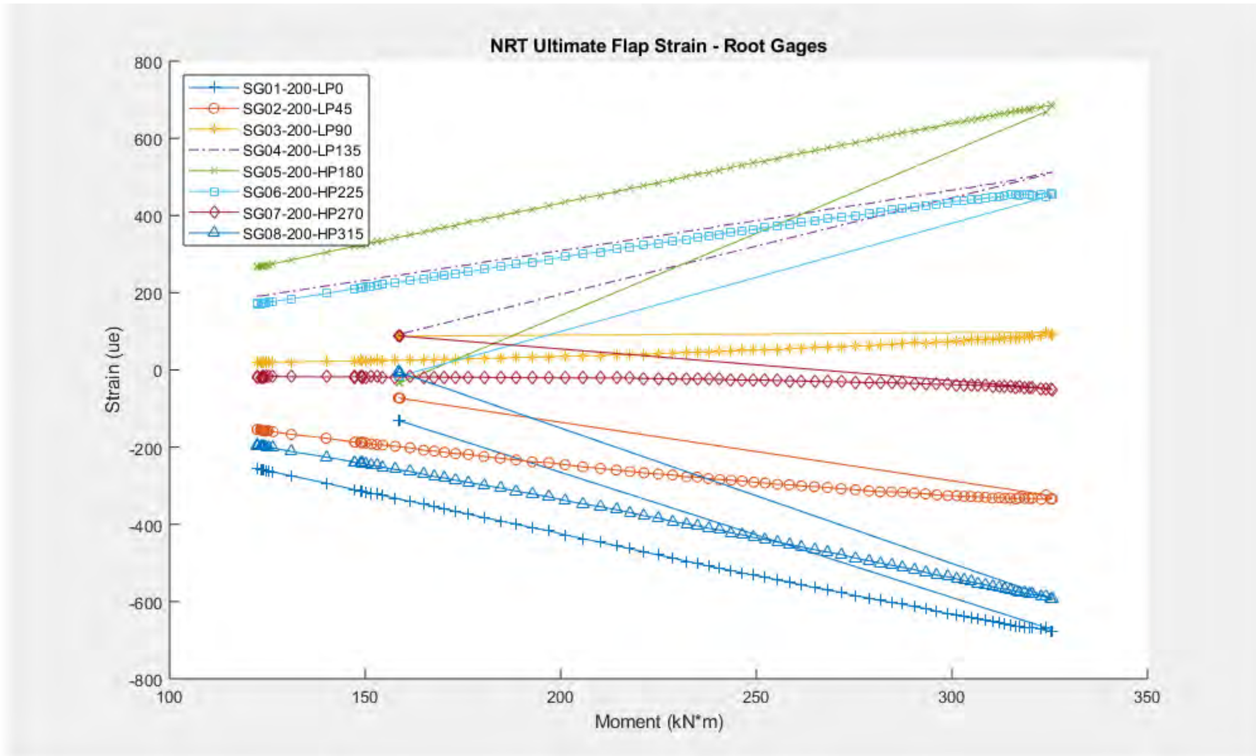

Figure H-9

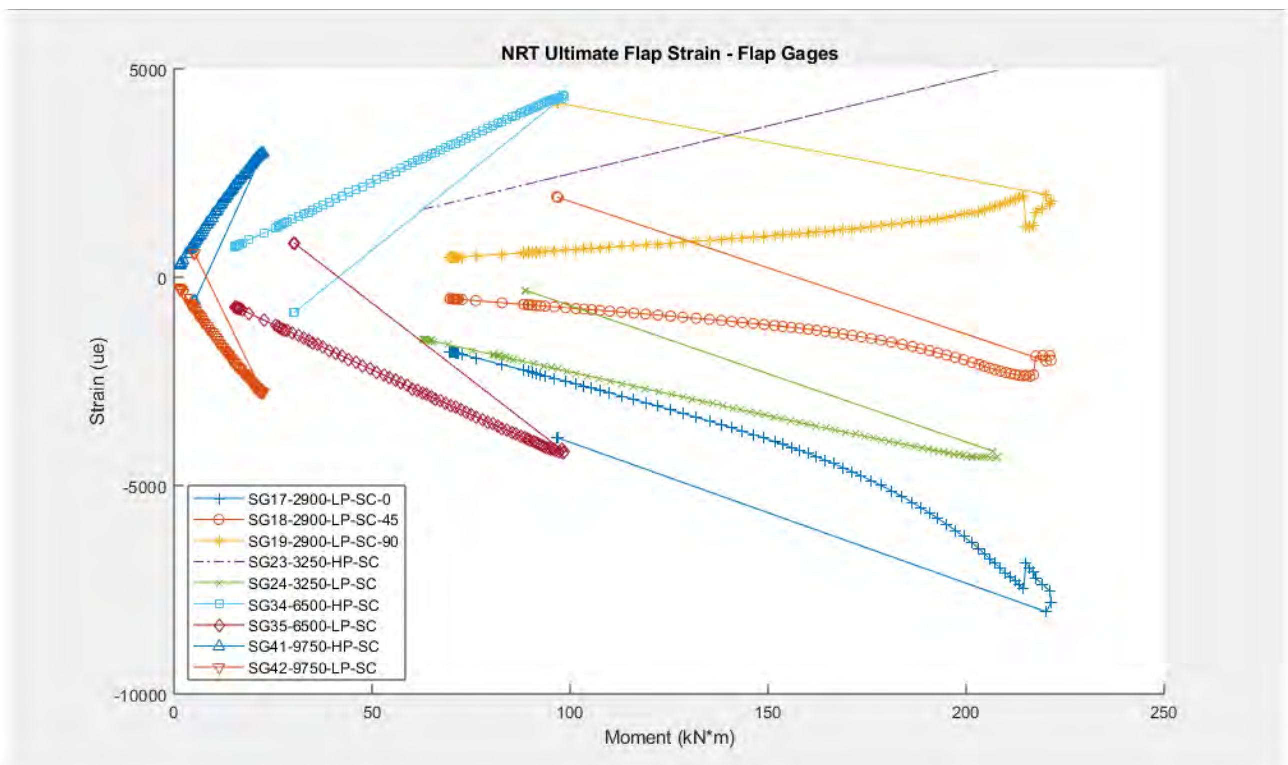

Figure H-10

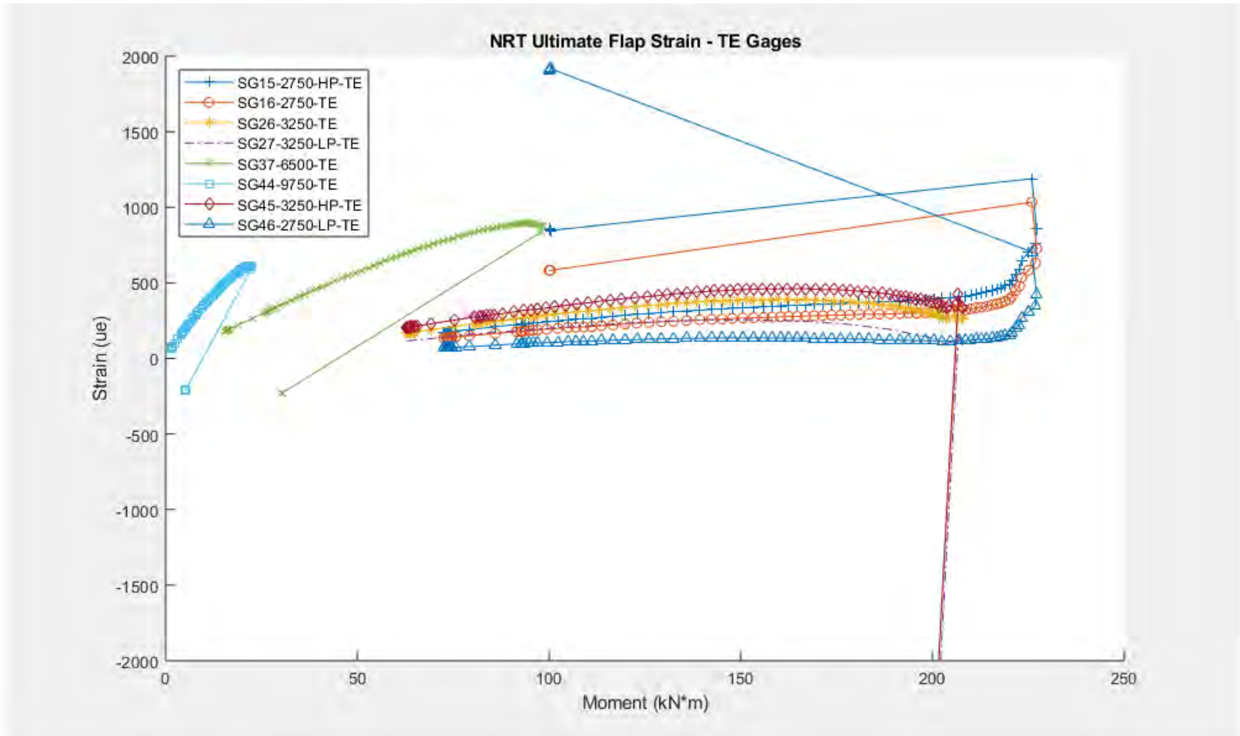

Figure H-11

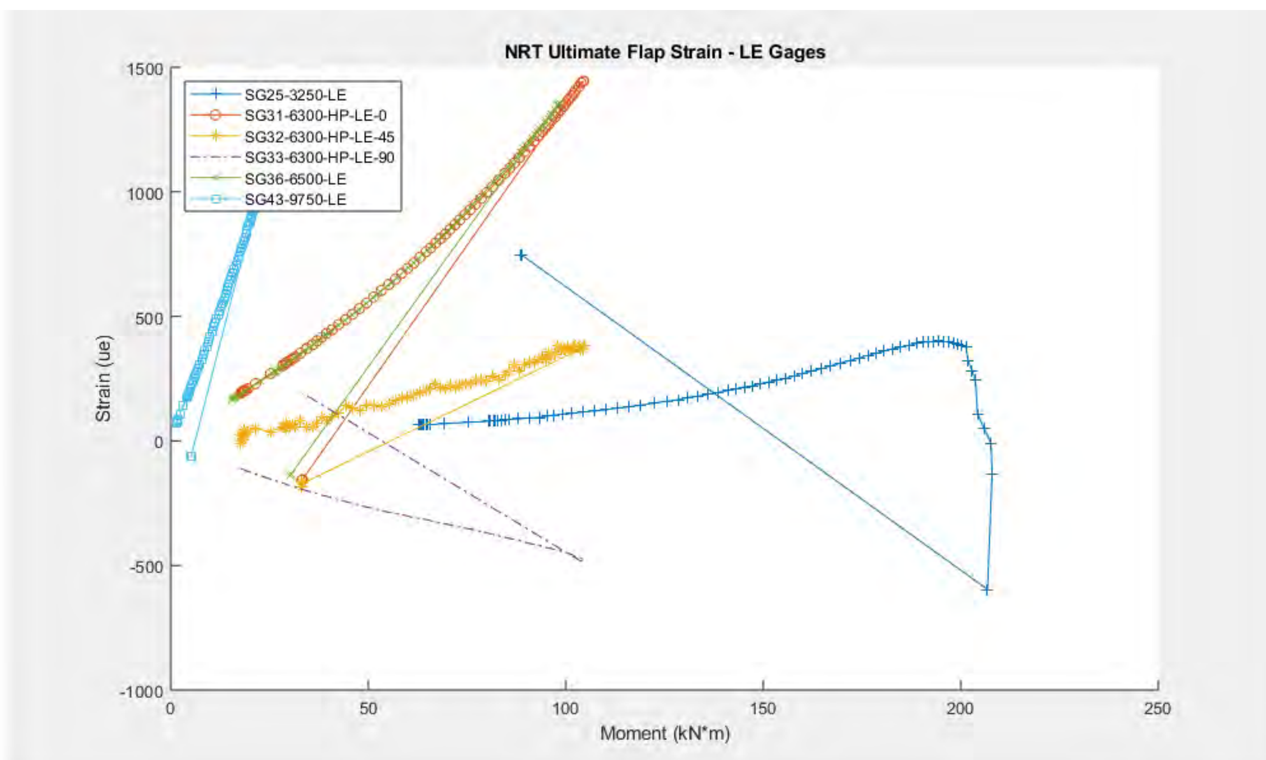

Figure H-12

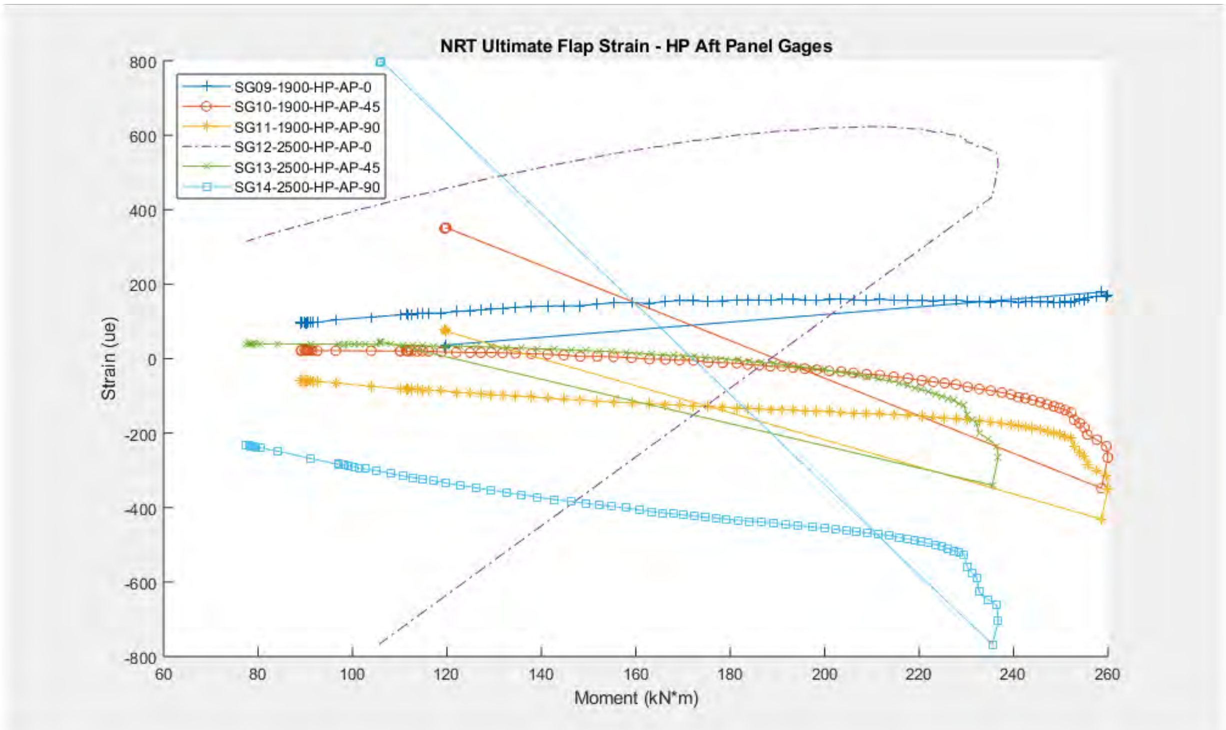

Figure H-13

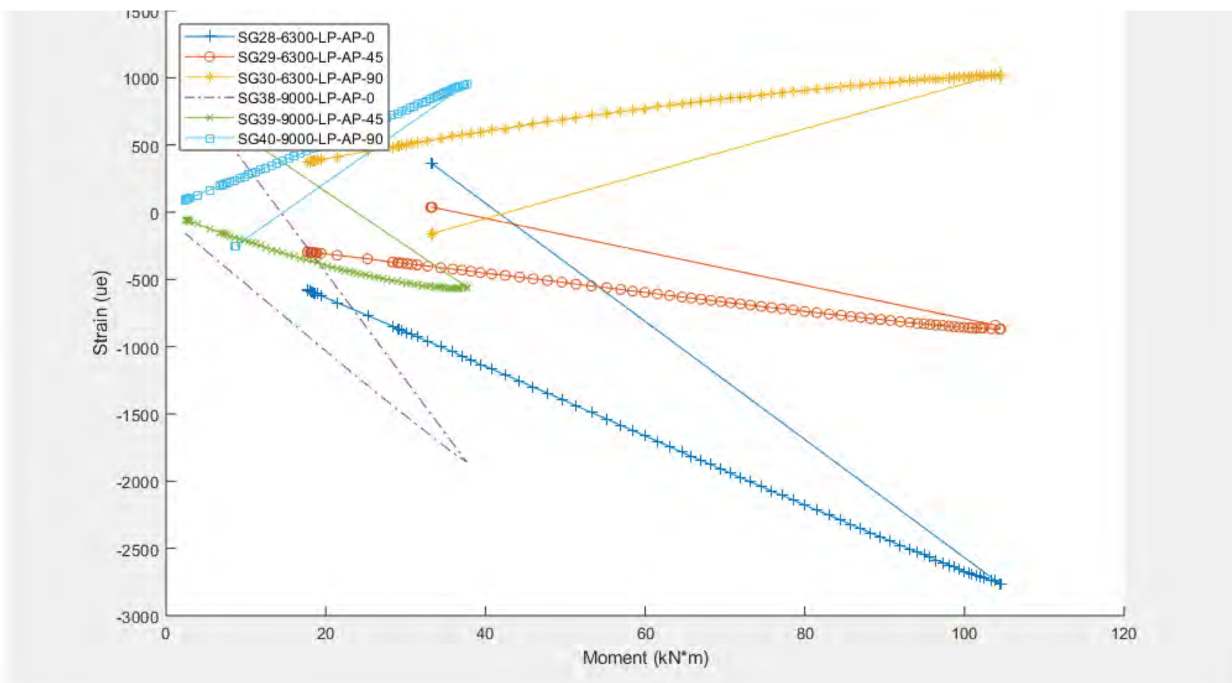

Figure H-14

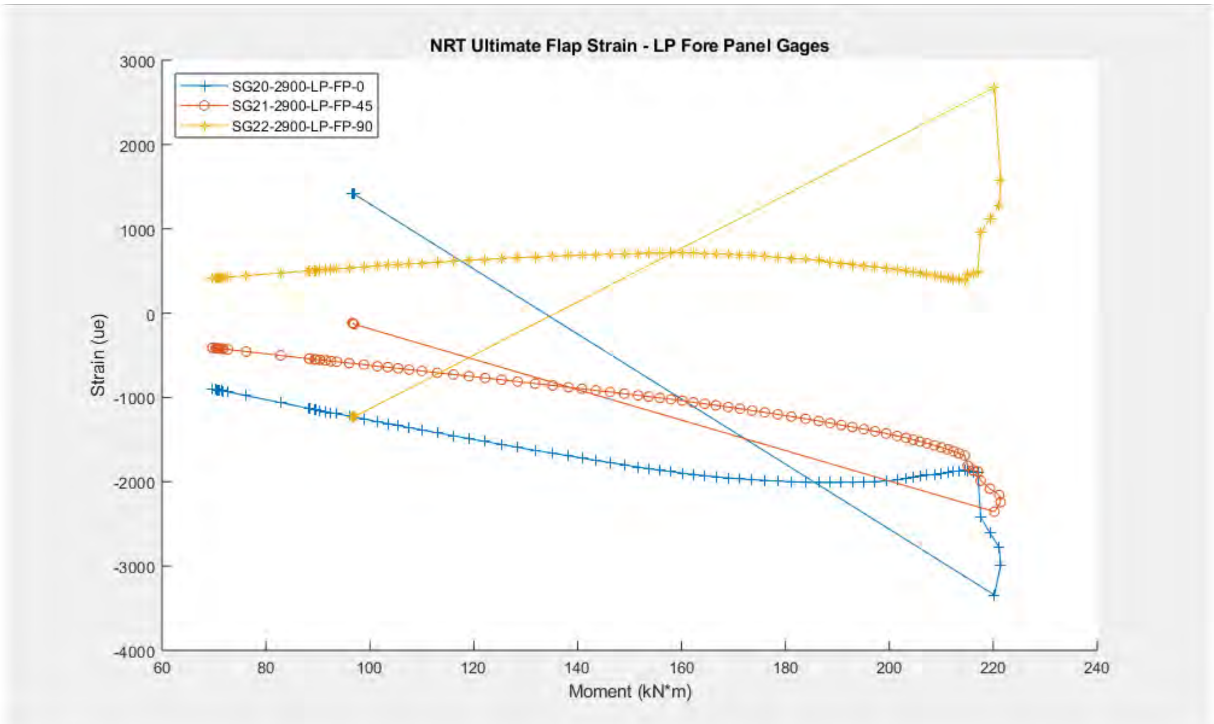

NRT Ultimate Flap Strain - LP Fore Panel Gages
SG20-2900-LP-FP-0
SG21-2900-LP-FP-45
SG22-2900-LP-FP-90
Strain (ue)
Moment (kN*m)
3000
2000
1000
0
-1000
-2000
-3000
-4000
60
80
100
120
140
160
180
200
220
240

Figure H-15

APPENDIX I – Test Photographs

Figure I-1. Adapter Plate Mounting Configuration for Static Proof Load Tests

Figure I-2. Preparing to Mount Blade for Maximum Flap Load Case

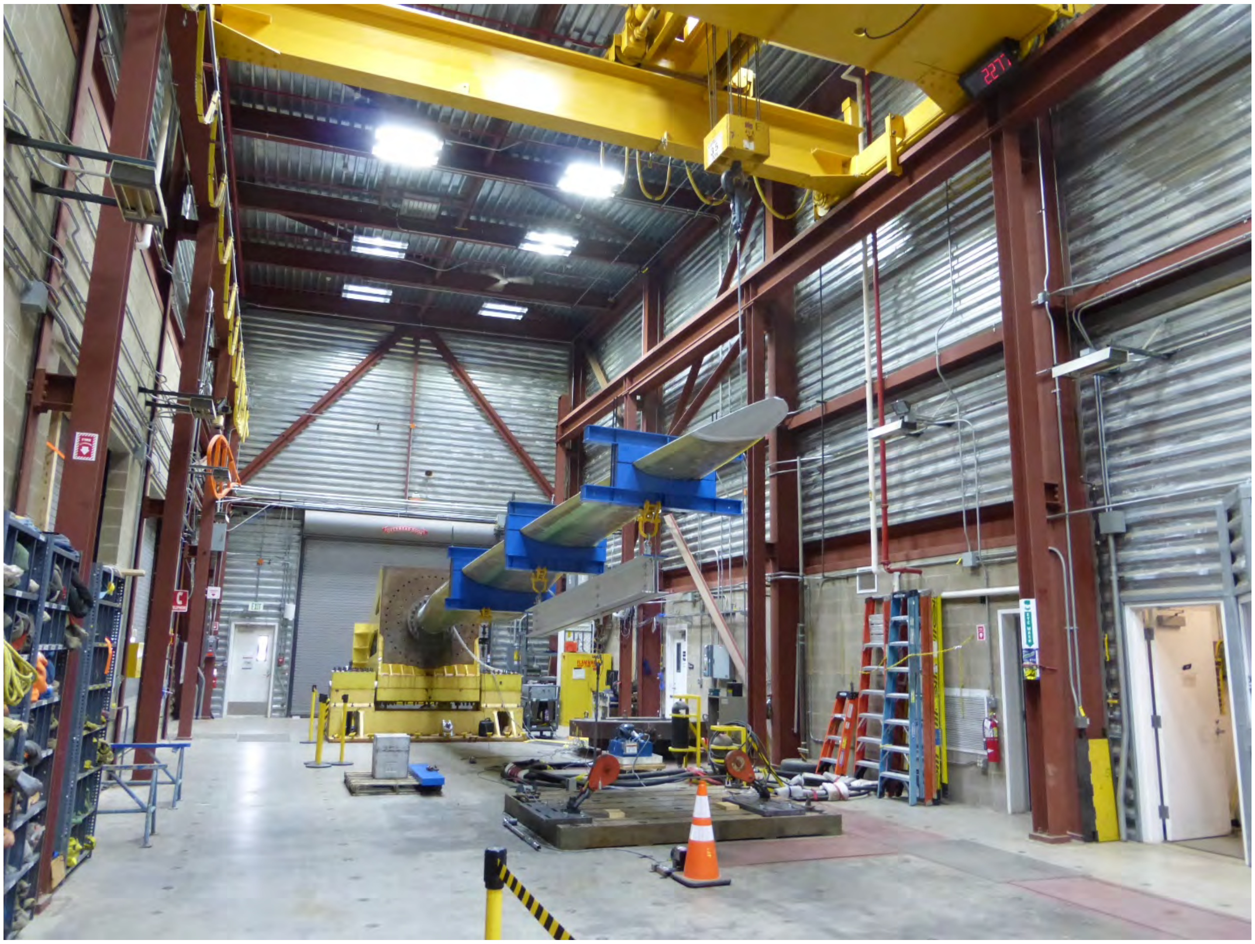

Figure I-3. Maximum Flap Test Setup

Figure I-4. Max Flap setup showing rigging line from spreader bar to overhead crane

Figure I-5. Maximum Flap near target 100% Applied Test Load

Figure I-6. Minimum Flap Test Setup

Figure I-7. Minimum Flap near Target Applied Test Moment

Figure I-8. Maximum Edge setup

Figure I-9. Maximum Edge Setup

Figure I-10. Maximum Edge, 7.55 m Saddle and Connection to Spreader Bar

Figure I-11 Minimum Edge Test setup

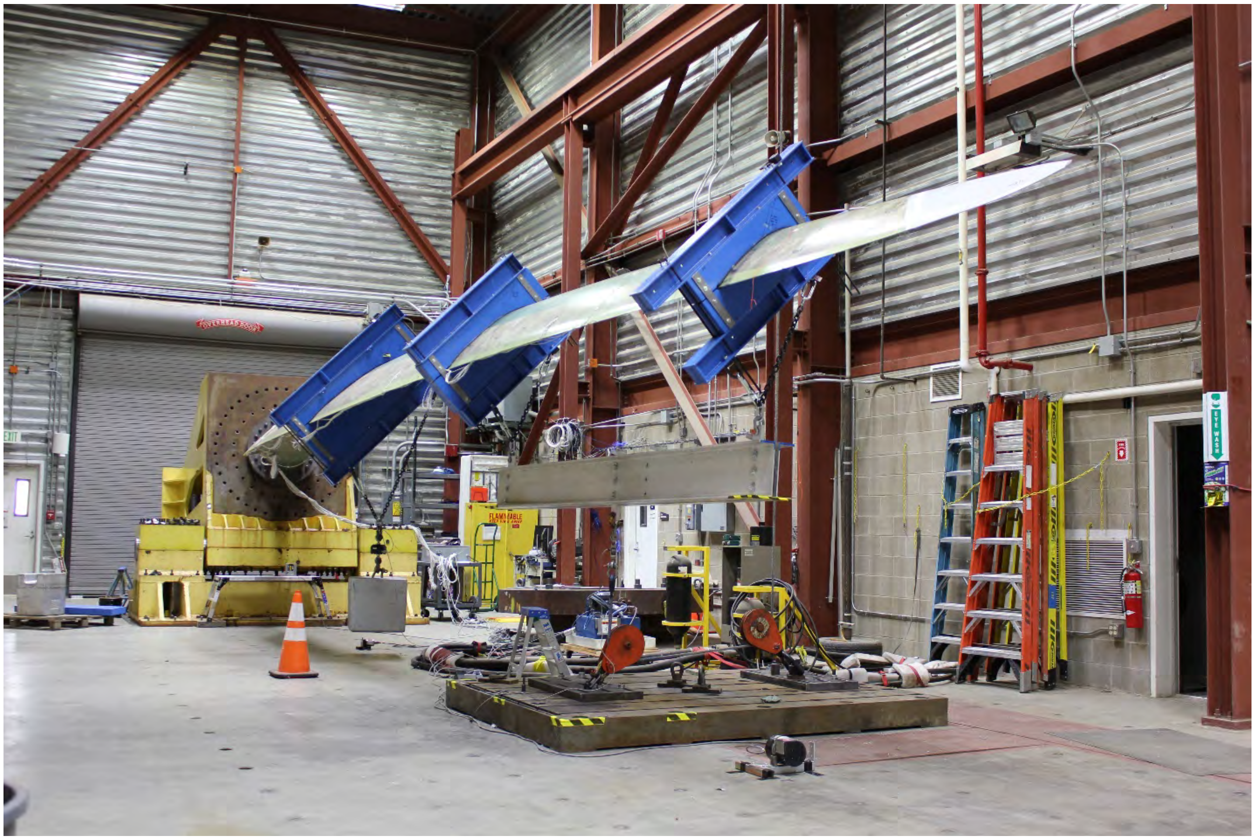

Figure I-12. Minimum Edge Near 100% Target Load

Figure I-13. Flapwise Calibration Pull for Fatigue Test Setup


Figure I-14. South UREX for Fatigue Testing

Figure I-15. Fatigue Test Setup. Single UREX on South, or Leading Edge side

Figure I-16. Winch used to apply loads for Ultimate Static Test

Figure I-17. Ultimate Static Test Setup

Figure I-18. Ultimate Static Test Near Tare Load

Figure I-19. Ultimate Static Test near failure load


Figure I-20. Ultimate Static Test – blade after failure, LP side

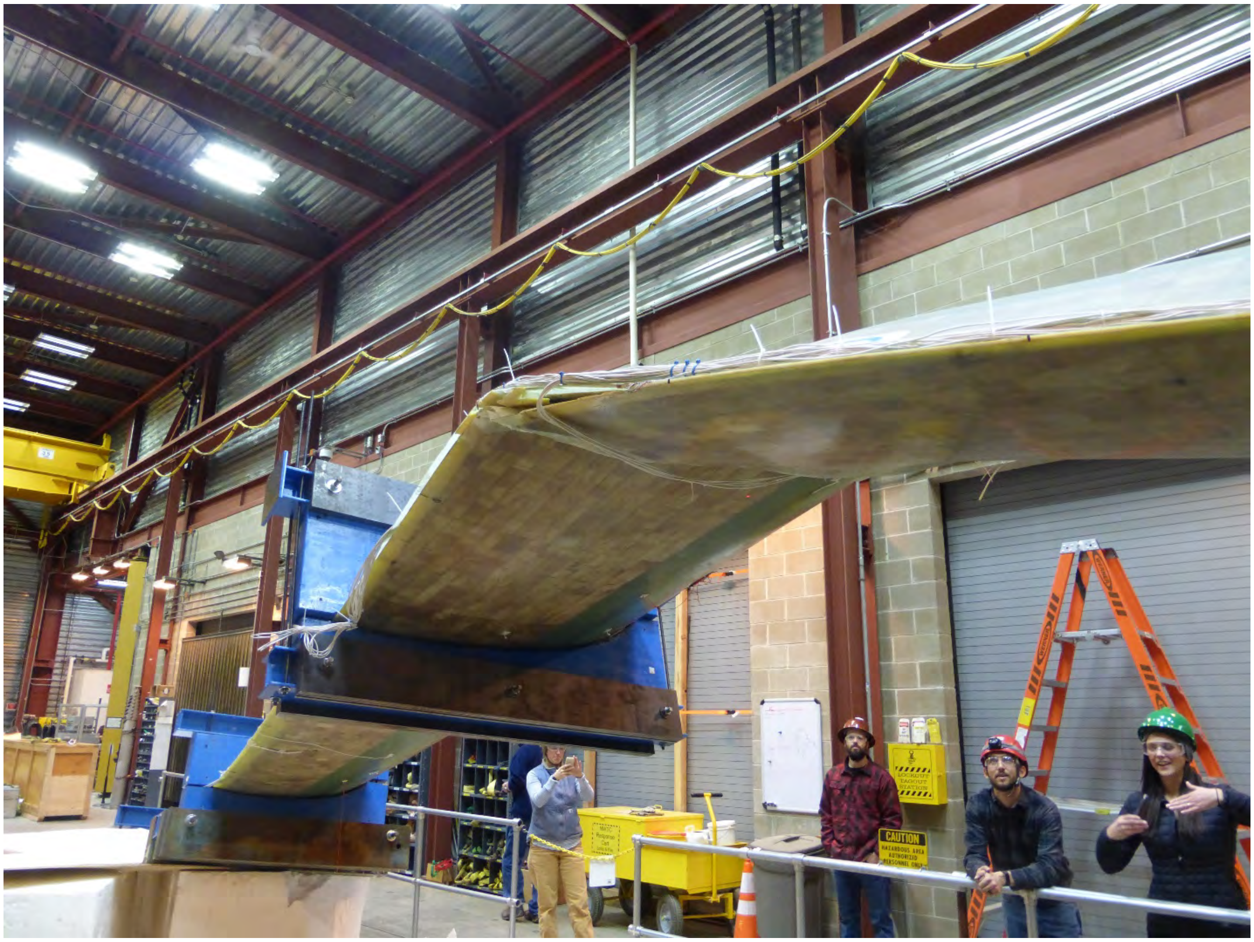

Figure I-21. Ultimate Static Test – blade after failure viewing LP from TE

Figure I-22. Ultimate Static Test post failure from LE

Figure I-23. Ultimate Static Test, HP side